University of Bremen

Institute for Psychology
Department of Neuropsychology and Behavioral Neurobiology

# Neural Correlates of Risk-Taking with Social and Financial Incentives – an fMRI Study

Dissertation submitted in partial fulfillment of the requirements
for the degree of Doctor rerum naturalium by

M.Sc. Niels Doehring

Supervision: Prof. Dr. Dr. Manfred Herrmann

First Reviewer: Prof. Dr. Bettina von Helversen
Second Reviewer: Dr. Peter Erhard

Colloquium date: 30.11.2022

# Acknowledgments

# Table of Contents

# Abstract (EN)

Humans take risks tied to different incentives - e.g., health, money, or social recognition. While changes in incentives are known to alter behavior, current neuropsychological research on risk-taking focuses almost exclusively on financial and token incentives. Whether and to what degree neural correlates depend on the incentive remains an open question, hindering transferability of findings from the laboratory context to the real world. This thesis is a first step in generalizing findings on the neural correlates of risk-taking to other incentive domains.

First, as a basis for further analyses, a meta-analysis of functional magnetic resonance imaging (fMRI) studies on human risk-taking was conducted. A general risk-taking brain-network was identified, and several experimental design parameters were found to have an influence on its extent. These findings help inform future experimental design decisions and serve to explain differences in findings of prior studies.

Second, brain activation during risk-taking with social and financial incentives was measured with fMRI in 40 participants. Findings on neural correlates were broadly similar across incentives, with their conjunction largely matching the network identified through the meta-analysis. However, the right inferior parietal lobule (IPL) was more strongly involved if incentives were financial compared to social. Exploratory correlational analyses tie this finding to participants behavior in the social condition. The findings place the IPL as a possible source of intra- and inter-individual differences in risk-taking propensity between domains. Future research making use of recent developments in bayesian multilevel modeling and precision fMRI could help understand its exact role.

# Abstract (DE)

Menschen gehen Risiken in Verbindung mit verschiedenen Anreizen ein - zum Beispiel Gesundheit, Geld oder soziale Anerkennung. Während es bekannt ist, dass Unterschiede in den Anreizen einen Einfluss auf das Verhalten haben, nutzt die neuropsychologische Forschung zu Risikoverhalten beinahe ausschließlich finanzielle oder symbolische Anreize. Ob und zu welchem Grad neuronale Korrelate von Verhalten abhängig sind von der Art der Anreize ist eine offene Frage, die die Übertragbarkeit von neuronalen Befunden zu Risikoverhalten aus dem Labor in die echte Welt einschränkt. Diese Doktorarbeit ist ein erster Schritt in Richtung einer Ausweitung der Befunde zu neuronalen Korrelaten von Risikoverhalten auf andere Anreizbereiche.

Zunächst, als Grundlage der weiteren Analysen, wurde eine Meta-Analyse angefertigt. Diese fasst Ergebnisse von Studien, die menschliches Risikoverhalten mit funktioneller Magnetresonanztomographie (fMRT) untersuchen, zusammen. Ein Netzwerk aus Hirnregionen zur Verarbeitung von Risikoverhalten wurde identifiziert. Weiterhin wurden verschiedene Parameter in experimentellen Designs gefunden, die einen Einfluss auf die neuronalen Korrelate haben. Diese Befunde helfen dabei, zukünftige Experimentaldesigns zu entwickeln und können darüber hinaus Unterschiede in den Ergebnissen vorheriger Studien erklären.

Anschließend wurde bei 40 Proband:innen Hirnaktivität während Risikoverhaltens mit sozialen und finanziellen Anreizen mittels fMRT gemessen. Ergebnisse hinsichtlich der neuronalen Korrelate ähnelten sich zwischen den Anreizen weitestgehend. Ausschließlich im inferioren Parietallappen (IPL) wurden stärkere Signale in der finanziellen Bedingung gemessen. Exploratorische Korrelationsanalysen bringen diese Ergebnisse mit dem Verhalten der Proband:Innen in der sozialen Anreizbedingung in Verbindung. Die Ergebnisse deuten auf den IPL als

mögliche Quelle von inter- und intraindividuellen Unterschieden in der Risikobereitschaft zwischen Anreizdomänen hin. Weitere Studien könnten neue Entwicklungen in bayesscher Modellierung von fMRT Daten und neue Ansätzen aus dem Bereich der Ruhemessungen nutzen, um die genaue Rolle des IPLs bei Risikoverhalten aufzuklären.

## Chapter 1: Introduction

Decisions govern our daily lives, on a large and small scale: "Where do I want to be in my life in three years?", "What do I want to eat this afternoon?". When making a decision, we are presented with at least two options. One way to distinguish such options is the risk associated with them. It might be considered riskier to aim for a career in a highly competitive field compared to one where new employees are sought after, at least in everyday understanding of the terms "risk" and "riskiness".

While most decisions entail options of varying riskiness, the resources at risk might differ. Decisions on what to eat entail, for example, a health risk – if decisions lead to an imbalanced diet, one's health might deteriorate. Decisions on what fund to invest in are coupled with a financial risk, and decisions on whether to go to a social event might include a possible social risk (if one does not go) and maybe even a health risk (if one does go and consumes too much alcohol). Thus, while risk-taking is a common component of decision-making, it takes place in different contexts, with different stakes and different incentives.

### 1.1 Relevance

Psychological research approaches human risk-taking from at least two angles. Firstly, by researching risk-taking in relation to judgment and decision-making in the general population. Here, understanding risk could inform better descriptions of and interventions in decision processes (Fischhoff & Broomell, 2020). Secondly, through the lens of clinical psychology, excessive risk-taking

is prevalent in specific age groups (Mata et al., 2011; Mamerow et al., 2016) and a component in the DSM-V based diagnosis of several psychiatric disorders – among them attention deficit hyperactivity disorder (ADHD), bipolar disorder, borderline personality disorder and substance abuse disorders (American Psychiatric Association, 2013). Excessive risk-taking is used here to describe maladaptive behavior where possible negative outcomes are undervalued in their severity or probability of occurrence. Such behavior can be problematic for the risk-taker. In young adults and adolescents, risk-taking is considered one of the main reasons for mortality and permanent injury (Kann et al., 2018). It furthermore contributes to harmful behavior in several psychiatric disorders, e.g., in alcohol use disorder (Ashenhurst et al., 2011), in ADHD (Pollak et al., 2017), and in biploar disorder and schizophrenia (Reddy et al., 2014).

Research related to risk-taking has led to a growing body of behavioral and neuroscientific findings on the topic ( Mohr et al., 2010; Schmitz et al., 2016; Wu et al., 2021). A common goal of both behavioral and neuroscientific research on risk-taking is a better understanding of the underlying mechanisms of - especially excessive - risk-taking behavior. Such understanding might pave the way to improved prevention and intervention regarding policy making and clinical applications. Neuropsychological approaches promise to elucidate how risk and its perception shape decisions (Chandrakumar et al., 2018) and highlight intervention targets to attenuate excessive risk-taking (Poudel et al., 2020).

Behavioral research on the context- and incentive-dependence of risk-taking is ongoing (e.g., Blais & Weber, 2006; Josef et al., 2016). However, most current

research into risk-taking and its neural correlates was conducted using financial (money) or arbitrary (token) incentives to model risk (cf. review articles by Schonberg et al., 2011; Chandrakumar et al., 2018; Poudel et al., 2020; Wu et al., 2021).

Minding the multitude of different incentives in everyday life, results from studies of risk-taking only using financial or arbitrary incentives may not be directly applicable to other contexts and incentives. A lack of studies with non-financial incentives has been recognized in the general decision-making research community in the last years, and the interest in neural correlates related to other incentives is on the rise (cf. e.g., Vrtička et al., 2014; Distefano et al., 2018). Conducted in October 2017, the systematic review by Chandrakumar et al. (2018) found no studies focusing on the neural correlates of risk-taking behavior with other incentives besides token and financial ones.

## 1.2 Overview

This thesis aims to broaden the study of neural correlates of risk-taking by comparing risk-taking in situations with financial incentives with situations with social incentives. Functional magnetic resonance imaging (fMRI) is employed to gain insights into the neuronal correlates of risk-taking behavior. Several designs for the laboratory assessment of risk-taking behavior with financial incentives were already implemented in studies using fMRI (cf. Sherman et al., 2018). This opens up the possibility of building upon well-tested designs and adapting them slightly to enable the use of social incentives.

During the development of the study design and detailed literature research, it became apparent that designs, results, and their interpretation in the study of

risk-taking with fMRI are very heterogeneous. Therefore, a meta-analysis was conducted to get an up-to-date overview of the field. A network of brain regions involved in risk-taking similar to that found in other meta-analyses was identified (Poudel et al., 2020; Wu et al., 2021). It encompasses the right dorsolateral prefrontal cortex and superior parietal lobule, and the bilateral dorsal anterior cingulate cortex (dACC), Insula, Caudate, and Brainstem. Furthermore, contrast analyses resulted in several detailed findings on the relationship between experimental design parameters and neuronal activation patterns. The results of the contrast analyses can be used to inform experimental design decisions in future studies on the neural correlates of risk-taking. They furthermore help explain differences in findings of previous primary studies that can now be linked to differences in their design. The meta-analysis serves as the starting point for the interpretation of the results of the fMRI study.

In the fMRI study, participants were asked to decide between risky and non-risky options tied to financial or social incentives. At the same time, neural correlates of their behavior were measured through fMRI. The design was an adapted version of an established, computerized instrument in risk-taking research, the "balloon analogue risk task" (BART, Lejuez et al., 2002). On the one hand, the analysis revealed a shared network of brain regions active independent of the incentive, spanning the bilateral dACC, occipital cortex, and the striatum. On the other hand, social versus financial incentives resulted in a significant difference in neuronal activation in the right inferior parietal lobule (IPL).

Further exploratory analyses link IPL-activation to risk-taking propensity in the social condition. Prior studies and exploratory analyses indicate that intersubject heterogeneity of functional topography in the IPL might be linked to domain-specific risk-taking propensity. These findings can be a starting point for more detailed analyses of the neural correlates of risk-taking. The incentive-independent network of brain regions identified assures that results from studies on risk-taking with financial incentives broadly apply to other incentive domains in most circumstances. However, for specific brain regions and under specific circumstances, neural activation patterns are dependent on the incentive domain, and the transferability of findings is not guaranteed.

The fMRI study was conducted during the onset of the severe acute respiratory syndrome coronavirus type 2 (SARS-CoV-2) pandemic. Thus, additional analyses were conducted to estimate the pandemic's influence on the results. Overall, results do not appear strongly influenced by the onset of the pandemic. However, results from these analyses should only be used to draw conclusions on the present data, as sample sizes are too small to permit adequately powered inferential statistics.

# Chapter 2: Theoretical Background

## 2.1 Definitions of Risk-Taking in Psychology and Economics

Risk-taking, as a component of decision-making, is ubiquitous in human life. Accordingly, various scientific fields have an interest in understanding it: from behavioral economics over clinical- to neuropsychology. Definitions of what exactly is meant by "risk" and "risk-taking" vary between the fields (Schonberg et al., 2011; Bran & Vaidis, 2019).

Knight (1921) defines "decisions under risk" as decisions where the probabilities of all possible outcomes are known. This would, for example, be the case in a lottery with a fixed chance of winning a fixed amount. Knight contrasts "decisions under risk" with "decisions under uncertainty", where the probabilities are not known in advance, for example when investing in the stock market. Knights' terminology is widely adapted in behavioral economics (De Groot & Thurik, 2018).

Authors with a background in psychology historically used definitions different from those in behavioral economics (Lipshitz & Strauss, 1997; De Groot & Thurik, 2018). Developmental and clinical psychology primarily use the term "risk-taking". It usually denotes "engagement in behaviors that are associated with some probability of undesirable results" (Boyer, 2006). This definition matches some instances of "decisions under risk", e.g., playing roulette or other games of chance where the probabilities of outcomes are known. However, many real-world decisions must be made without knowing the exact probabilities of possible outcomes. Developmental risk-taking research often

focuses on behaviors like drug consumption, unprotected sexual encounters, and dangerous driving (Boyer, 2006) – all "decisions under uncertainty" according to the definition by Knight (1921).

The differences in the usage of the word "risk" have led to economists criticizing psychologists for not correctly addressing the difference between "decisions under risk" and "decisions under uncertainty" (De Groot & Thurik, 2018). This critique ignores that the differentiation between known and unknown probabilities is of little importance for clinical researchers, who are trying to investigate excessive engangement in possibly harmful activities, be it in a lottery or while driving a car. Nevertheless, clear differentiation between "risk-taking" and "decisions under risk" allows for a separation of the different theoretical concepts from clinical and developmental research and from behavioral economics, respectively.

The term "risk" on its own is used in publications in psychology to refer to various different concepts (e.g., Chandrakumar et al., 2018: explicit definition of risk, differing from that of Knight; Rao et al., 2018: definition of risky situations analogous to situations where risk-taking can happen; Buckert et al., 2014: definition used by Knight). Bran and Vaidis (2019) note in their work on terminology in risk-taking research that disagreement on exact definitions and measurement instruments was already remarked upon in the 1960s. Review articles stated diverging evidence, originating in different scales using different concepts behind the same terminology - without any changes in their wake (Bran & Vaidis, 2019).

This thesis will use the following definitions: "Decisions under risk" and "decisions under uncertainty" will be used analogously to Knight (1921). Both

terms and definitions are widely adapted in behavioral economics (De Groot & Thurik, 2018). Their specificity offers a clarity other definitions lack. Regarding risk-taking, the definitions suggested by Bran and Vaidis (2019) will be used: "Risk-taking" and "risk-taking behavior" will describe a behavior where actions are taken that involve potential risks or uncertainties. The term can be differentiated from "self-reported risk-taking behavior" or "hypothetical choices". The former denotes all measures of risk-taking as reported by participants themselves, i.e. in a questionnaire. The latter relates to decisions made in hypothetical scenarios that participants are asked to imagine.

"Risk-taking propensity" indicates markedness of a person's tendency to choose an option with a higher probability of undesirable results. Because risk-taking propensity might be domain-specific, as explained in more detail below, "general" and "domain-specific" risk-taking propensity will be differentiated.

## 2.2 Domain Specificity in Risk-Taking

In part of the literature, risk-taking propensity is treated as a domain-general trait, not unlike measures of personality (Mata et al., 2018; Zhang et al., 2019). An instrument for measuring this supposed trait is the "general risk propensity scale (GRiPS)" developed by Zhang and colleagues (2019). However, other research indicates risk-taking to be more domain-specific, with little or no convergence across domains – the related measure being the domain-specific risk-taking scale (DOSPERT, Blais & Weber, 2006). The discussion up until 2017 is summarized by Mata and colleagues (2018). They recapitulate the evidence as pointing towards a trait-like domain-general risk-taking propensity, with notable convergence across domains (ibid.). Mishra (2014) argues that strong

enough differences in participants' valuation of incentives from different domains might mask a common trait. Other recent studies, however, find indications of strong domain specificity in various contexts: correlations between risk-taking propensity and disgust sensitivity (Sevi & Shook, 2021), in decisions under ambiguity akin to that under risk-taking (Shou et al., 2020), and gender effects unique to social risk-taking (Friedl et al., 2020).

The question has gained interest from other research fields, with a study by Nicolaou and Shane (2020) finding a common genetic component accounting for a part of the relationship between general and domain-specific risk-taking propensity and behavior. These findings explain some portion of the source of inter-subject variability in domain-specific risk-taking as a genetic effect. They also add to the evidence pointing to some domain generality of risk-taking. The mechanism, origin and full extent of domain specificity, however, remain unclear.

Neuroscientific research on reward consumption has shown that rewards from different domains activate dissociable neural networks (Rademacher et al., 2010; Flores et al., 2015; Gu et al., 2019). Behavioral research on risk-taking with different incentives found an effect of the incentive type on the behavior. Sunstein and colleagues (2011) observed that people's willingness to get paid in exchange for a painful yet safe electric shock did not change if the probability of receiving the shock changed. People accepted a 1% and 100% chance of receiving an electric shock for the same amount of money, demonstrating indifference to the actual size of the risk (ibid.), a behavior different from that observed in financial risk-taking (Wu et al., 2021). Rosati and Hare (2016) used a more complex design to compare risk-taking propensity for financial

rewards, food, and office supply prizes and found significantly lower risk-taking for non-financial incentives. They argue that financial rewards are different from other reward domains, as they enable the acquisition of other rewards. Lastly, von Helversen and colleagues (2020) compared risk-taking with money and odors as incentives. They found a lower sensitivity to probabilities and stronger deviations from optimal behavior if bad odors were used as negative incentives. They attribute this to the bad odor being richer in affect, i.e. evoking a stronger affective response compared to a financial loss. In conclusion, the behavioral literature agrees on a difference in risk-related behavior between financial rewards and at least some other rewards in an experimental setting (Sunstein et al., 2011; Rosati et al., 2016; von Helversen et al., 2020), with affect-richness and the special status of money probably influencing behavior. How broadly such effects apply and if they have a measurable effect on the neuronal correlates of risk-taking remains an open question.

Financial and token incentives have many advantages over other incentive types: they are easy to quantify, can be divided into smaller subunits, are related to participants' everyday life, and are easy to disburse after the experiment. However, the extent to which findings on risk-taking with financial incentives are generalizable to other domains remains unclear. Investigating whether neural networks found in risk-taking differ based on the incentive domain would lead to a better understanding of the mechanisms and extent of domain specificity in human risk-taking.

## 2.3 Risk-Taking Designs in Experimental Studies

A variety of risk-taking designs were developed over the years. Schonberg and colleagues (2011), among others, compared different study designs. They propose three criteria for evaluating laboratory risk-taking tasks. (1) Task results should be decomposable into the different aspects underlying risk-taking, (2) they should show external validity, and (3) the participants should be emotionally engaged in the task.

One of the more frequently used designs in the research on risk-taking is the BART, developed in 2002 by Lejuez and colleagues (Schonberg et al., 2011; Schmitz et al., 2016; Poudel et al., 2020; Wu et al., 2021). In the BART, participants are instructed to inflate a virtual balloon via button presses. After each inflation, they have to decide whether they want to continue inflating or stop and continue with the next balloon. The reward participants get for a balloon increases with every inflation, but so does the probability of the explosion of the balloon. If the balloon explodes, the accumulated reward for that balloon is lost. If the participants decide to stop inflating, the accumulated reward is added to their final payout, and they continue with the next balloon. The participants know that the probability of an explosion increases with every inflation. However, they do not know the exact probability for each size. They thus have to decide under incomplete information whether they want to inflate the balloon further or stop and collect the accumulated reward. Usually, multiple virtual balloons are inflated by the participants, and the average size of non-exploded balloons is taken as a measure of risk-taking propensity (Schmitz et al., 2016). This measure is called the "adjusted BART score" (ibid.). Multiple research groups examined the BART's validity in the years after its

publication. It was shown that the adjusted BART score correlates with various forms of real-world risk-taking, such as alcohol consumption, criminality, and drug consumption (Aklin et al., 2005; Skeel et al., 2008). Additionally, Hunt and colleagues (2005) found that psychopathy and impulsivity, two attributes strongly related to excessive risk-taking, affect the risk-taking behavior in the BART. Furthermore, the correlation between self-reported risk-taking and behavior in the BART is stronger than that between self-reported risk-taking and hypothetical or financial gambles (Lauriola et al., 2014).

Regarding the criteria mentioned above (decomposability, external validity, and emotional engagement), the BART is considered satisfactory in the second and third domain by Schonberg and colleagues (2011). Schmitz and colleagues (2016) bring forward a possible reason for the comparatively high external validity based on neuropsychological findings by Ulrich and colleagues (2014). The BART's intuitiveness and low cognitive demand might encourage more spontaneous decisions that are more in harmony with one's personality dispositions than more abstract choices (Schmitz et al., 2016).

However, it has two major flaws: One is the complete correlation of expected value and risk in the design, the other its demand on the learning capacity of the participants. As explosion probabilities are unknown to participants, they must be learned during the experiment. Mata and colleagues (2011) showed that experimental designs with such properties tend to mix up learning capacity and risk-taking propensity and should thus be applied with caution. While the first concern is harder to dispel, the second can, at least partly, be addressed by a homogeneous cohort of participants of a similar age and comparable level of education. Another approach to limit the effects of inter-

subject differences in short-term memory is to focus on the comparison of different measures within instead of between subjects.

Lejuez and colleagues, the inventors of the original BART, parameterized risk-taking by calculating participants' average number of inflations over all balloons that did not explode. However, several different ways to parameterize the BART have since been established. Schmitz and colleagues (2016) discuss various scoring alternatives in detail and suggest using the "burst-score", calculated by taking the sum of exploded balloons for each participant.

## 2.4 Neural Correlates of Risk-Taking - a Meta-Analysis

Studies on the neural correlates of risk-taking are, like the studies on the behavioral level, heterogeneous in approaches and findings (cf., Mohr et al., 2010; Chandrakumar et al., 2018; Poudel et al., 2020; Wu et al., 2021). A meta-analysis on the topic was conducted with the goal to describe and summarize the current state of the field, and to inform experimental design and interpretation of further fMRI studies on the topic. The following chapters detail the hypotheses, methods, results, and discussion of the meta-analysis.

### 2.4.1 INTRODUCTION TO THE META-ANALYSIS

No systematic review articles on fMRI measurements of neural correlates of human risk-taking capturing the present state of the field existed in 2019, to the best of the author's knowledge. Systematic reviews existed on risk-taking studies using electroencephalography (EEG, Chandrakumar et al., 2018) and adolescents' neural correlates of risk-taking (Sherman et al., 2018). EEG measurements are precise in time, but despite recent progress limited in their

spacial resolution (Seeber et al., 2019). Studies on risk-taking on the behavioral and neuropsychological levels found notable differences between adolescents and adults, and results can thus not be transferred from one group to the other. Furthermore, a review article using a very narrow interpretation of the concept of "decisions under risk", as introduced by Knight (1921), was published by Levy in 2017. The definition of risk-taking commonly used in psychology is broader, as detailed above, and neural correlates likely differ depending on which one is used (cf. Wu et al., 2021).

Since then, two relevant meta-analyses have been published by other research groups: one by Poudel and colleagues (2020) and one by Wu and colleagues (2021). The following paragraphs will summarize their findings, followed by an overview of the additional insight the present meta-analysis can provide.

Prior meta-analyses of the topic can be grouped based on the concept they focus on - either the psychological concept of risk-taking or broadly defined decision-making under risk, as used in economics. Mohr and colleagues (2010) compared the findings of 30 fMRI studies. They oriented their analysis on the psychological concept of "risk-taking", focusing on designs where probabilities of outcomes were known or could be inferred or learned. Another approach to the topic is the comparison of decisions under risk and ambiguity (cf. Krain et al., 2006). Poudel and colleagues (2020) and Wu and colleagues (2021) worked on two broadly similar meta-analyses on the question. Both use a broader definition of decision-making under risk, including studies where probabilities can be inferred or learned.

Previous primary studies on risk-taking use various designs (cf. Mohr et al., 2010; Poudel et al., 2020; Wu et al., 2021 for fMRI; Chandrakumar et al., 2018

for EEG; Schonberg et al., 2011 for behavioral research). Studies offer different rewards to subjects, and fMRI studies differ in the contrasts they employ. Contrasts reach from decisions for save compared to risky options (e.g., Bjork et al., 2007, Brevers et al., 2015; Funkunaga et al., 2018) over decisions for options with high risk compared to decisions for low risk (e.g., Paulus & Frank, 2006; Miedl et al., 2010) to decisions for risk compared to various baselines (e.g., Congdon et al., 2013).

The present study adds to the field in two ways: Study selection criteria were more specific compared to other current meta-analyses on the topic (cf. Poudel et al., 2020; Wu et al., 2021). Especially the work by Poudel and colleagues (2020) uses broad inclusion criteria, e.g., mixed samples of healthy controls and patient groups. Their approach allows for a large number of primary studies to be included and results in higher statistical power and better generalization over various groups of subjects. In comparison, the present analysis is more focused, e.g. including only healthy young adults. Accordingly, statistical power is lowered, but more specific observations can be made, adding a new perspective. Furthermore, two subgroup analyses are added. Studies contrasting risky and save options are compared to those contrasting different levels of risk, and studies using financial rewards are contrasted with those using tokens or similar rewards that cannot be kept after the study.

An activation likelihood estimation (ALE; Turkeltaub et al., 2002) will be used to summarize the findings of primary studies. The present analysis results can be of use to highlight moderators of neural correlates of risk-taking, thereby

advancing future design decisions and helping to generate specific hypotheses. To this goal, the following questions are investigated:

> 1. What are common brain areas found in fMRI studies on human risk-taking?

Including all studies in one analysis promises to reveal structures that are mostly independent of the specific task and common to most or all designs falling under the here-used definition of risk-taking (Eickhoff et al., 2012). It is also the first step to, akin to Laird and colleagues (2009) and Wu and colleagues (2021), conduct contrast analyses on subsets of all studies to identify moderating factors. The following research questions are based on previous meta-analyses and differences in the designs of primary studies identified before the measurement.

> 2. What are the differences in brain activation between risk-taking in the win and the mixed domain?

Previous meta-analyses (Mohr et al., 2010; Wu et al., 2021) compare neural correlates of risk-taking in the win and loss domain. Both groups contrast designs that allow only for gains with designs where gains and losses were possible - studies on pure losses were too rare to allow for statistical comparison (Wu et al., 2021). Both studies found significant differences in neuronal activation patterns associated with risk-taking in the win and the mixed domain: Wu and colleagues report a broader involvement of the left anterior insula in study designs allowing losses. Mohr and colleagues report foci in multiple regions. They find the left anterior insula (aINS), left superior temporal gyrus (STG), and left precentral gyrus more likely to be activated in the mixed domain. In the win domain, the dorsomedial prefrontal cortex

(dmPFC), dorsolateral prefrontal cortex (dlPFC), right parietal cortex, parts of the thalamus, and the occipital cortex (OC) were more likely to be activated.

The results of the present analysis are expected to be closer to the findings of Wu and colleagues (2021). The ALE-meta analysis algorithm was updated multiple times since the study by Mohr and colleagues (cf. Turkeltaub et al., 2012; Eickhoff et al., 2012), and the overlap in primary studies is larger between the present study and the work of Wu and colleagues compared to that of Mohr and colleagues. If the results of the present analysis differ from those of Wu and colleagues, it will likely be caused by the study selection criteria.

For the present work, "win domain" will refer to designs where only gains were allowed, and "loss domain" refers to designs where only losses were possible. "Mixed domain"-designs include both.

### 3. What are the differences in brain activation between financial and arbitrary incentives?

Due to its relevance for the current thesis, the effect of differences in incentives was analyzed. Previous research shows that different incentives can activate different neural structures. A study on the delivery and consumption of financial and social rewards by Rademacher and colleagues (2010) found differences in the neural networks associated with the different incentives, particularly during consumption. Accordingly, research on differences in the anticipation and consumption of different rewards is ongoing. Regarding the anticipation phase, a study by Flores, Münte & Donamayor (2015) found differences in the event-related potentials (ERPs) measured through EEG during the anticipation of social versus financial rewards. As another example, a current review of fMRI studies on reward anticipation and delivery expressly

excludes non-financial rewards to preempt the included studies from being too heterogeneous due to different reward types (Jauhar et al., 2021). In the light of differences in the neural networks associated with anticipation and consumption of rewards, differences in the neural networks related to risk-taking based on whether financial incentives are given to participants or not seems plausible. To the author's knowledge, no comparable analysis has been conducted on risk-taking studies.

> 4. What are the differences in brain activation between the comparison of different risk levels and contrasts between risky and save decisions?

Studies on the neural correlates of risk-taking differ in the type of analyses they conduct: different levels of risk – either binary or parametric – can be compared, and decisions for save and risky options. While the difference between risky and save options is qualitative, differences between varying levels of risk are quantitative. Investigating if such differences in analysis lead to differences in findings will advance the current understanding in multiple ways. On the one hand, differentiating brain regions sensitive to the pure presence of risk and those changing in their activation with the actual level of risk can help in understanding brain activation patterns in primary studies. On the other hand, it might guide future studies in their choice of analysis approach.

Wu and colleagues (2021) conducted a similar analysis, focusing on the methodological decision for parametric vs. binary analyses. Based on their findings, the left aINS and thalamus are more reliably active in parametric designs. The left OC and right inferior frontal gyrus (IFG) are more reliably active in binary contrasts. In the present analysis, not enough primary studies were found on parametric designs to replicate that analysis. However, the

present analysis can offer a different perspective, and comparisons between the findings of the present analysis and that of Wu and colleagues are likely to shed further light on the moderating effects of the analysis approach.

## 2.4.2 Research methods

The meta-analysis was oriented on the "Preferred Reporting Items for Systematic Reviews and Meta-Analyses" Statement (PRISMA 2020 Statement, Page et al., 2021). The databases Scopus, PubMed, Web of Science, PsycInfo, and ScienceDirect were searched for relevant peer-reviewed articles written in English. The search was conducted on the 23rd of March, 2019. A second search with the same parameters was conducted on the 25th of February 2022 to find any additional studies published in the meantime. For the second search, The database PsycInfo could not be accessed due to technical problems and was thus excluded from the second search. No further exclusion criteria were set regarding the publication date of primary studies.

### 2.4.2.1 Study selection, preparation, and data extraction

Inclusion criteria were a sample of at least ten healthy young or middle-aged adults (minimum age >= 18, maximum age < 65) and the use of fMRI to investigate differences in blood-oxygen-level-dependent (BOLD) signal strength in whole-brain analyses. Region of interest (ROI) studies violate the assumptions of ALE meta-analyses and were thus excluded (Turkeltaub et al., 2002). In addition, studies had to include a paradigm where participants were actively engaged in a task in which they had to choose between options differing in the probabilities of positive or negative outcomes. In contrast to other meta-analyses on the topic, anticipation risk - the process of risk processing without a choice (Mohr et al., 2010) - was excluded from the present

analysis for two reasons. First, stricter selection criteria reduce heterogeneity while maintaining a large enough database for adequately powered analyses. Second, the neural network involved in risk-taking as proposed by Mohr and colleagues (2010), did not differ between anticipation risk and actual risk-taking during the first stages of processing, while the later stages were only present in actual risk-taking. A focus on designs involving the latter might thus allow for the whole network to be observed in every primary study.

Overall, inclusion criteria were more narrow compared to other current meta-analyses on the topic (cf. Poudel et al., 2020; Wu et al., 2021). Studies comparing risk and ambiguity, studies using fixation or rest periods as a contrast (compared to decisions for different risk levels, save options, or conceptually similar tasks), and studies involving experimental manipulation before each risk-taking trial were excluded to decrease heterogeneity.

For inclusion, studies needed to use an fMRI analysis comparing levels of riskiness with a contrast design (e.g., risk vs. no risk, active vs. passive risk, or high vs. low risk) or a parametric regressor varying with the level of risk. The term "risk" here denotes the probability of an undesirable outcome, akin to definitions commonly used in psychology (cf. Boyer 2006, Bran & Vaidis 2019). This definition mostly matches what other meta-analyses termed "decisions under risk" (c.f. Poudel et al., 2020; Wu et al., 2021). Studies furthermore had to report the coordinates of peaks of significant differences in BOLD signal strength in a known standardized reference frame.

Tasks using a choice paradigm with a clearly optimal choice option were not included to assure that participants treated the decision as purely perceptual. A commonly used design in the study base excluded for this reason is the Iowa

Gambling Task (IGT, Bechara et al., 1994). In the IGT, participants can choose multiple times to draw a card from one of two decks: One deck has a higher variability of rewards but lower expected value than the other. After a learning period, choices for risk in the IGT are strictly disadvantageous (ibid). As soon as participants learn the respective probabilities, they should be able to pick only the options leading to the best outcomes, leaving little room for intentional risk-taking.

Some previous meta-analyses of decision-making studies included the IGT as "decision making under risk" in their study sample (Krain et al., 2006; Poudel et al., 2020). This point can be argued, as it seems relatively certain that behavior in the IGT can be driven by risk-seeking behavior in some individuals (Dunn et al., 2006; Bull et al., 2015). However, Bull and colleagues (2015) found results from the IGT concerning risk-taking strongly influenced by minor details in the design choices. At least during the first 100 trials, task understanding and risk-taking are correlated in at least some individuals (ibid.). The IGT was therefore excluded from the present meta-analysis as it is unclear how well it captures risky decision-making and how strong the influence of minute differences in designs might be.

Table 1 reports the number of articles identified through each database and the exact search string used. For the second search, the search was adapted only to include results published after the exact date of the first search. For search engines where only full years could be excluded, the search was rerun for 2019 and later.

**Table 1**

*Databases, search terms and results of the primary literature search and the update*

| Database | Search String | first search | updated search |
|---|---|---|---|
| Scopus | TITLE-ABS-KEY ( ( fmri OR "functional magnetic resonance" OR "functional MRI" ) AND ( "risk taking" OR "risk-taking" OR "risk perception" OR "risk propensity" ) )[b] | 408 | 98 |
| PubMed | ( fmri OR "functional magnetic resonance" OR "functional MRI" ) AND ( "risk taking" OR "risk-taking" OR "risk perception" OR "risk propensity" ) | 545 | 116 |
| Web of Science | ALL= ( ( fmri OR "functional magnetic resonance" OR "functional MRI" ) AND ( "risk taking" OR "risk-taking" OR "risk perception" OR "risk propensity" ) ) | 466 | 112 |
| PsycInfo | ( ( fmri OR "functional magnetic resonance" OR "functional MRI" ) AND ( "risk taking" OR "risk-taking" OR "risk perception" OR "risk propensity" ) ) | 262 | –[a] |
| ScienceDirect | ( ( fmri OR "functional magnetic resonance" OR "functional MRI" ) AND ( "risk taking" OR "risk-taking" OR "risk perception" OR "risk propensity" ) ) | 102 | 33 |

*Note*: Search strings for the updated search were limited to studies published after the date the first literature search was conducted.

[a] PsycInfo was not available for the updated search due to technical issues.

[b] Reviews were excluded through the user interface.

22

The first search returned a total of 1783 reports, 808 of whom were duplicates and thus removed from the analysis. Two independent investigators screened abstracts and titles. Any disagreement on whether to include a report in the next step was solved by consensus. When no consensus was reached, reports were included in the next step. During the first step, 834 reports were excluded based on their title and abstract, leading to 141 papers remaining for full-text analysis. Of these 141 reports, 55 reports were excluded as they did not report any relevant contrasts. A further 47 papers were excluded for various reasons detailed in the PRISMA-Flowchart in figure 1. The second search resulted in 359 papers that went through the same process. Only one additional study was eligible, increasing the number of included studies to 36. Detailed data for exclusion numbers of the second search can be found in the figure 1. Data were extracted by two independent researchers. Any disagreements were discussed until consensus was reached.

**Figure 1**

*PRISMA-Flowcharts of the primary systematic literature search and the update*



PRISMA-Flowchart of the first systematic literature research, conducted on the 23rd of March 2019

- Identification (n = 1783)
  - Scopus: 408
  - PubMed: 545
  - Web of Science: 466
  - PsycInfo: 262
  - Science Direct: 102
  → Duplicate records removed (n = 808)
- Records Screened (n = 975) → Records excluded (n = 834)
- Reports sought for retrieval (n = 141) → Reports not retrieved (n = 0)
- Reports assessed for eligibility (n = 141) → Reports excluded (106):
  - No relevant contrast (58)
  - No healthy-adults only (25)
  - Clearly superior option in design (12)
  - Design unsuitable (5)
  - No whole brain analysis (4)
  - Not a paper (1)
  - Sample size <10 (1)
- Studies included in ALE-Meta Analysis: (n= 35)

PRISMA-Flowchart of the systematic literature research update, conducted on the 25th of February, 2022.

- Identification (n = 359)
  - Scopus: 98
  - PubMed: 116
  - Web of Science: 112
  - PsycInfo: /
  - Science Direct: 33
  → Duplicate records removed (n = 175)
- Records Screened (n = 184) → Records excluded (n = 161)
- Reports sought for retrieval (n = 20) → Reports not retrieved (n = 2)
- Reports assessed for eligibility (n = 18) → Reports excluded (17):
  - No relevant contrast (8)
  - No healthy-adults only (7)
  - Design unsuitable (2)
- Studies included in ALE-Meta Analysis: (n= 1)

*Note.* Only one reason for exclusion is counted for every study, even if multiple reasons applied. The reported reason is the most specific, i.e. a study including a clearly superior choice option is counted in that category, although it would also qualify for the less specific "design unsuitable" category.

## 2.4.2.2 Calculation of the ALE-meta analyses

Current practice in fMRI research is to only report the coordinates of peaks of significant activation together with their effect size, resulting in large parts of the results - all non-peak voxels - not being eligible for meta-analyses. The method used here to circumvent this problem quantitatively is the ALE approach developed by Turkeltaub and colleagues in 2002.

Coordinates were extracted from the primary studies. Coordinates in Talairach space (Talairach, 1967; Talairach & Tournoux, 1988) were converted to the MNI152-2009a template (Fonov et al., 2011) through the Lancester Transformation (Lancester et al., 2007; Laird et al., 2010) as implemented in GingerALE 3.0.2. (Eickhoff et al., 2009). Results were reversed in polarity where necessary to ensure that significant positive differences in BOLD-signal strength always indicate a positive relation between BOLD-signal strength and risk level. Significant negative BOLD-differences vice versa implied a negative relation.

ALE analyses were conducted in GingerALE 3.0.2 (Eickhoff et al., 2009), a software solution implementing the updated ALE algorithms described by Turkeltaub and colleagues (2012) and Eickhoff and colleagues (2012). For all research questions detailed above, separate analyses were conducted. The ALE algorithm convolutes the foci-data with a three-dimensional Gaussian probability distribution with the width determined by the sample size of primary studies. The resulting maps for each study are superimposed, with the value in the final map being set to the maximum value from the individual studies maps. This method is recommended over simple addition, as the latter can lead to distortions if a single study reports multiple foci close to each other (Turkeltaub et al., 2012). When multiple analyses from one study were eligible for analysis, they were grouped as a single analysis (Turkeltaub et al., 2012) to avoid an inflation of the contribution of a single study to the analysis. Next, a map of so-called "ALE-values" is created as the union of all study-specific maps. Significant differences from zero are calculated via cluster-thresholding to account for multiple comparisons: For several iterations, the coordinates in the dataset are replaced by random coordinates, ALE values are calculated,

thresholded, and the size of the resulting clusters is recorded as a null distribution. The cluster-forming threshold in the present study was set to $p$ < .001, the cluster threshold to $p$ < .05. 1000 permutations were used to generate the null distribution.

Some software packages for the analysis of fMRI data only report one-directional tests if standard settings are used (cf. Cox et al., 2017), and some primary studies do not report whether one-directional or bidirectional analyses were conducted. As the bias induced by this possibly selective reporting cannot be estimated accurately, only positive relations between risk level and BOLD-signal strength were analyzed. Contrast analyses, as described by Eickhoff and colleagues (2012), were conducted with GingerALE to compare different conditions for research questions two to four. For contrast analyses, a null distribution was calculated from 10000 permutations of the data. The statistical threshold was set at p<.05, and clusters below 200mm³ volume were rejected.

Anatomical labels and brain parcellations were based on the human Brainnetome Atlas (Fan et al., 2016) as implemented in AFNI's "whereami" function. All figures used for illustration in this chapter were created in AFNI (Version 'Galba' - 20.0.17, Cox, 1996). For better comparability, composite images of different analyses were generated using the 3dcalc++ function from AFNI.

### 2.4.2.3 Additional analyses

A strong correlation between any two of the three variables used for contrast analyses would impede a clear attribution of neuronal findings to the variables. Correlations between all three variables were calcculated to describe any such effects in the present sample. Furthermore, correlations between each variable

and the year of publication of the primary studies were calculated and tested for significance to identify any trends in experimental design choices. Trends in the development of sample sizes over time were analyzed with a correlation between the year of publication and the sample size. Studies with a sample size of 3 standard deviations above or below the mean were excluded from the analysis.

### 2.4.3 RESULTS

#### 2.4.3.1 Study characteristics

The 35 studies reporting significant changes in BOLD signals depending on variations in risk contained a total of 44 statistical analyses. Only a single study (Gillman et al., 2011) reported no significant effects of risk-taking on neuronal activation patterns. The analyses will be called "experiments" in the following, as proposed by Laird and colleagues (2009). A list of all included experiments can be found in table 2. Studies reported positive and negative relationships between increased risk and BOLD signals for a total of 95 negative and 392 positive peaks.

Mean ages varied from 20.2 to 41 years, with the youngest participants being 18 and the oldest being 56 years of age. Sample sizes for fMRI analyses reached from 10 to 157 participants ($m = 28$, $sd = 25.3$). Six studies recruited exclusively male samples. No exclusively female sample was investigated, although some studies had considerably more female than male participants (e.g., Pletzer et al., 2016 with 41 female and 18 non-female participants). One study (Macoveanu, 2016 -2) did not report on the gender of its participants. Information on the sample sizes and gender ratio of all studies can be found in table 2.

**Table 2**

*Experiments identified in the literature search for the ALE meta-analysis*

| Author | Year | n (female) | age (sd) | peaks reported | experimental design | win/mixed domain | incentive | contrast type |
|---|---|---|---|---|---|---|---|---|
| Bjork et al. | 2007 | 20(10) | 28.5(3.2) | 22 | risky gains task | win | money | risk vs save |
| Bjork et al. | 2007 | 20(10) | 28.5(3.2) | 21 | risky gains task | mixed | money | risk vs save |
| Bjork et al. | 2007 | 20(10) | 28.5(3.2) | 3 | risky gains task | mixed | money | high vs low risk |
| Bjork et al. | 2008 | 17(7) | 33.5(NR) | 22 | risky gains task | win | money | risk vs save |
| Bjork et al. | 2008 | 17(7) | 33.5(NR) | 27 | risky gains task | mixed | money | risk vs save |
| Brevers et al. | 2015 | 10(2) | 36.2 | 5 | Choice between bet or save | win | random trial | risk vs save |
| Campbell et al. | 2008 | 23(10) | 25.68 | 16 | Choice between bet or save | loss | arbitrary | risk vs save |
| Cohen et al. | 2005 | 16(7) | NR(NR) | 5 | Choice between bets | win | not reported | high vs low risk |
| Congdon et al. | 2013 | 23(13) | 25.65(4.43) | 3 | ART – choice for risk | win | money | high vs low risk |
| Engelmann et al. | 2009 | 10(3) | NR(NR) | 25 | Choice between bets | win | money | risk vs save |
| Fukunaga et al. | 2012 | 16(8) | 20.19(NR) | 4 | BART – choice for risk | win | money | risk parametric |
| Fukunaga et al. | 2012 | 16(8) | 20.19(NR) | 2 | BART – choice for save | win | money | save parametric |

| Author | Year | n (female) | age (sd) | peaks reported | experimental design | win/mixed domain | incentive | contrast type |
|---|---|---|---|---|---|---|---|---|
| Fukunaga et al. | 2018 | 25(14) | 24.24(3) | 11 | Choice between bet or save | mixed | money | variance parametric |
| Gilman et al. | 2012 | 20(12) | 26.1(2.8) | 0 | Choice between bet or save | mixed | money | risk vs save |
| Haeusler et al. | 2018 | 165(0) | 38.9(6.7) | 3 | Choice between bet or save | mixed | random trial | risk vs save |
| Kohno et al. | 2015 | 60(27) | NR(NR) | 8 | BART – choice for risk | win | money | risk parametric (choice for risk) |
| Kohno et al. | 2015 | 60(27) | NR(NR) | 5 | BART – choice for save | win | money | risk parametric (choice for save) |
| Lee et al. | 2008 | 12(0) | 19.9(6.2) | 3 | risky gains task | mixed | arbitrary | risk vs save |
| Li et al. | 2020 | 34(18) | 32.5(8.7) | 11 | BART – choice for risk | mixed | not reported | risk parametric |
| Liu et al. | 2017 | 27(0) | 22.74(2.35) | 2 | cups task | mixed | arbitrary | risk vs save |
| Losecaat et al. | 2014 | 26(12) | 22(2.68) | 12 | choice between bet or save | mixed | money (capped) | risk vs save |
| Macoveanu, Fisher et al. | 2016 | 32(0) | NR(NR) | 14 | choice between bets | mixed | not reported | risk parametric |
| Macoveanu, Miskowiak et al. | 2016 | 62(NR) | NR(NR) | 18 | choice between bets | mixed | not reported | risk parametric |
| Matthews et al. | 2004 | 12(5) | 34(NR) | 7 | choice between bet or save | mixed | not reported | risk vs save |

| Author | Year | n (female) | age (sd) | peaks reported | experimental design | win/mixed domain | incentive | contrast type |
|---|---|---|---|---|---|---|---|---|
| Meder et al. | 2016 | 20(9) | NR(NR) | 17 | cummulative gambling task | win | not reported | risk parametric |
| Miedl et al. | 2010 | 12(0) | 33.4(8) | 11 | blackjack task | mixed | money | high vs low risk |
| Paulus et al. | 2003 | 16(6) | 41(2.1) | 5 | risky gains task | mixed | arbitrary | risk vs save |
| Paulus et al. | 2006 | 17(6) | 38.3(1.4) | 15 | choice between bet or save | win | arbitrary | high vs low risk |
| Pletzer et al. | 2016 | 59(41) | 22.39(5.14) | 4 | BART | win | money | risk vs save |
| Pletzer et al. | 2016 | 59(41) | 22.39(5.14) | 2 | Game of Dice Task | win | money | high vs low risk |
| Rao et al. | 2008 | 14(6) | 25.1(NR) | 15 | BART – choice for risk | mixed | arbitrary | risk parametric |
| Rao et al. | 2008 | 14(6) | 25.1(NR) | 7 | BART – active vs. passive | mixed | arbitrary | active vs passive risk taking |
| Roy et al. | 2011 | 23(15) | 27.6(7.9) | 72 | choice between bet or save option | mixed | money | risk vs save |
| Schonberg et al. | 2012 | 16(10) | 23.6(2.9) | 8 | BART – choice for risk | win | money | risk vs control parametric |
| Smith et al. | 2009 | 25(12) | 29.1(5.5) | 2 | choice between bets | win | money | high vs low risk |
| Symmonds et al. | 2011 | 23(11) | 24(NR) | 12 | choice between bet or save option | win | money | risk vs save |
| Symmonds et al. | 2011 | 23(11) | 24(NR) | 3 | choice between bet or save option | win | money | variance parametric |
| Weber et al. | 2008 | 23(11) | 23(NR) | 10 | choice between bets | win | money | high vs low risk |

| Author | Year | n (female) | age (sd) | peaks reported | experimental design | win/mixed domain | incentive | contrast type |
|---|---|---|---|---|---|---|---|---|
| Wright et al. | 2013 | 22(16) | 22(NR) | 9 | choice between bet or save option | mixed | money for a random trial | risk vs save |
| Wright et al. | 2013 | 25(10) | 24(NR) | 18 | choice between bets | mixed | money for a random trial | high vs low risk |
| Xue et al. | 2009 | 13(5) | 23.6(6) | 6 | Cups Task | mixed | arbitrary | risk parametric |
| Yu et al. | 2016 | 25(14) | 21(1.6) | 8 | BART – choice for risk | win | money | risk vs control parametric |
| Yu et al. | 2016 | 25(14) | 21(1.6) | 9 | BART – choice for risk | win | money | risk vs save |
| Zhang et al. | 2019 | 25(14) | 20.64(2.06) | 16 | choice between bet or save option | mixed | random trial | risk vs save |

*Note.* Some studies consist of multiple experiments and thus fill multiple rows. The contrast analyses are based on the columns "win/mixed domain", "incentive", and "contrast type". Peaks reported include positive and negative peaks. For information on the individual peaks, location and effect sizes, please refer to appendix table 1. Full citations for all studies can be found in section two of the references.

For correlation analyses including the sample size, the study by Haeusler and colleagues (2018) was excluded, as its sample is more than three standard deviations larger than the average. Correlations between the variables used for contrast analyses revealed small to medium correlations between the variables (incentive and domain: $r$ = .33; incentive and contrast condition: $r$ = .15; contrast condition and domain: $r$ = -.19). No significant correlations between the year of publication and any of the three variables were found (incentive: $r(37)$ = .16, $p$ = .32; domain: $r(35)$ = -.09, $p$ = .59; contrast condition: $r(40)$ = .05, $p$ = .78. Sample sizes of primary studies got significantly larger over time ($r(41)$ = .54, $p$ < .001).

### 2.4.3.2 Common neuronal activation patterns in risk-taking over all studies and conditions

Two experiments were excluded from the overall analysis as they reported on changes in risk-related activations when the save option was picked, and the respective studies both included an experiment on signals related to decisions for the risky option. The remaining 42 experiments report a total of 396 peaks.

The ALE analysis found 8 clusters of peaks. Peaks in ALE-values were located in the anterior cingulate cortex (ACC), left and right insula, bilaterally in the Caudate, in the right superior parietal lobule (SPL), the right midbrain extending to the right thalamus, and the right dlPFC. A detailed breakdown of all foci, their locations, and the associated anatomical regions can be found in appendix table 1. Figure 2 illustrates the findings superimposed on the MNI152-2009a standard brain (Fonov et al., 2011).

**Figure 2**

*Findings of the main meta-analysis*
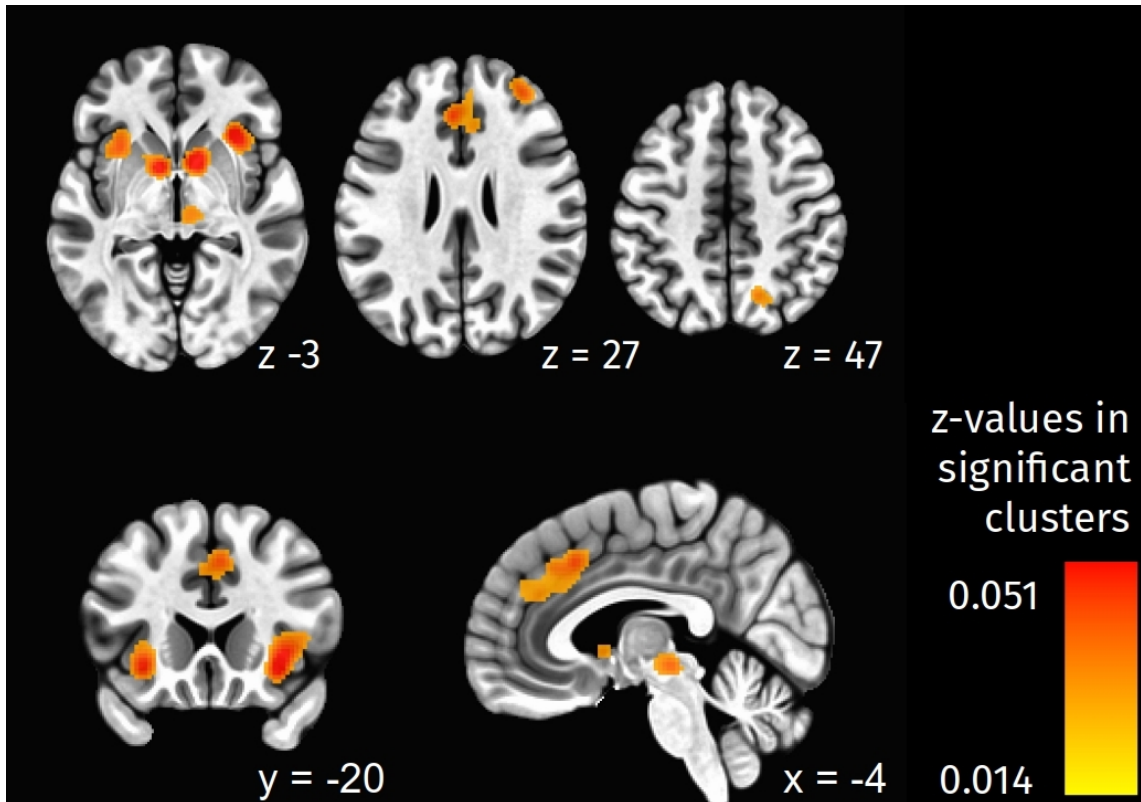


*Note.* Significant overlap of all positive foci identified in the primary studies, superimposed on MNI152-2009a brain (Fonov et al., 2011). All clusters identified are partially covered by the depicted slices. Left-right orientation follows psychological norm: participants' left is depicted left. Details on clusters can also be found in table 3.

2.4.3.3 Differences in brain activation during risk-taking in the win and mixed domain

Sixteen primary studies were identified, including 19 experiments investigating risk-taking only in the win domain. They reported a total of 148 positive peaks of BOLD-signal differences. No study examining risk-taking only in the loss domain was found. Nineteen studies containing 21 experiments investigated risk-taking in both the win and the loss domain. These studies identified a total

of 244 positive peaks. Some studies included experiments on both risk-taking in the win domain and risk-taking in the mixed domain. E.g. both studies by Bjork and colleagues (2007 & 2008) calculated a contrast for gambles in the win domain and a separate contrast for gambles allowing for losses. Therefore, different experiments from these studies appeared in different groups of the present contrast.

**Figure 3**

*Results of ALE contrast-analyses*
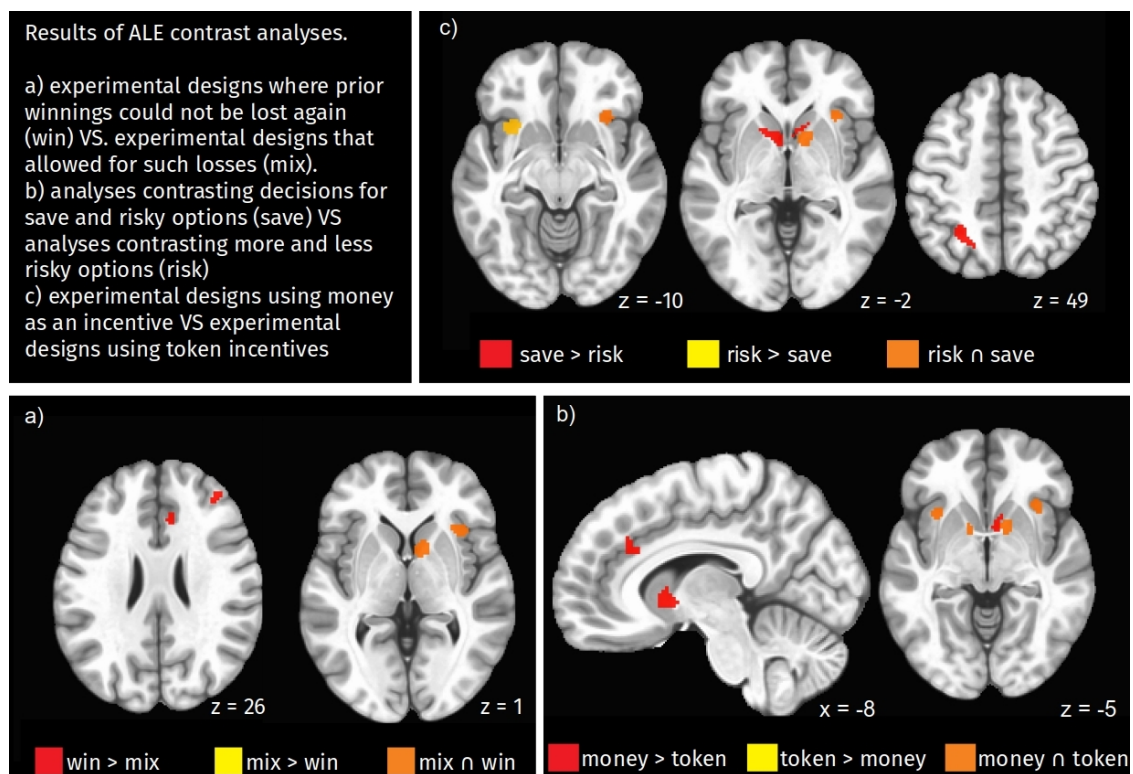


*Note.* Significant findings superimposed on MNI152-2009a brain (Fonov et al., 2011). Left-right orientation follows psychological norm: participants' left is depicted left. x and z denote slice numbers in the respective orientation. Details on clusters can be found in table 3.

Contrasting the two conditions revealed significant differences in the convergence of peaks over studies. No peaks exclusively found in studies in the mixed domain could be identified. Clusters of convergence exclusive for studies in the win domain were found in the right dorsal ACC and dlPFC. Details on the clusters can be found in table 3 and figure 3a.

A conjunction analysis revealed converging clusters of peaks in the right insula and caudate.

### 2.4.3.4 Differences in brain activation during risk-taking depending on the incentive

*Different types of Incentives*

Primary studies could be grouped into four groups based on their reward schemes. Some of the studies were based on a design where participants received a performance-based financial reward directly influenced by their behavior in the risk-taking task. These represent the majority of the financial-reward-based studies. In the study by Vermeer and colleagues (2014), the previously explained reward scheme was used, albeit with a maximum return defined beforehand that was known to the participants. If participants regularly reached this ceiling is not evident from the report. The study is grouped with the above-described financial reward schemes for the present analysis.

In five experiments, participants were instructed that they would be rewarded with real money but that one or several trials would be chosen randomly, and the payoff would be based only on those trials. For the present analysis, these experiments were excluded. While they could fit in the financial-reward group,

the difference is notable, and it is uncertain what effect these different instructions have on participants' perception of the task. Thus, excluding them allows for a decrease in heterogeneity and increased interpretability of the results.

Eight studies clearly stated that no incentives besides "points" or virtual money were given to the participants. These studies belong to the "non-financial" group. Five studies did not specify whether any form of financial reward was used or not. A financial reward is expected to increase ecological validity. Thus, authors are likely incentivized to report on using financial rewards explicitly. Therefore, studies not reporting on their reward scheme will be considered not to have rewarded participants' performance with money.

Of all experiments found in the primary studies, 22 used real financial incentives (248 peaks), while 13 used arbitrary or token incentives (109 peaks). The conjunction of both groups revealed shared clusters bilaterally in the caudate and insula region.

Significant differences were found as follows: Studies working with financial rewards found stronger convergence of peaks in the bilateral dACC and the right caudate. No stronger convergences were found for studies with arbitrary rewards. The results of both contrasts and conjunction can be found in figure 3b and table 3.

### 2.4.3.5 Differences in brain activation depending on the contrast condition

Five experiments could not be sorted in either category for this contrast and were thus excluded from the analysis. Kohno and colleagues (2015) and Fukunaga and colleagues (2012) investigated decisions for risky and save

options with separate contrasts. The analyses focusing on decisions against a risk were excluded from the analysis. Rao and colleagues (2008) used a contrast with a "passive risk-taking" condition that could not be assigned to either group. Schonberg and colleagues (2012) and Yu and colleagues (2016) compared a parametric correlate of risk-taking with a parametric control condition, straddling the line between the two categories defined for the meta-analysis and will thus be excluded.

Eighteen studies compared different levels of riskiness over 18 experiments, either with a simple contrast design (k=8) or a parametric design (k=10), containing a total of 129 peaks. 17 studies amounting to 19 experiments compared risk with either a save or similar non-risky decision (240 peaks).

The conjunction of primary studies from both groups showed shared clusters in the right caudate and insula. Contrasting the two conditions, unique clusters of peaks were found for both conditions. Experiments comparing risky and save decisions had stronger convergences of foci bilaterally in the caudate and the left superior parietal lobule. Experiments comparing more and less risky decisions showed a stronger convergence of foci in the left anterior insula. Contrasts and conjunctions are illustrated in figure 3c. Detailed data on the contrast can be found in table 3.

**Table 3**

*Size of clusters and location of their peaks determined through ALE-meta-analyses*

| cluster # | location of peak | MNI coordinates of peak | | | effect at peak | cluster size (mm$^3$) |
|---|---|---|---|---|---|---|
| | | X | Y | Z | | |
| All studies | | | | | | |
| 1 | dACC | 4 | -34 | 28 | ALE = 0.030 | 4288 |
| 2 | insula (R) | -32 | -24 | -6 | ALE = 0.052 | 3496 |
| 3 | caudate (R) | -10 | -8 | 0 | ALE = 0.049 | 2824 |
| 4 | insula (L) | 30 | -16 | -6 | ALE = 0.038 | 2480 |
| 5 | red nucleus | -6 | 22 | -6 | ALE = 0.030 | 2128 |
| 6 | caudate (L) | 10 | -6 | -2 | ALE = 0.039 | 1992 |
| 7 | dlPFC (R) | -36 | -46 | 26 | ALE = 0.031 | 1344 |
| 8 | superior parietal lobule (R) | -16 | 64 | 48 | ALE = 0.020 | 656 |
| win ∩ mix | | | | | | |
| 1 | caudate (R) | -10 | -10 | 0 | ALE = 0.024 | 1256 |
| 2 | insula (R)/orbital gyrus (R) | -32 | -24 | -4 | ALE = 0.019 | 1152 |
| win > mix | | | | | | |
| 1 | dlPFC (R) | -38 | -42 | 20 | z = 2.09 | 304 |
| 2 | dACC (R) | -12 | -28 | 28 | z = 2.42 | 272 |
| money ∩ arbitrary | | | | | | |
| 1 | Insula (R) | -32 | -22 | -8 | ALE = 0.019 | 872 |
| 2 | Insula (L) | 28 | -22 | -2 | ALE = 0.017 | 592 |
| 3 | caudate (R) | -14 | -10 | -6 | ALE = 0.019 | 456 |
| 4 | caudate (L) | 12 | -6 | -4 | ALE = 0.014 | 272 |

| cluster # | location of peak | MNI coordinates of peak | | | effect at peak | cluster size (mm³) |
|---|---|---|---|---|---|---|
| | | X | Y | Z | | |
| money > arbitrary | | | | | | |
| 1 | caudate (L) | -10 | -16 | 2 | z = 2.39 | 784 |
| 2 | dACC | -6 | -28 | 26 | z = 2.81 | 520 |
| contrast with risk ∩ contrast with save | | | | | | |
| 1 | insula (R) /orbital gyrus (R) | -32 | -22 | -8 | ALE = 0.021 | 720 |
| 2 | caudate (R) | -12 | -8 | -4 | ALE =0.020 | 632 |
| contrast with risk > contrast with save | | | | | | |
| 1 | insula (L) | 30 | -16 | -12 | z = 2.46 | 616 |
| contrast with save > contrast with risk | | | | | | |
| 1 | caudate (L) | 8 | -12 | -6 | z = 2.60 | 848 |
| 2 | caudate (R) | -12 | -16 | 4 | z = 2.52 | 680 |
| 3 | superior parietal lobule (L) | 18 | 66 | 48 | z = 2.64 | 648 |

*Note.* Contrasts not resulting in significant findings are omitted from the table. Coordinates are in RAI format. Effect sizes for contrasts are given as Z-Values. Effect sizes for conjunctions are given as ALE-values. (L) and (R) denote the hemisphere where the peak effect size of a cluster was located.

## 2.4.4 Discussion

A peak activation coordinate-based meta-analysis was calculated to identify brain regions commonly found in fMRI studies investigating neural correlates of risk-taking. The primary analysis, focusing on commonalities between studies, demonstrated convergent activity in a network spanning the prefrontal, parietal, insular, and cingulate cortex and parts of the striatum and brainstem. The contrast analyses on specific features of the primary studies found multiple moderating effects.

*Convergence of findings in the insular cortex*

A significant convergence of foci was identified bilaterally in the insula, similar to findings from comparable meta-analyses (Mohr et al., 2010; Wu et al., 2021). While the cluster extends into the orbitofrontal regions, its peak is in the anterior insula.

Involvement of the insular cortex has been described in various processes: from the processing of interoceptive sensory information (Afif et al., 2010) to complex cognitive tasks like intentional action and consciousness (Gasquoine, 2014). The findings largely overlap with the anterior-dorsal part of the insula, as described by Kurth and colleagues (2010), which is likely involved in the functional integration of information from the rest of the insula (Kurth et al., 2010; Uddin et al., 2017).

The insula is described in the context of affect and reward processing (Eickhoff et al., 2016), with its role in decision making backed by lesion studies: Patients with lesions affecting the insula show less gamblers fallacy and are less motivated by so-called "near misses" (Clark et al., 2014). Furthermore, von

Siebenthal and colleagues (2016) found that patients with a perculo-insular resection were insensitive to the expected value in the loss domain in both the IGT and the Cups Task (Levin & Hart, 2003).

Insula function is likely lateralized (Kurth et al., 2010). Comparing decisions under risk and ambiguity, the left insula seems more strongly related to ambiguity and the right to risk (Wu et al., 2021). The left and right insula have previously been discussed in relation to parasympathetic and sympathetic activity, respectively (Strigo & Craig, 2016). In the present study, analyses comparing different levels of risk led to a significantly higher convergence of foci in the left anterior insula than analyses relating risky and save options. A similar pattern has been described when comparing parametric and contrast approaches to the study of risk-taking (Wu et al., 2021). While the current data is still inconclusive, it seems plausible that a positive affective component in choosing a riskier option might be reflected by stronger involvement of the left insula compared to when a save option is chosen or under ambiguity.

*Convergence of findings in the thalamus*

While some primary studies reported activity in various parts of the thalamus correlated with risk-taking (e.g., Bjork et al., 2007; Macoveanu et al., 2016; Meder et al., 2016), no convergence of primary studies was found in it in the present meta-analysis. However, a cluster found in the midbrain in the present analysis extends into the most ventral parts of the thalamus. The peak and most of its extent (66.2%) are located close to the thalamic nuclei, yet outside of it.

The thalamus has come to be understood not as a relay nucleus but as a mediator of cortico-cortical communication, interacting with multiple functional networks and integrating and gating information flows between them (cf. Sherman, 2016; Hwang et al., 2017). Furthermore, it is engaged in many different cognitive functions (Hwang et al., 2017) and thus a prime candidate to be involved in a complex tasks such as risk processing and -taking. The present results do, however, not support the previous model by Mohr and colleagues (2010), where the posterior and dorso-medial Thalamus act as a core component in human risk-processing.

Instead, the activation reported by primary studies in various parts of the thalamus seems most likely to be a byproduct of the specificities of the experimental designs rather than a component of the risk-processing network itself. Poudel and colleagues (2020) report on convergent activity in the red nucleus, right below the thalamus and partly overlapping with present findings, but do not further discuss it.

Additional analyses could reveal if any specific features of task designs or analysis procedures reliably lead to the recruitment of thalamic nuclei. Such an analysis might also disentangle why Mohr and colleagues (2010) found a convergence of foci that could not be found in the present analysis.

*Convergence of findings in the right dlPFC*

A convergence of peaks from all primary studies was found in the right dlPFC). This area has previously been repeatedly described in the context of risk-processing (Schonberg et al., 2011). Mohr and colleagues (2010) found it to be active only when actual risks are taken by participants and not when risky

situations are perceived. As the current analysis only focused on studies of the former type, no such distinction will be made here.

The dlPFC has been previously associated with domain-general executive control and conflict management (Oehrn et al., 2014), a role it likely fulfills in a network with the dACC (Smith et al., 2009). Hertrich and colleagues (2021) report that the dlPFC is involved in decisions if task inhibition, task switching, or engagement in memory systems can be observed. The dlPFC is involved in the dynamic updating of executive control processes and the adaption to changing environments (ibid.), fitting well with the observation that the dlPFC is more consistently found in designs on ambiguity than risk (Wu et al., 2021).

Executive control functions in the dlPFC are lateralized (Seikel et al., 2018; Ngetich et al., 2020). The right dlPFC is related to nonverbal working memory (Baddeley, 2003) and error awareness (Harty et al., 2014). Several primary studies introduced experimental designs where probabilities were not known to the participants but had to be estimated and learned during the task and thus could have caused an involvement of the dlPFC. The learning component inherent to many risk-taking designs has been pointed out before (Schonberg et al., 2011). It might lead to systematic biases in studies on risk preference when comparing different groups of participants (Mata et al., 2011).

In studies where no prior earnings could be lost, the convergence of findings from primary studies in the right dlPFC was stronger. Gowin and colleagues (2013) draw a link between dlPFC activity and the deliberation between risk and rewards that seemingly contradicts the current finding. As dlPFC activation has been discussed in subjective utility calculation (Fiore & Gu, 2019), it seems plausible that systematic differences between the groups of

primary studies introduced stronger recruitment of the dlPFC. The BART, for example, is one of the designs commonly used only in the win domain (cf. Schmitz et al., 2016). It furthermore contains a learning component that also might lead to dlPFC involvement.

If dlPFC involvement reflects a learning component, the following line of argumentation should hold: In more ambiguous situations, where behavior needs to be dynamically updated based on the environment and errors have to be observed, right dlPFC involvement should be observable. Such is the case for risk-taking designs that do not offer explicit information on probabilities, such as the BART. If this holds, lower dlPFC activation should be measured in risk-taking designs with explicit information on probabilities. It could thus be investigated in a further subgroup meta-analysis, comparing studies with ambiguity in their tasks to those that had no ambiguity. However, as the dlPFC is part of several different networks (cf. Ferbinteanu et al., 2019; Panikratova et al., 2020; Xiong & Newman, 2021), this is unlikely to form an exhaustive theory of dlPFC involvement in decision making.

*Convergence of findings in the parietal lobe*

A significant overlap of peak activations was found in the right SPL, mostly in Brodmann area 7, peaking in a7c in the Brainnetome Atlas nomenclature (Fan et al., 2016). In contrast analyses, the left SPL was found more consistently in studies contrasting decisions for risky and save options. In the same analysis, a convergence was observed in the bilateral caudate, a region functionally linked to parts of the dACC and SPL (Robinson et al., 2012).

Findings of prior meta-analyses do not agree on the parietal cortex (Mohr et al., 2010; Poudel et al. 2020; Wu et al. 2021). Activation of the medial SPL has been linked to sensory processing through functional decoding. This link might explain why it is more reliably found in perceptual decision-making compared to decision-making under risk or ambiguity (Poudel et al., 2020). However, results seem inconclusive, as do interpretations of parietal findings in primary studies (cf. Symmonds et al., 2011; Losecaat et al., 2014; Zhang et al., 2019).

The parietal cortex is part of the resting state network (RSN). Gilmore and colleagues (2021) found that differences between participants in the topography of the RSN might hide commonalities in activations if standard group analysis techniques are used for the analysis of fMRI data. For example, nine different subnetworks of the RSN were found that were only discernible in single subjects and did not show up in group analyses, as their exact location differed between participants (Gordon et al., 2020). Individual differences in parietal network architecture might be one reason for inconclusive findings in the literature. Especially comparisons in single subject activation patterns akin to the single subject RSN studies by Gordon and colleagues (2020) might explain some differences between current studies.

*Convergence of findings in the dACC and dmPFC*

The primary meta-analysis found a bilateral cluster spanning the dmPFC and the dACC. dACC and dmPFC activation are often co-occurring (Kolling & O'Reilly, 2018), and activation in a similar cluster has been found in another meta-analysis on the topic (Mohr et al., 2010). Furthermore, the regions have

been discussed as involved in decision and strategy control, thus likely playing a role in the cognitive processing of risk stimuli (Venkatrama et al., 2009).

Based on more recent theories, the dACC and dmPFC-region is concerned with evaluating the entire situation an organism is currently experiencing. It uses information on the situation to trigger a change of context, if necessary (Kolling & O'Reilly, 2018). dACC activation can, for example, result in seeking new options in foraging designs (Kolling et al., 2012) or abandoning an old strategy in favor of searching for a new one (Karlsson et al., 2012).

Activation of the dACC was observed in monkeys that acted self-initialized (Shima et al., 2007). In humans, Kolling and colleagues (2016) postulate that during learning, the dACC encodes the degree to which a model of the current environment must be updated. When faced with a decision, the dACC encodes the average value of exploring alternative behaviors (ibid.). More general, differences in activations in the dACC serve behavioral adaptation to the task – an interpretation substantiated by computational models (Holroyd et al., 2021), finding dACC activation related to actuation of the implementation of higher-level strategies.

Involvement of dACC and dmPFC was stronger when financial compared to token incentives were used in the experimental design. Executive control has been described as a limited resource requiring participants' effort to be employed (Kurzban et al., 2013), a process probably implemented through dACC activation (Shenhav et al., 2013). Participants likely felt higher motivation when faced with financial rather than token incentives, leading to more substantial employment of executive control functions for the task.

A further region directly linked to the tasks of the dACC is the dlPFC. It has been described to implement behavioral adaptations initiated by the dACC (Voloh et al., 2015). In studies where accumulated gains could be lost again, the convergence of foci was stronger in the dlPFC and dACC/dmPFC simultaneously. Comparable to the dlPFC activation described above, this could be an artifact of systematic differences between studies allowing losses and those that do not.

*Convergence of findings in the striatum*

The primary meta-analysis revealed two clusters spanning multiple regions of the ventral and dorsal striatum, focused on the head of the caudate but including parts of the nucleus accumbens (NAc). The clusters are located symmetrically in both the left and right hemispheres. In both hemispheres, their majority (left hemisphere 44%, right hemisphere 38%) and their peaks are located in the head of the caudate. As the Gaussian distribution used in the ALE analysis is not constrained by neural anatomy, peaks from separate regions close to each other can blur together, as was likely the case in the present cluster. Peaks reported in primary studies are partly located in the head of the caudate and partly spread over neighboring regions. A meta-analysis based on the full results of primary studies and not limited to peaks could yield more detailed results on the exact localization of activation.

The ventral caudate is known to be involved in reward processing (Liu et al., 2010) and was observed in action selection, the initiation in decision making (Balleine et al., 2007), and reward valuation (Lau & Gilmcher, 2008). It was more reliably found in studies comparing risky and save decisions compared to studies comparing levels of risk in the present meta-analysis. Based on prior

studies and the present findings, the ventral caudate seems more likely to be a general component of decision-making and valuation, not necessarily involved in evaluating risk specifically.

In previous findings, lateralization of activation in the striatum can be observed. The left caudate seems more directly linked to risky decision-making than other types of decisions (Poudel et al., 2020) and is more reliably found if financial incentives are part of the design. Arsalidou and colleagues (2020) describe lateralization in basal ganglia depending on the type of reward and find activation for financial incentives in both hemispheres in the caudate. It thus seems likely that differences in reward might be at least partially responsible for the lateralization of brain activations.

### 2.4.4.1 Correlations between contrast variables and experimental designs over time

Correlations between the variables used for contrast analyses vary between small and medium effects, with the strongest correlation having a coefficient of $r = .33$. Accordingly, results in one contrast are likely to be slightly influenced by the effects from other contrasts. However, to the best of the authors knowledge, no tested approaches for more complex statistical models such as multiple regression or ANOVAs exist for ALE analyses. As the intercorrelations are not excessive in size, they have to be noted as a possible source of limited systematic noise in the present analysis but will not be discussed further.

During the years of publication of the primary data, fMRI measurement and analysis techniques have steadily improved, as argued above. Any notable correlations between the variables used in contrast analyses and the year of publication would therefore hint at a possible distortion, when newer, more

reliable studies all belong to one group while older, less reliable studies make up the other group. Correlations between the contrast variables and publication year were all small ($r < .16$) and non-significant. Thus, descriptively, no major effect of advancements in methods on the contrast analyses is to be expected.

### 2.4.4.2 Limitations of the present approach

Several limitations of the present study have to be considered. As a meta-analysis, it is influenced by all potential limitations of primary studies: experimental designs (Schonberg et al., 2011), imaging parameters and procedures (Feinberg & Setsompop, 2013), data processing and analysis (e.g., Eklund et al., 2016; Cox et al., 2017) and recommended minimal sample sizes (Poldrack et al., 2017) went through notable changes between the first and last study included in the meta-analysis. While the ALE approach accounts for differences in sample size, other parameters cannot be taken into account without major changes to the procedure and are still likely to affect the result.

The ALE algorithm simplifies the data by only integrating peaks of significant activation and ignoring cluster forms or non-significant data. Accordingly, ALE-analyses do not have the capacity of traditional meta-analyses to detect smaller effects that were not measurable in primary studies. While ALE analyses allow to include most of the published literature, future meta-analyses based on the actual contrast volumes of previous studies could allow far more detailed analyses and might detect previously unobservable small differences in BOLD signal.

While the strict criteria for study inclusion keep the heterogeneity of the present analysis comparatively low, heterogeneity is still present and

noteworthy - studies used different experimental designs and took place in different countries and laboratories using different equipment. A bias, while partly addressed through contrast analyses, cannot be excluded and is likely to exist to some extent. Furthermore, the strict criteria led to a smaller sample size than other meta-analyses on the topic (Poudel et al., 2020; Wu et al., 2021).

A notable source of heterogeneity is differences between experimental designs that require learning of probabilities (e.g., the BART) and those that do not (e.g., the choice between bets). As noted by Wu and colleagues (2021), learning processes are likely to occur in the earlier stages of the task. Participants did not learn the probabilities yet in that phase, and decision-making can be assumed to happen under ambiguity. After learning, decision-making could be assumed to happen under risk in the later stages. Risk-taking and learning are intertwined and can not easily be separated in the analysis. In the contrast analyses conducted in this meta-analysis, designs requiring learning were not evenly spread over conditions and could therefore introduce systematic bias (cf. table 2).

For some studies, assumptions had to be made about characteristics of the primary studies as reported data was incomplete or other necessary information was missing. This holds particularly for missing indications of the direction of the reported effects, most prevalent in older studies. The direction of effects can sometimes be inferred from how contrasts are communicated, but it is often unclear if tests were conducted two-sided. Furthermore, some primary sources were missing information on the reference space. In such cases, it was assumed that the standard reference space of the reported

analysis software was used. Last, as mentioned above, not all primary studies communicated if financial- or token incentives were used.

### 2.4.4.3 Reccomendations for future studies

Based on the contrast analyses, recommendations for future studies on the neural correlates of risk-taking can be made. Whether performance in the task is incentivized with money or abstract tokens is associated with different neural activation patterns, with the caudate and dACC being more reliably reported in studies using money as an incentive. This finding seems to be related to higher engagement of the respective human subjects. Using arbitrary points leads to no additional convergence in findings. In combination with general differences in neural networks based on differences in incentives (Arsalidou et al., 2020) and the ongoing discussion of domain-specificity of risk-taking, this also calls for future studies on the effects of different incentives on human risk-taking.

The exact contrast chosen for the analysis of risky decision-making has a notable influence on the findings. Wu and colleagues (2021) describe a difference in findings when using parametric or categorical approaches to fMRI analysis. The present study adds to this by finding differences depending on the condition that risk-taking is compared to, i.e., lower-risk or save. Using a save condition as contrast leads to a more extensive network, including left caudate and left superior parietal lobule. Contrasting with lower-risk leads to a stronger convergence of findings in the left Insula.

### 2.4.4.4 Summary and perspectives for the present thesis

This meta-analysis investigated commonalities in findings of previous studies on human risk-taking as measured through fMRI. A network of regions was

found involving multiple regions previously linked to decision-making and risk. Based on these findings, the following neuronal processes occurring during risky decision-making can be deduced: At the cognitively higher levels, the currently employed strategy is continuously monitored and adapted through the dACC (Kolling et al., 2016; Kolling & O'Reilly, 2018). Changes in strategy instigated by the dACC are implemented through dlPFC activation (Voloh et al., 2015) as part of the executive control network (Smith et al., 2009; Shenhav et al., 2013). Insula activation is likely linked to an affective or heuristic component in processing, as substantiated by lesion studies (Clark et al., 2014; von Siebenthal et al., 2017). Insula activation is lateralized, with the exact implications of the lateralization remaining unclear (cf. Wu et al., 2021). Another open question is the lateralization of caudate activation observable in several contrasts (cf. Poudel et al., 2020) and possibly linked to differences in reward processing (Arsalidou et al., 2020). The role of the superior parietal lobule and Brodmann area 7 (BA7) is the least clear. Inconsistent findings in that region might be based on interindividual differences in functional localization (Gordon et al., 2020; Gilmore et al., 2021). Future research on individual differences in risk-taking, in general, could help to illuminate correlates of pathological risk-taking and might also identify neural correlates of non-pathological elevated risk-taking propensity.

The present findings might help to understand differences in findings of previous studies related to heterogeneous and partly incomparable experimental study designs. Furthermore, they allow for more precise design suggestions for future studies on human risk-taking.

This concludes the meta-analysis. In the following paragraphs of the introduction, one last set of studies relevant for the experimental design of this thesis will be discussed.

## 2.5 Risk-Taking for Oneself and Others

Some inference about different incentives can be made from the research comparing risk-taking for oneself with risk-taking for others. Studies on the topic were conducted on the behavioral level (e.g., Stone et al., 2002; Stone et al., 2013) and on neural correlates of both conditions (Ogawa et al., 2018; Zhang et al., 2019). Ogawa and colleagues (2018) let participants take risks for themselves or an anonymous other. They conducted fMRI-based region of interest (ROI) analyses of the right temporoparietal junction (TPJ), medial orbitofrontal cortex (mOFC), and ventral striatum. The authors report that participants adopted a more risk-neutral approach when deciding for others.

Research on differences in risk-taking for oneself and others developed partially from the research on differences between outside advice and inside perspective (Kray & Gonzalez, 1999; Stone et al., 2002). Accordingly, it assumes that both parties are in a similar situation and have similar preferences (Zhang et al., 2019: "Participants were told that the other person was randomly selected from among the participants of another experiment", p. 3). Furthermore, current fMRI studies on the topic communicate the reward as being the same in both conditions, with just the recipient differing (Ogawa et al., 2018; Zhang et al., 2019).

## 2.6 Experimental Approach of the Present Study

This study investigates differences in the neural correlates of human risk-taking dependent on the incentive domain. To that end, the BART was adapted for use in fMRI and different incentive domains, namely financial and social domains. Financial rewards were paid out after the measurement. In the social incentive condition, participants were instructed that their performance influences how many gift bags would be handed out to children at a later date and received a certificate on the number of gift bags after the measurement.

Unlike studies on risk-taking for oneself and others, this study undertook an effort to maximize the difference between the different reward types. Several steps were taken to make social rewards more distinct: The reward was not communicated through numbers but through simplistic smiley faces whose degree of smiling corresponded to the height of the reward. Furthermore, the recipients were no young adults in a similar situation as the participants, but pre-school children.

fMRI measurements were conducted to compare neural activation patterns during risk-taking in both conditions. First, a general linear model approach was used to contrast parametric regressors of active and passive risk-taking within each incentive condition (financial and social). In a second step, differences and similarities of the within-condition contrasts were analyzed to compare neural activation patterns between the two incentives.

## 2.7 Research Questions and Hypotheses

Human risk-taking behavior seems to be, at least partially, domain-specific (Mishra et al., 2014; Sevi & Shook, 2021). Moreover, research on reward anticipation found dissociable neural networks for different incentives (Rademacher et al., 2010; Flores et al., 2015, Gu et al., 2019). Therefore, the neural network responsible for active risk-taking is hypothesized to encompass different brain regions, depending on the incentive at stake. However, a general risk-taking factor influencing behavior across different domains is broadly discussed in the literature (Mishra et al., 2014, Mata et al., 2018, Nicolaou & Shane, 2019), and studies on reward anticipation found considerable overlap in neural activation patterns independent of the type of reward (Gu et al., 2019). Integrating this information and the fact that many processes might be necessary components of risk-taking across domains (e.g., value estimation, strategy formation, and selection), an overlap in the neural network is expected to be active independent of the incentive domain.

No prior fMRI studies on risk-taking comparing different incentive conditions are known to the author. Accordingly, the present study has to be understood as exploratory. All studies analyzed in the above meta-analysis used financial or arbitrary incentives. Any inference from these studies on possible findings in risk-taking with social incentives are possibly incomplete. However, preliminary assumptions on the neuronal basis of incentive-dependence in risk-taking can be made based on the meta-analysis described above and other prior literature.

The network of brain regions associated with risk-taking in prior research contains components unlikely to be directly related to the incentive (cf. Poudel

et al. 2020; Wu et al., 2021). Activation in the dACC and dlPFC has been associated with strategy adaption and implementation of such adaptions, respectively (Voloh et al., 2015; Kolling et al., 2016; Kolling & O'Reilly, 2018). In addition, both regions are connected to various tasks involving cognitive control as part of the executive control network (Shenhav et al., 2013; Smith et al., 2019). While the dACC was observed to be more strongly involved if financial instead of arbitrary incentives were used in the above meta-analysis, this likely reflects increased engagement in the task (Kurzban et al., 2013; Shenhav et al., 2013).

Differences in the neural correlates of risk-taking based on the incentive are more likely found in the insular cortex or the striatum based on the previous literature. Both regions are associated with risk-taking (cf. meta-analysis; Poudel et al., 2020; Wu et al., 2021), and their involvement in reward consumption has been shown to depend on the type of reward offered (Arsalidou et al., 2020). Due to the findings on risk-taking in the parietal lobule being heterogeneous in the prior literature, no assumptions on a possible reward dependency can be made here.

Findings on active risk-taking contrasted with passive risk-taking are hypothesized to resemble the network identified in the meta-analysis. Right dlPFC, bilateral dACC, dmPFC, insula and striatum, and right SPL showed convergent activation in prior studies on risk-taking and were likely to be found in the contrast of active and passive risk-taking with financial incentives in this study. Rao and colleagues (2008) calculated a similar contrast to the present study and found differences in bilateral dlPFC, striatum, insula, and dACC.

On a behavioral level, response-time differences between incentives were analyzed (e.g., Zhang et al., 2019). From prior literature, it is unclear if or how these are affected by differences in incentives. Zhang and colleagues (2019) found no significant difference in response time between participants taking a risk for themselves or others which serves as a first reference point. However, due to the difference in focus between the work by Zhang and colleagues and this study, as well as the higher sample size acquired here, differences in findings are possible but no detailed hypotheses on the direction can be made.

Risk-taking propensity probably changes depending on the incentive. Results based on the DOSPERT (Blais & Weber, 2006) indicate substantial variation in risk-taking propensity between participants and domains (Blais & Weber, 2006). Furthermore, risk-taking behavior is known to change in the presence of peers (Haddad et al., 2014) and if decisions are made for other people (Zhang et al., 2019). Effects from peers and risk-taking for others are only loosely related to the present study and the effects depend on additional design variables, such as whether risk-taking happens in the win- or loss- domain and the variance of outcomes (Haddad et al., 2014; Zhang et al., 2019; Sun et al., 2020). As such, risk-taking propensity was hypothesized to differ between incentives, but based on the limited prior literature, no clear hypotheses can be made on the size or direction of the effect.

## 2.8 Addendum: The SARS-COV-2 Pandemic

This study was conducted partly during the SARS-COV-2 pandemic. A total of 20 participants were measured before data collection was stopped due to the pandemic in March 2020. Measurements could be resumed in June 2020 under

a strict hygiene protocol and at a slower pace. Data from 20 further participants were measured to balance the final sample with equal numbers of participants from before and during the pandemic. As detailed below, participants' behavior might have been affected by the pandemic.

*Self-selection bias*

Both during previous pandemics, such as the H1N1 pandemic in 2009, and during the ongoing SARS-COV-2 pandemic, a link between risk perception and adaption in behavior was found (Bish & Mitchie, 2010; Wise et al., 2020, respectively). The higher a person judges their risk of infection or its adverse health effects, the more they commit to protective behavior, such as hand washing or social distancing (Bish & Mitchie, 2010; Wise et al., 2020). In this study, such changes in behavior could lead to a selection bias, with fewer risk-averse or less risk-perceptive individuals participating during the pandemic compared to before its start.

*Changes in risk-taking propensity*

During the first months of the pandemic, negative economic influences were perceivable in the German population: Hövermann and Kohlrausch (2020) analyzed a data set compiled in June 2020, in the same time frame as the second wave of fMRI measurements for the present work was conducted. They found less than 20% of the participants reporting that they were not likely to be financially affected by the pandemic in a negative way. It was shown that financial losses decrease people's willingness to take financial risks, both in experts in a short-term experimental setting (Cohn et al., 2015) and in the general population over larger timescales (Malmendier & Nagel, 2011).

Worldwide, governments tried to combat the pandemic by mandating lockdowns of varying intensity, prohibiting gatherings, limiting the number of people allowed to meet, and other social distancing measures (Solomou & Constantinidou, 2020). These measures likely had at least a short-term detrimental effect on the mental health of the affected populations (Solomou & Constantinidou, 2020; Williams et al., 2020). Evidence indicates that health shocks, such as severe diseases or accidents, can decrease self-reported risk-taking propensity (Decker & Schmitz, 2016). This influence is likely not mediated through a decrease in financial resources following a health shock (ibid.).

In summary, individuals experiencing adverse health events, either directly through SARS-CoV-2 or indirectly through the detrimental health effects of the measures taken to combat the pandemic, might have a decreased risk-taking propensity. The same goes for participants that are financially burdened by the pandemic. Thus, further analyses were conducted to explore possible distortions in the data that the pandemic may have induced.

*Effects on neuronal activation patterns and BOLD-signal*

The two factors detailed above, self-selection bias and crisis-related changes in risk-taking propensity, might also impact the neuronal correlates of risk-taking measured via fMRI. Furthermore, participants measured during the pandemic wore a surgical mask in the fMRI scanner, possibly influencing blood-oxygenation levels.

Law and colleagues (2021) investigated the effects of surgical mask wearing on resting-state and task-based BOLD signals in eight participants. They used two

ways to manipulate fresh air available to participants: by directly comparing mask-on and mask-off conditions and by supplying fresh air underneath the mask through a nasal cannula. The experimental manipulation results in a substantial decrease in gray matter BOLD-signal baseline (30%) when wearing a mask, but only minimal effects on task-based activation. In a sensory-motor task, 2.5% of task activation was related to fresh air supply through the nasal cannula (ibid.).

Scholkmann and colleagues (2021) critically comment on the work by Law and colleagues (2021). They base their argument on Chan and colleagues (2020) not finding any significant effect of mask-wearing on arterial oxygenation and suggest some improvements to the experimental protocol. Scholkmann and colleagues (2021) expect an even lower true effect of mask-wearing on blood oxygenation.

In an EEG study, Tamimi and colleagues (2022) found no effects of surgical mask wearing on blood gas, oxygen saturation, or EEG data. Fisher and colleagues (2021), using fNIRS, find results between those by Tamimi and colleagues (2022) and Law and colleagues (2021): wearing a surgical mask leads to small but significant changes in cerebral hemodynamics in their sample of 13 healthy adults.

Due to the inconclusive results of the prior literature, task-based BOLD-signal correlates of participants before and during the pandemic were compared. On the one hand, the present study can add to the literature on the topic by possibly clarifying if any measurable effects persist in studies that do not explicitly focus on the effects of mask-wearing. Whether a mask is worn in the fMRI scanner during a pandemic is a weighing between participants' safety and

epistemological interest for high data quality. If the effects of mask-wearing on BOLD signals are negligible, the ethical consideration should favor participant safety. On the other hand, any significant effects between groups would restrict generalization over all 40 participants and have to be considered for the principal analysis.

# CHAPTER 3: RESEARCH METHODS

## 3.1 Participants

A sample of 30 participants was aimed for in the present study, meeting the previously recommended sample size to obtain reliable and replicable results (Murphy & Garavan, 2004) and exceeding it in the light of more recent literature on the topic (Poldrack et al., 2017). Due to the SARS-CoV-2 pandemic, measurements were halted after data from 20 participants was collected. Data collection could only resume after 3.5 months. Immediately after measurements had to be stopped, a decision was made to increase the sample size to 40 participants. The increase resulted in an equal number of participants before and during the pandemic. The data from one participant from the time after the onset of the pandemic had to be excluded for technical reasons, leaving the final sample size at 39 (28 female), with 20 participating before and 19 during the pandemic (16 and 12 female, respectively).

Participants were recruited through mailing lists, mainly from the University of Bremen student body. Participants received the money they accumulated during the trials with financial incentives and a certificate stating the amount of gift bags they won after the measurement. In addition, students of psychology received course credit for participating.

Older adults were excluded as they behave differently from younger adults in risk-taking designs (Best & Charness, 2015). Furthermore, neural activity patterns elicited by risk-taking vary during the adult human lifespan (Yu et al., 2016). Accordingly, recruitment was limited to participants between 18 and 35

years of age for the present study. The average age in the final sample is 23.9 years (*sd* = 3.8), with the youngest participant being 19 and the oldest 33 years old.

## 3.2 Task and Procedure

For the present thesis, a classic risk-taking design - the Balloon Analogue Risk Task (BART, Lejuez et al., 2002) - has been adapted in several ways. In the first section of this chapter, the design is explained and the reasons for its selection are detailed. Following, adaptions of the task to both the research question and the prerequisites of fMRI measurements are detailed.

A behavioral pilot study was conducted to investigate whether these design decisions had the desired effect. Details on this study can be found in the second section of this chapter. The results of the pilot study and its influence on the main study are laid out in the third section. The chapter continues with a section on the secondary measures taken during the study and the detailed fMRI scanning parameters. It ends with a summary of the measurement process as participants experienced it.

### 3.2.1 THE TASK

The word "Trial" is ambiguous in the BART. In the following, it is used to denote a full balloon, usually comprising several decisions to inflate and the outcome: a payout or the explosion of the balloon. The period from one decision phase to the next – presentation of the balloon, decision, inter-trial interval (ITI), feedback, inflation animation – will be referred to as one inflation.

*Incentives*

In the present work, changes to the classic design were made in order to directly compare the influence of social and financial incentives on risk-taking. Participants were instructed to imagine themselves having a balloon inflation machine and being at a funfair. Furthermore, they should imagine being approached by both adults and children. In the setting, adults pay for balloons with money (financial incentive condition), while children get them without paying (social incentive condition).

All trials had the same overall sequence of events. The only difference was in the presentation of the current reward for a balloon and the final reward. In financially incentivized trials, the exact amount accumulated was shown in a yellow circle. If a balloon exploded, 0.00€ was displayed in the same way. In the socially incentivized trials, feedback on the current reward was given through a smiley that smiled more strongly the larger the balloon was, with the corners of its mouth rising with each inflation. If a balloon exploded in the social incentive condition, a neutral smiley with a flat line as its mouth was shown. Participants were informed before the measurement that gift bags containing buttons, stickers, balloons, small gadgets, and other toys appropriate for children would be handed out to real children later. The amount of gift bags was dependent on the degree of smiling of the smileys in the socially incentivized condition. Participants were also informed that, together with the money from the financial condition, they would receive a certificate stating the amount of gift bags they won in the social condition. One gift bag in the social condition was equivalent to one euro in the financial condition.

*The BART and fMRI*

Measuring neural correlates via fMRI usually requires some adaptions to the tasks: Breaks must be introduced between different tasks to allow for adequate measurement of the hemodynamic response function (cf. Brigadoi et al., 2018). Furthermore, multiple repetitions of the same event can increase the signal-to-noise ratio (Chen et al., 2022). Previous studies employing the BART in an fMRI setting arrived at a suitable number of events by reducing the maximal capacity of the balloons from the original 100 inflations (with an average capacity of 50 inflations) to a maximum of 8-12 with an average number of 4-5 inflations (numbers vary between studies, compare e.g. Lei et al., 2017; Rao et al., 2018). Fewer inflations result in less time required for each balloon. As a result, participants can inflate more balloons in a reasonable time frame, increasing the number of events in each condition and thereby increasing the signal-to-noise ratio. In the present study, balloons can be inflated 4.5 times on average, with a maximum of 8 and a minimum of 1 before the balloon explodes.

Previous studies using the BART in an fMRI context use a variety of contrast conditions (e.g. Rao et al., 2008; Hulvershorn et al., 2015; Kohno et al., 2015). The present study uses a "passive-viewing" condition where participants see the same stimuli as in the active condition but have no influence on whether the balloons are inflated or not. Instead, the decision is made automatically for them. A similar condition was previously used in other fMRI studies of risk-taking in the BART (Rao et al., 2008; Lei et al., 2017; Rao et al., 2018)

While inflating a balloon in the BART, phases of risky decision making (when deciding to inflate the balloon or not) are interwoven with phases of reward

consumption (when the current accumulated winnings are depicted). Differences in reward consumption might therefore carry over to brain activation measurements during the decision phases. Previous research has shown that neural activation patterns are sensitive to differences in the types of rewards consumed (e.g., Rademacher et al., 2010; Flores et al., 2015) and anticipated (Nummsen et al., 2021). By using a passive-viewing condition with real incentives, rewards are consumed in both conditions. Any effect purely based on reward consumption should therefore exist in the passive and active condition and thus not turn up in the contrast.

In the classic BART-Design, balloons grow by the same amount with each inflation. Accordingly, participants can decide on their behavior for the subsequent inflation as soon as they see the feedback on the previous one. Thus, an outside observer cannot differentiate between the feedback and the decision phase. The present work decouples decision- and feedback phases in the following way: Participants are instructed that balloons grow by different amounts with each inflation. The new balloon size is shown only after the feedback that the balloon did not explode. The size increases by 1 to 3 steps, with the increase being fixed a priori in a pseudo-randomized order. An abbreviated example trial can be found in figure 4.

*Trial structure*

Before each trial, participants are given information on whether a balloon was part of the passive or active condition through the words "Aktiv" and "Passiv" (active and passive in German). Whether a balloon was active or passive is also indicated through its color. Yellow and blue were assigned to active and passive balloons balanced over participants. Furthermore, it was indicated

what type of incentive was used in the current trial through a stylized picture of either an adult or a child. Both information were shown for 1.5 seconds.

A sequential presentation of information similar to the one described by Schonberg and colleagues (2012) was chosen for the current study to reduce visual cluttering and control the exact point in time when participants acquire information. First, participants were shown the balloon until they communicated via button presses whether they wanted to inflate it or not. Then, a fixation cross was shown for 500±200 ms before the currently accumulated reward was presented. Afterward, an animation of the balloon inflating to its new size (taking 500ms) was displayed before participants could decide again.

**Figure 4**

*Abbreviated example of a trial with financial incentive*
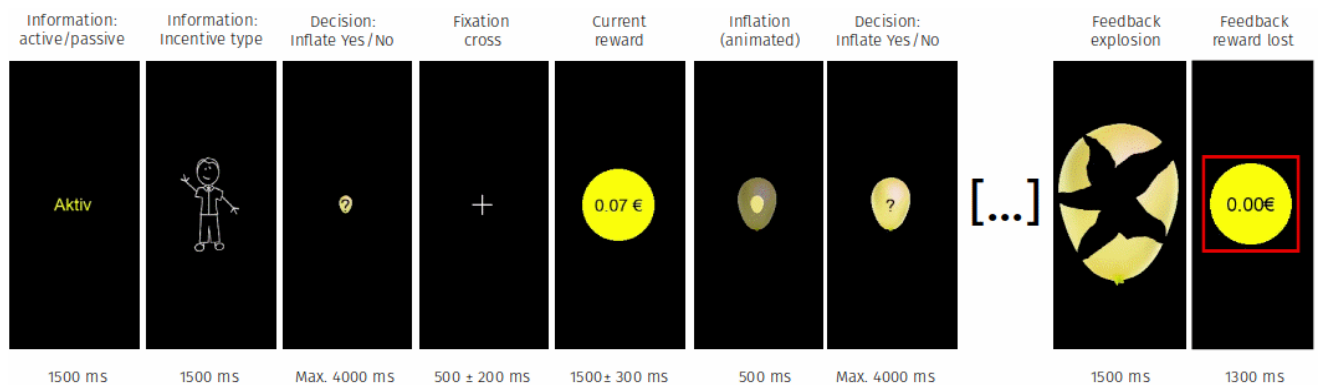


*Note.* The incentive type is communicated in the beginning via a drawn representation of an adult (financial) or a child (social). Images are cropped for representation: the screen used in the pilot- and fMRI study had a side ratio of 4:3, with the screen being black except for the stimuli depicted here. Balloons were separated by a 3000 ms ± 1500 ms ITI (Inter trial interval).

Participants had a maximum of 4 seconds to decide on whether to inflate a balloon or not. They were instructed to take enough time to make a sound decision while not overthinking their decisions and staying within the time frame. If participants failed to respond within 4 seconds, the text "zu langsam" ("too slow" in German) was displayed in red letters, the current balloon was aborted without any reward, and the next balloon started. Figure 4 depicts an abbreviated version of an example trial. Between trials, a fixation cross was shown for an interval of 3000ms ± 1500ms, uniformly distributed.

*Trial Order*

Participants were shown 120 balloons distributed equally over all four combinations of active and passive and socially and financially incentivized trials. The balloons' capacity ranged, in integrals, from 2 to 16. All four conditions contained two balloons reaching each different size. As balloons increased in size in steps of 1 to 3 with each inflation, the largest balloons exploded after nine inflations. The average number of inflations before the explosion was 4.5, the minimum 1.

The design was split in two halves. The order of the halves was alternated between participants for counterbalancing. The trial order was pseudorandomized, and the order of presentation was the same for all participants in the same counterbalancing group. The experiment had three breaks of variable length at regular intervals during the task. During these breaks, participants were shown their cumulative earnings from the social and financial condition and were instructed to continue with the task whenever they were up to it.

*Experimental Setup*

The experiment was scripted in Octave (Version 4.2.1; Eaton et al., 2017), using the Psychophysics Toolbox extensions (Brainard, 1997; Pelli, 1997; Kleiner et al., 2007) and running under Ubuntu for high timing precision (cf. Bridges et al., 2020). During feasibility- and pilot studies, participants were seated in a darkened room in front of a computer screen and used a regular computer mouse for responses. In fMRI measurements, participants laid in the MRI scanner, and stimuli were projected onto a screen outside the scanner. Participants saw the stimuli through a mirror mounted on the head coil. In all setups, stimuli were presented such that participants saw them straight ahead at what they perceived as eye level. Responses in the scanner were communicated via button presses of the right index, middle and ring finger on an input device resembling a three-button mouse. The mapping of buttons to responses was counterbalanced over participants.

*Feasibility study*

The adapted BART design was tested in a feasibility study with 4 participants. The study goal was to uncover significant flaws in the design and determine whether a blocked or pseudo-randomized design should be used. A pseudo-randomized design offers to keep the participants engaged by not having too many passive trials one after the other. However, frequent changes between the different conditions (social vs. financial, active vs. passive, differing balloon inflations) might confuse participants.

Interviews conducted with the participants after the measurement and the analysis of the behavioral data showed that participants in both conditions had

no problems understanding the task. As participants who were shown a blocked design reported boredom during blocks of passive balloons, it was decided to use a pseudo-randomized design for the behavioral pilot study.

### 3.2.2 BEHAVIORAL PILOT STUDY – GOALS AND SETTING

After the feasibility study, a behavioral pilot study was conducted with 10 participants with both financial and social rewards. Measurement conditions were closely adapted to the fMRI environment where the actual study took place. Participants sat in a darkened room in front of a computer screen and used a similar device to communicate responses as participants later on in the scanner used.

Participants were asked how motivated they felt by the social and financial incentives and overall design after the measurement. Answers were given on a 10-point discreet scale ranging from "Not motivated at all" to "Highly motivated". In addition, during the short interview after the measurement, participants were explicitly asked whether they had problems with the pace or structure of the design and if they got bored or stressed out by it. Participants were furthermore asked if they had any more general problems in understanding the design. Due to the small sample size and the resulting low power, no statistical analyses were conducted on the data from the pilot study.

### 3.2.3 BEHAVIORAL PILOT STUDY – RESULTS AND ADAPTIONS

The behavioral pilot study revealed no need for extensive revisions regarding the design. All participants reported a motivation higher than the neutral point on the 10-point self-report scale ($m$ = 8.3, $sd$ = 1.55, $min$ = 6, $max$ = 10). Both social and financial incentives were on average rated as motivating ($m_{soc}$ = 7.95,

$sd_{soc}$ = 1.21; $m_{fin}$ = 7.1, $sd_{fin}$ = 1.85). Detailed ratings are shown in figure 5. While the lowest ratings for the social incentive were still above the middle of the scale, the lowest rating for the financial incentive was at 3. The respective participant reported only studying half-time and working the other half of the day. Thus, care was taken in the actual fMRI study to record the employment status. If the design were utilized in a setting with a non-student population, the financial incentives might have to be increased.

Most participants had no complaints about the design. Some remarked that the experiment was a bit too long (n = 2) but also reported no notable problems with their concentration regarding the overall length. Three participants reported boredom when there were more than three passive trials, one after the other. The highest number of recurring passive trials was five, which only happened once in the design. Two times, four passive balloons were presented back to back, making this a concern for a minority of trials, affecting a minor number of participants. Furthermore, the reported overall motivation was nonetheless satisfactory. It was thus decided not to change the design.

Task understanding was good, albeit not perfect, with two participants showing understanding problems that only became apparent during the ten testing balloons. All problems in understanding could, however, quickly be resolved. In addition, an analysis of participants' behavior shows reasonable choices by all participants - they always inflated tiny balloons, seldom inflated large balloons, had very few missing responses, and overall short response times. The instructions were further standardized and written down in plain text instead of the bullet points used for the pilot study to maximize understanding of the task and increase objectivity and reliability.

**Figure 5**

*Ratings of motivation in the pilot study*
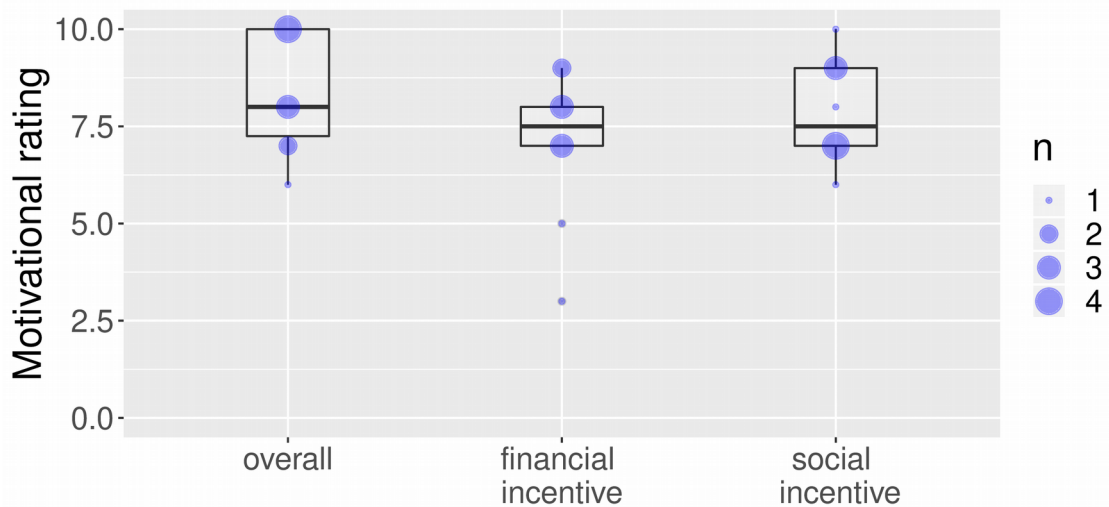


*Note.* Participants were asked to indicate on a 10-point scale how motivated they felt due to the financial incentives, the social incentives and how motivated they were in the overall design.

### 3.2.4 SELF-REPORT SCALES

The GRiPS (Zhang et al., 2019) was used to measure self-reported general risk-taking propensity. In addition, domain-specific risk-taking propensity was measured with the DOSPERT (Blais & Weber, 2006). As altruism and social orientation, might influence differences in behavior, participants were furthermore asked to complete the Social Value Orientation scale (SVO-scale) by Murphy and colleagues (2011).

### 3.2.5 fMRI SCANNING PARAMETERS

MRI and fMRI data were acquired with a Siemens Magnetom 3-Tesla system. Structural T1-weighted images with a 1mm isometric voxel size (R = 2400 ms, TE = 2.43 ms, TI = 900 ms, flip angle = 8°; FOV = 256*256mm; 176 slice) were

recorded for alignment of individual functional data to a template. T2-weighted images were recorded to be used for diagnostic confirmation in case of incidental findings. Structural measurements preceded functional measurements so participants had time to adapt to the scanner environment.

Functional data were acquired using an echo-planar imaging (EPI) sequence with a GRAPPA acceleration factor of two (echo time = 30 ms, repetition time (TR) = 2500 ms, 46 slices interleaved). Measurements were oriented parallel to an imaginary line connecting anterior- and posterior commissure. Voxels had a size of 3 mm isometric with an in-slice field of view of 64*64 voxels. The number of volumes recorded was dependent on participants behavior, as both response time and choices had an effect on the experiment's duration. Functional scanning was expected to take 34 minutes per participant, excluding breaks. This would have resulted in 816 functional volumes recorded per participant.

### 3.2.6 EXPERIMENTAL PROCEDURE AND SETTING

After arriving on-site, participants were instructed about the study's outline and gave their informed consent. During the pandemic, participants were required to wear a surgical mask and disinfect their hands before entering the laboratories. Demographic data, information on illnesses, medication, drug use, and sleep quality were gathered in a small interview. All consent forms, participant information and demographic questionnaires can be found in the appendix (document 2). In the next step, participants were introduced to the specific implementation of the BART with a standardized text. Finally, they were informed about the different incentives before starting the test trials of the BART.

The experimental procedure was approved by the ethics committee of the University of Bremen, the approval vote can be found in the appendix (document 1A). Furthermore, a hygiene concept (appendix document 1B) was implemented before measurements were resumed during the SARS-COV-2 pandemic. Participants furthermore signed a consent form informing them of the steps taken to reduce a risk of infection (appendix document 1C). The local pandemic crisis board of the university approved the procedure.

## 3.3 Data Analyses

Response times and risk-taking was analyzed based on the behavioral data collected during the fMRI measurement. These behavioral analyses are detailed in the first paragraphs of this section. Following the behavioral analyses, details on the fMRI analysis are presented.

### 3.3.1 BEHAVIORAL ANALYSES

All behavioral analyses were conducted in R (version 3.6.3; R Core Team, 2020) with RStudio (version 1.1.456; RStudio Team, 2016). Data from all 40 participants was used for behavioral analyses.

Absolute and relative numbers of missing trials were calculated, once over all participants and once separately for each participant, to gauge whether any participants had to be excluded due to excessive amounts of missing trials. Assumptions of normal distribution were checked with Shapiro-Wilk tests before conducting any analysis depending on them.

Differences in response times in the four conditions resulting from the two factors - trial type (active/passive) and incentive (financial/social) - were investigated using a 2x2 repeated measures analysis of variance (ANOVA).

Associations between behavior in the BART and the incentive type were analyzed as follows. Burst-scores (total number of exploded balloons, Schmitz et al., 2016) were calculated for each participant to estimate risk-taking propensity. The burst-score was used as it is reported to be most consistently related to real-world risk-taking between several different scoring methods (Schmitz et al., 2016). Balloons stopped because participants missed the 4-second response interval were omitted from analyses of risk-taking propensity. The relative number of exploded balloons in each category was used for analyses so that missing trials did not interfere with the comparison between participants.

### 3.3.2 FMRI PREPROCESSING AND ANALYSIS

Analyses of structural and functional data were conducted in AFNI (Cox, 1996; Cox & Hyde, 1997). For preprocessing, a script was created through AFNIs "uber_subject.py" function, adapted manually, and applied to the data of all participants. The script can be found in the appendix (document 3).

MRI data were preprocessed as follows: Dicom files were converted to NIfTI format (Li et al., 2016) and structural data were defaced through AFNI's @afni_refacer function to decrease the risk of de-anonymization (cf. Theyers et al., 2021). Slice timing was corrected before movement parameters were estimated with rigid-body transformations. Any volumes where a participant's head moved by more than 0.3 mm within one TR were censored from the

analysis. The functional and structural alignment was performed using Afni's "lpc+ZZ" cost function (Saad et al., 2009). Structural normalization was based on the MNI152-2009c template as packaged with AFNI (Fonov et al., 2011). Functional volumes were registered based on the volume determined to have a minimum number of outlier voxels (+/- 3 standard deviations from average). Nonlinear warping was used to register structural scans to the template volume as described by Cox and Glen (2013). Data were checked for accidental left-right flips (cf. Glen et al., 2020). Data were blurred with an 8 mm full-width-half-maximum gaussian kernel. Functional data were masked based on the structural scan, and voxel wise scaling was applied as described by Chen and colleagues (2017). Volumes where 5% of voxels or more were found to be outliers (± 3 standard deviations from voxel average), were censored in the regression model. AFNIs quality-control scripts were used to check for mistakes in preprocessing, and two independent researchers evaluated the results.

*First level analysis*

A general linear model approach was used for fMRI analysis. Three different types of stimuli were modeled separately for all four combinations of active and passive and social and financial incentives – social incentive active ($soc_{act}$), social incentive passive ($soc_{pas}$), financial incentive active ($fin_{act}$) and financial incentive passive ($fin_{pas}$). Decision periods before decisions to inflate were modeled with two regressors each: A constant regressor for the average effect and a mean-centered regressor parametrically modulated by the explosion probability of the current balloon. Regressors for the decision periods were based on a duration modulated BLOCK regressor, an incomplete gamma

function convolved with a boxcar function equaling one during the decision period and zero everywhere else. In addition, negative feedback in the form of an exploded balloon was modeled with a fixed duration BLOCK regressor, as was positive feedback in the form of the current reward. The overall number of regressors of interest was 16.

Added to the model were motion estimates for translation and rotation in all directions (6 regressors) and their derivatives (6 regressors) to account for movement-related effects. In addition, Legendre polynomials were added to the regression model for baseline detrending. The number of polynomials added was determined through AFNIs afni_proc.py script and varied between 15 and 17, depending on the measurement duration.

General linear tests (GLTs) were calculated on the subject level for the decision period regressors. For both types of incentives, a GLT was calculated to compare parametric regressors in active and passive trials.

*Second level analysis*

Second level analyses were based on the GLTs calculated at the subject level. Non-parametric cluster analyses were used for statistical interference and calculated through the -ClustSim option of AFNIs 3dttest++ function. Residuals of the GLM were used with randomized signs to simulate 10000 volumes of null results. Based on this data and the cluster forming threshold ($p < .001$), the cluster size threshold is calculated so that the false discovery rate is held below 5% (cf. Cox et al., 2017a; Cox et al., 2017b). Voxels were considered to belong to a cluster if their edges or faces touched. All tests were conducted two-sided.

Group-level contrasts were calculated for parametric regressors only. Voxel-wise t-tests between beta-values were used to compare active and passive risk taking within both incentive conditions ($soc_{act}$ - $soc_{pas}$ and $fin_{act}$ - $fin_{pas}$). The contrast calculated within the financial incentive domain is a loose conceptual replication of prior studies on risk-taking with financial incentives (cf. Lei et al., 2017, Rao et al., 2018). It will be discussed in comparison to these prior studies. Because the individual data of these prior studies is not available, the thresholded results must be used for comparison. This procedure increases the likelihood that small differences in findings where results are close to the threshold of significance are overinterpreted (cf. Chen et al., 2017). For the contrast within the social condition, no similar prior studies exist, and the findings of this analysis will not be analyzed on their own. Instead, the analyses detailed in the following paragraph will be used.

A symbolic GLT was calculated to determine whether the difference between the inter-incentive contrasts significantly differed from zero (($soc_{act}$ - $soc_{pas}$) - ($fin_{act}$ - $fin_{pas}$)). To analyze overlapping regions between incentives a conjunction analysis was used (($soc_{act}$ - $soc_{pas}$) ∩ ($fin_{act}$ - $fin_{pas}$)). Anatomical labels were drawn from the human brainnetome atlas (Fan et al., 2016) as implemented in AFNI's "whereami" function.

*Additional exploratory analyses*

In case significant differences in brain activation between the social and financial incentive conditions were found, further exploratory analyses of the findings were conducted. The exploratory analyses were based on the symbolic GLT comparing the two incentive conditions (($soc_{act}$ - $soc_{pas}$) - ($fin_{act}$ - $fin_{pas}$)). The average beta-estimate over voxels of this GLT was calculated for each

participant. Calculations were conducted separately for each cluster of significant differences found at the group level. These calculations result in a single value for each participant and cluster, signifying the average difference between the incentive conditions for each participant in each cluster.

The resulting data were used for strictly exploratory regression analyses. Average beta-estimates were used in a multiple regression model with six predictor variables:

- participants' risk-taking-propensity for social and financial incentives (burst-score)

- self-reported probabilities to engage in risky financial and social behavior taken from the DOSPERT

- self-reported general risk-taking propensity as measured with the GRiPS

- social value orientation measured with the SVO-scale

While other data on participants' risk-taking preferences were available, the variables included in the model had to be limited. The measured risk-taking propensity was included as it is directly related to the central question of this thesis and the only measure of actual risk-taking available. DOSPERT-Scales and the GRiPS were included as domain-specific and -general measures of reported risk-taking propensity. Lastly, the SVO scale is related to self-other differences in behavior that were previously investigated in the context of risk-taking by other groups (e.g., Stone et al., 2002; Stone et al., 2013; Ogawa et al., 2018; Zhang et al., 2019) and might influence present results. A second multiple regression model was calculated with all predictor variables significantly contributing to the previous model at $p < .1$.

## 3.4 Estimation of Influences of SARS-CoV-2 Pandemic

### 3.4.1 Influences on behavioral measurements and self-report scales

As argued in the chapter on the theoretical background, the onset of the SARS-CoV-2 pandemic might have influenced participants' risk-taking propensity in two different ways. First, an overall risk-taking reduction due to negative experiences might have occurred. Second, self-selection toward more risk-taking individuals might have influenced the sample selection during the pandemic.

*Estimation of self-selection bias*

The data compiled from each participant include various self-report measurements of both general- and domain-specific risk-taking. A multivariate ANOVA (MANOVA) was calculated to estimate differences between participants from before and during the pandemic.

The GRIPS score and the DOSPERT-Scales for financial, social, and health risk-taking propensity were used as dependent variables. Financial and social scales are of specific interest as these are the two types of incentives used in the present study. Risk-taking propensity in the health domain was added as it is related to the risks imposed by a pandemic. A similar analysis was conducted on the behavioral measures, namely the BART burst-score. The predictor variables were the burst-scores for balloons with social and financial incentives, the predicted variable the date of the measurement, dichotomized to "before" and "during" the pandemic.

*Estimation of changes in risk taking propensity*

To estimate whether the pandemic changed risk-taking behavior in the study's sample, participants from before the pandemic were contacted again in September 2020. They were asked to participate in an additional online survey to help estimate the effects of the pandemic on risk-taking. Within the data collected in the follow-up study were the DOSPERT scales for health, social and financial risk-taking and the GRIPS. All scales mentioned above were added as independent variables to a repeated measures MANOVA predicting the timepoint of the measurement. Of the 20 participants that were contacted, 16 took part in the follow-up study.

The two likely effects of the pandemic, overall risk-taking reduction due to negative experiences and self-selection towards more risk-taking individuals, act in opposite directions. As it is unclear how strong they are relative to each other, all tests in the above section were conducted two-sided.

### 3.4.2 Influences on fMRI measurements

To estimate the effects of the pandemic and mask-wearing on the BOLD-signals, beta-weights of the main parametric regressors of interest were compared between participants from before and during the pandemic. To this goal, three two-sample t-tests with cluster simulations were calculated for the symbolic GLTs within the social and financial conditions ($soc_{act}$ - $soc_{pas}$ and $fin_{act}$ - $fin_{pas}$) and the difference between the two conditions (($fin_{act}$ - $fin_{pas}$) - ($soc_{act}$ - $soc_{pas}$)).

# Chapter 4: Results

## 4.1 Behavioral Results

### 4.1.1 Response times, missing trials and overall performance measurement

Over all participants and trials, the maximal response time of 4 seconds was exceeded 31 times, or in 0.17% of all trials. 27 participants never took too long to decide on whether to inflate a balloon or not. The highest relative amount of exceed response time windows for a single participant was 4.6%. No participants had to be excluded from the analysis due to missing trials.

Participants took on average 542ms (sd = 384ms) to respond, measured from the beginning of the decision window. As part of the behavioral analysis, average response times in the different conditions (active and passive balloons and social and financial incentives) were calculated for each participant and compared in a 2x2 factorial within-subject ANOVA. Shapiro Wilk tests confirmed that the response times in three of the four conditions were normally distributed ($p$ > .05). Response times in the active social condition significantly deviated from a normal distribution ($W_{soc-act}$ = .94, $p_{soc-act}$ = .040). False positives in ANOVA are not strongly influenced by slight deviations from normality (Harwell et al., 1992; Lix et al., 1996; Schmider et al., 2010). The ANOVA was thus calculated, but results from this analysis should be interpreted with adequate caution.

No interaction effect between the two factors was found ($F$(1,38) = .01, $p$ = .091). Main effects of both the balloon type ($F$(1,38) = 37.33, $p$ <.001, $\eta_p^2$ = .50) and the incentive type ($F$(1,38) = 10.82, $p$ = .002, $\eta_p^2$ = .22) on the response time were

found. Participants took longer to decide when balloons were active compared to passive ($m_{act}$ = 592 ms, $sd_{act}$ = 186 ms; $m_{pas}$ = 492 ms, $sd_{pas}$ = 146 ms). Balloons with a social incentive elicited longer response times compared to balloons with a financial incentive ($m_{soc}$ = 552 ms, $sd_{soc}$ = 175 ms; $m_{fin}$ = 532 ms, $sd_{fin}$ = 174 ms). Data on response-times are illustrated in figure 6.

**Figure 6**
*Boxplots of average response times in all conditions*
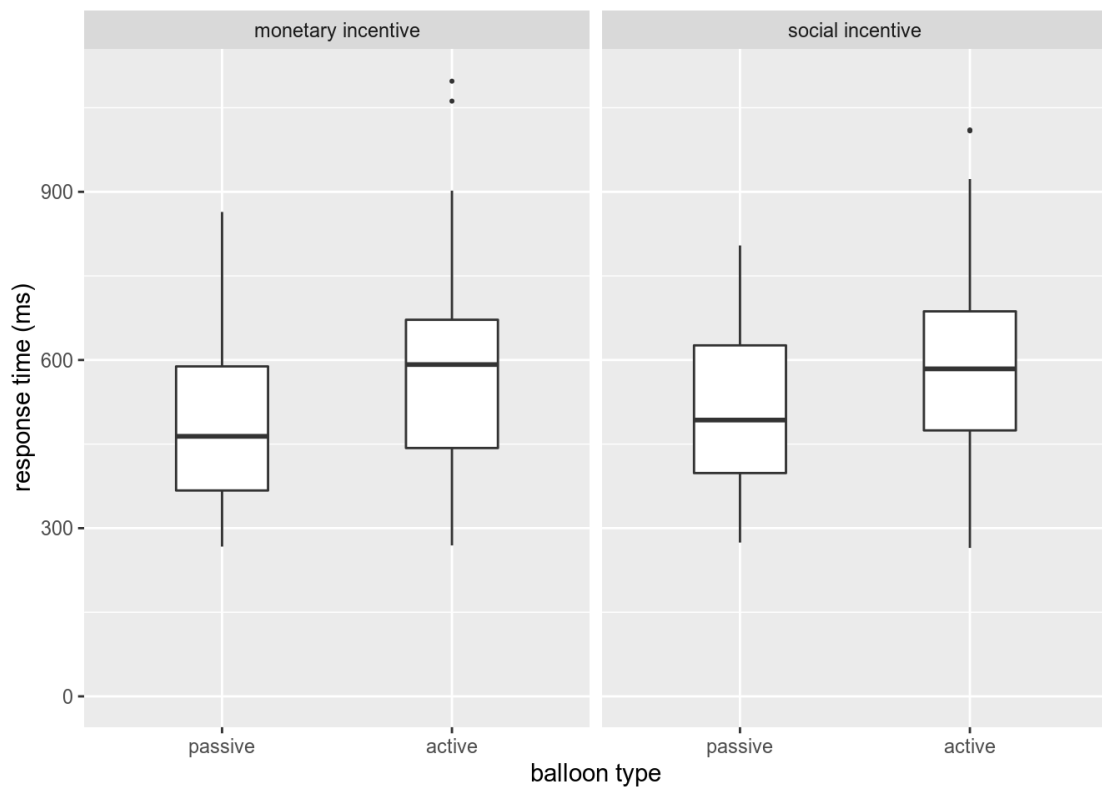


*Note.* Mean response times within each combination of conditions were calculated on the individual level.

### 4.1.2 Behavioral risk measurements

The behavioral risk measurement was compared between the different incentives in active trials. The relative burst score (Schmitz et al., 2016) was used to estimate risk taking in the BART. The number of balloons completed under each condition varied slightly over participants due to missed response time windows. Thus, the relative number of exploded balloons was used for the analysis instead of the absolute amount.

Burst-scores in both groups were normally distributed ($W_{soc}$ = .97, $p_{soc}$ = .44; $W_{fin}$ = .97, $p_{fin}$ = .15). A paired t-test shows significant differences between risk-taking measures of the two incentive types ($t(38)$= 3.64, $p$ = .001). With social incentives, participants were less risk-seeking ($m$ = 35%, $sd$ = 8 percentage points) compared to financial incentives ($m$ = 39%, $sd$ = 9 percentage points).

### 4.1.3 Influences of SARS-CoV-2 pandemic on behavioral results

Data of participants from before and during the pandemic were compared to test for self-selection bias. Data from a follow-up survey and retrospective self-report scales were used to estimate changes in the risk-taking propensity caused by the pandemic.

*Self-selection bias*

A MANOVA using Pillai's trace was calculated to compare the DOSPERT risk-taking propensity scales for the social, economic and health domains as well as the GRIPS score between the data sets collected before and during the pandemic. No significant difference between the groups were found ($V$ = .073, $F(4, 35)$ = 0.63, $p$ = .64). A power analysis conducted with G*Power (Version

3.1.9.7, Faul et al., 2009) revealed a power of .18 to reveal effects of a medium size based on the aquired sample size. Figure 7 depicts the relevant DOSPERT-scales and the GRiPS for both groups.

**Figure 7**

*Comparison of selected self-report scales between the participants partaking before and during the SARS-COV-2 pandemic*
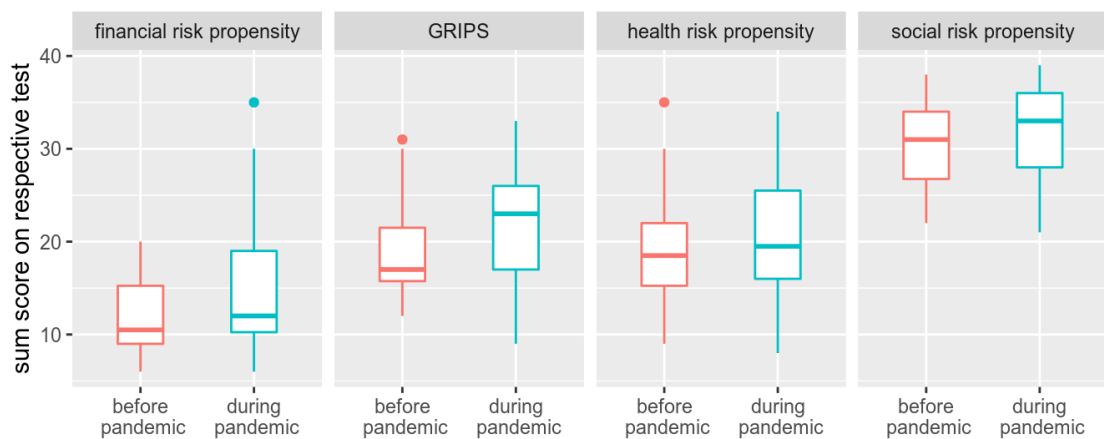


A second MANOVA, comparing the burst-scores with social and financial incentives between the two groups found no significant differences either ($V = 0.050$, $F(2,35) = 0.92$, $p = .410$). A power analysis based on the aquired sample size resulted in a power of .25 to reveal effects of medium size. The underlying data are depicted in figure 8.

**Figure 8**

*Comparison of burst-scores in the BART between the participants measured before and during the SARS-COV-2 pandemic*
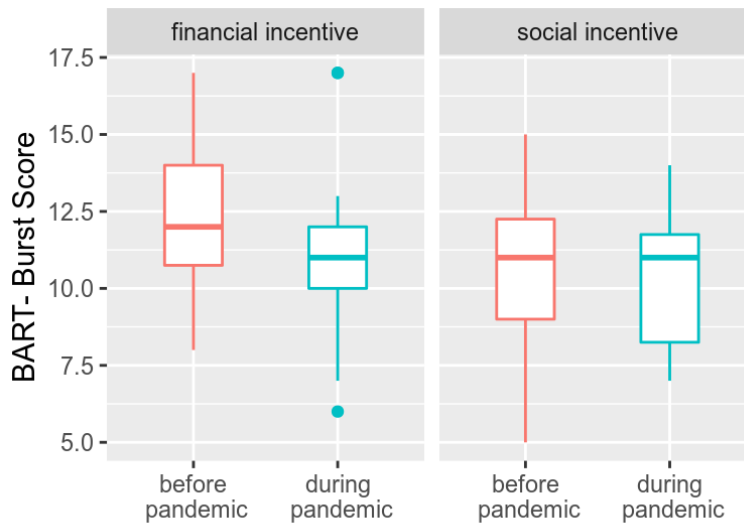


*Changes in risk-taking propensity*

Comparing data on social, financial, health and general risk taking propensity from participants before the pandemic with data from the same participants collected during the follow up study with a repeated measures MANOVA using Pillais trace found no significant difference in measurements between the two time points ($V = 0.379$, $F(3, 13) = 2.65$, $p = .093$).

## 4.2 fMRI Results

The number of volumes recorded differed between participants due to differences in response times and decisions in the task. The average number of TRs was 894 ($SD = 43$), the minimum 818, and the maximum 1016.

### 4.2.1 Social and financial incentives

*Risk-taking with financial incentives*

Six clusters of significant differences in beta-estimates were found in the contrast of active and passive risk-taking with financial incentives. For all clusters, beta-estimates were higher in the active compared to the passive condition. Clusters were located in the left striatum stretching to the left insula, in the right striatum, dorsal anterior cingulate cortex (dACC), right insular cortex and bilaterally in the occipital cortex. Detailed information on cluster sizes, extent, and peaks can be found in table 4 and figure 9.

**Figure 9**

*Significant results of the contrast within the financial incentive condition*
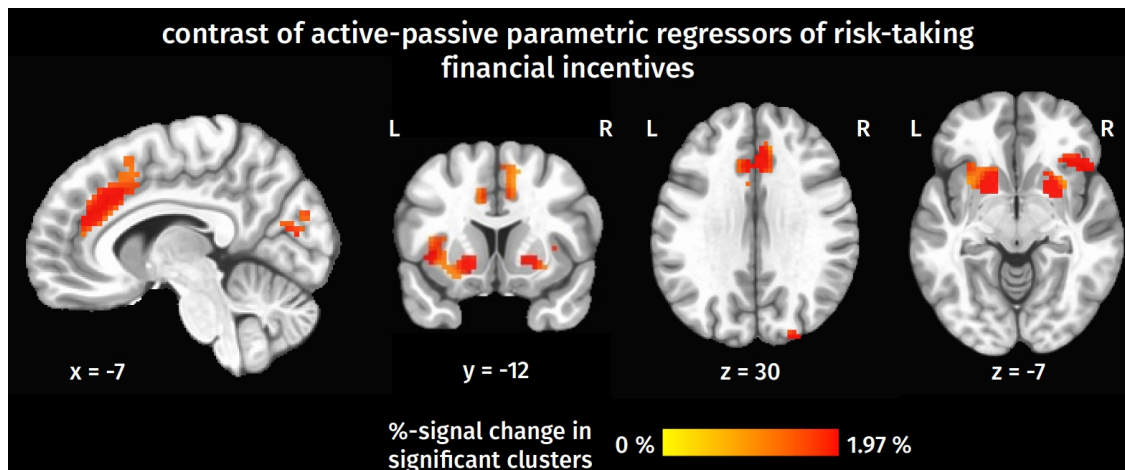


*Note.* Significant differences in beta-estimates of active and passive risk-taking within the financial incentive condition, superimposed on the MNI152-2009c brain (Fonov et al., 2011).

*Risk-taking with social incentives*

Seven clusters of significant differences were found by contrasting active and passive risk taking within the social incentives condition. Beta-estimates were higher in the active condition in a large cluster spanning much of the occipital cortex and three smaller clusters, one in the bilateral dACC and right BA9, one spanning the left striatum, insula, and IFG, and the last in the right striatum. Beta estimates in the passive condition were significantly higher in three clusters, all located in the left hemisphere: In the IFG and the middle and inferior frontal gyrus. The exact location of peaks and more detailed information on the extent can be found in table 4 and figure 10.

**Figure 10**
*Significant results of the contrast within the social incentive condition*
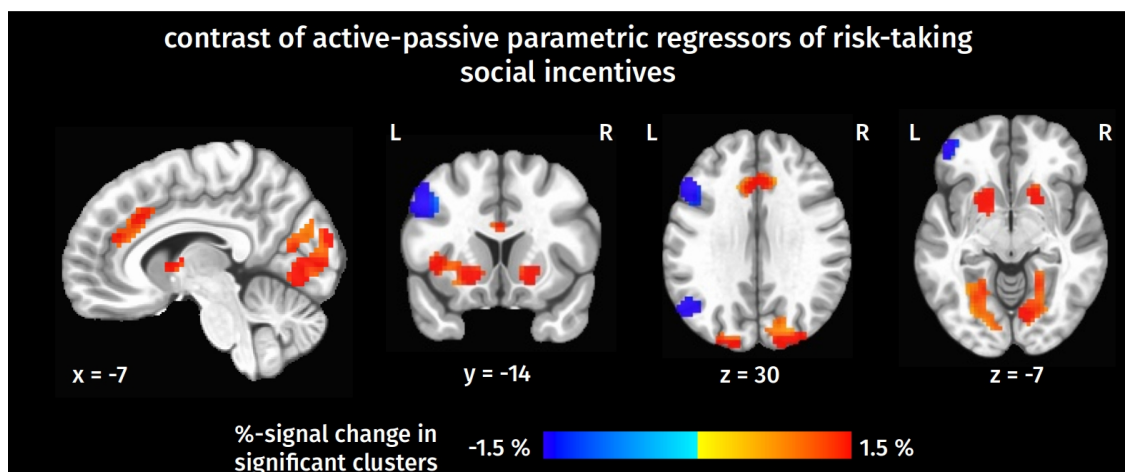


*Note.* Significant differences in beta-estimates of active and passive risk-taking within the financial incentive condition, superimposed on the MNI152-2009c brain (Fonov et al., 2011).

*Contrast between risk-taking with social and financial incentives*

Contrasting the results of both prior analyses and thus comparing differences between the two incentive types resulted in a single cluster of significant differences in the right inferior parietal lobule (IPL) in Brodmann areas 39 and 40. The findings are detailed in table 4 . Figure 11 depicts the results superimposed on a standard MNI152_2009c brain (Fonov et al., 2011).

*Conjunction analysis of risk-taking with social and financial incentives*

A conjunction analysis of findings from contrasting both active conditions with the respective passive conditions within each incentive found five clusters of overlapping activation. Clusters were located in the dACC, bilateral striatum and bilateral OC. Again, details can be found in table 4. The findings are depicted in figure 11.

**Figure 11**

*Contrast and conjunction of the results from both incentive conditions*
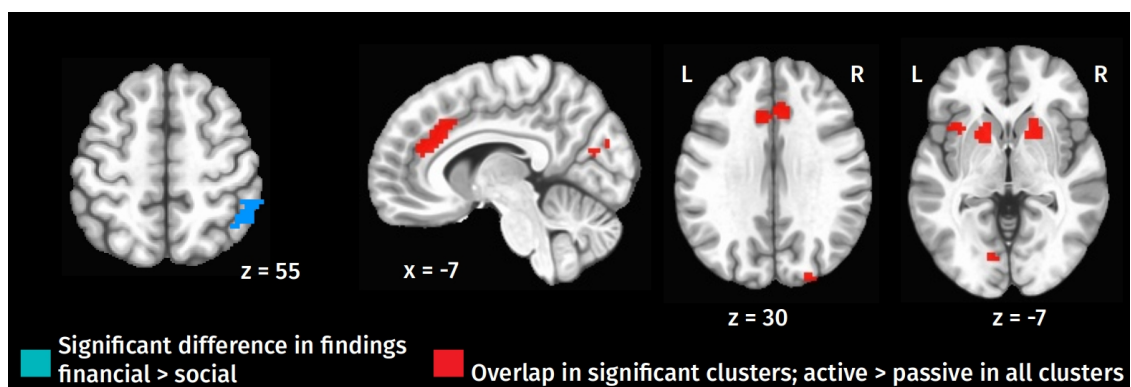


*Note.* Significant differences and commonalities of the social and financial risk-taking contrasts, superimposed on the MNI152-2009c brain (Fonov et al., 2011).

**Table 4**

*Results of all fMRI analyses on neural correlates of risk-taking*

| Nr. | location of peak | extent | peak coordinates | | | peak | size |
|-----|------------------|--------|---|---|---|------|------|
| | | | | | | Z-score | voxels |
| | | | X | Y | Z | (*p*) | (mm³) |
| **ea - ep** minimal cluster-size for significance: 55 voxels | | | | | | | |
| **ea > ep** | | | | | | | |
| 1 | Left orbital gyrus, <2mm from left nucleus accumbens | Left striatum (Putamen, caudate, nucleus accumbens, globus pallidus) Left inferior frontal gyrus Left dorsal insular lobe | 19.5 | -4.5 | -16.5 | 4.416 (<.01) | 230 (6210) |
| 2 | Right dorsal anterior cingulate cortex (dACC) <2mm from right medial BA9 | Right dACC, right medial and dorsolateral SFG, left ACC | -1.5 | -25.5 | 34.5 | 4.587 (<.01) | 227 (6129) |
| 3 | Right occipital cortex | Bilateral rostral cuneus, right occipital cortex | -25.5 | 91.5 | 34.5 | 4.142 (<.02) | 141 (3807) |
| 4 | Right putamen | Right striatum (putamen, caudate) | -10.5 | 1.5 | 13.5 | 4.211 (<.02) | 111 (2997) |
| 5 | Left occipital cortex (1mm: cCunG_left) | Left occipital cortex and caudal cuneus | 1.5 | 103.5 | 4.5 | 4.367 (<.03) | 94 (2538) |
| 6 | Right dorsal agranular insula (1mm: A12/47l_right) (2mm: A44op_right) | Right orbital gyrus and opercular IFG, right dorsal insula | -49.5 | -19.5 | -7.5 | 4.079 (<.03) | 79 (2133) |
| **ea < ep** | | | | | | | |
| No significant clusters matching criteria | | | | | | | |
| **sa – sp** minimal cluster-size for significance: 57 voxels | | | | | | | |
| **sa > sp** | | | | | | | |
| 1 | Medial superior occipital gyrus | Right occipital cortex, bilateral parietooccipital sulcus, bilateral lingual gyrus | -13.5 | 85.5 | 46.5 | 3.406 (<.01) | 1480 (39960) |

| Nr. | location of peak | extent | peak coordinates | | | peak Z-score (*p*) | size voxels (mm³) |
|---|---|---|---|---|---|---|---|
| | | | X | Y | Z | | |
| 2 (3) | Right dACC <1mm from left dACC <1mm from right subgenual ACC | Bilateral dACC, right medial BA9, right subgenual ACC | -1.5 | -37.5 | 19.5 | 3.945 (<.01) | 300 (8100) |
| 3 (6) | Left dorsal disgranular insula <1mm from left opercular IFG < 2mm from left ventral IFG < 2mm from left agranular insula | Left striatum (Putamen, caudate, nucleus accumbens), left insula, left opercular IFG | 43.5 | -13.5 | -1.5 | 3.834 (<.01) | 176 (4752) |
| 4(7) | Right nucleus accumbens | Right striatum (caudate, putamen, nucleus accumbens) | -16.5 | -4.5 | -10.5 | 3.292 (<.02) | 97 (2619) |
| **Sp > sa** | | | | | | | |
| 1 (2) | Left inferior parietal lobule (IPL), BA39 | Left IFP, BA39 & BA40 | 34.5 | 76.5 | 52.5 | -3.297 (<.01) | 366 (9882) |
| 2(4) | <3mm from left inferior frontal junction | Left middle and inferior frontal gyrus | 52.5 | -22.5 | 40.5 | -4.114 (<.01) | 225 (6075) |
| 3(5) | <2mm from left orbital gyrus (A12/47l) | Left middle frontal, orbital and inferior frontal gyrus | 49.5 | -46.5 | -16.5 | -4.159 (<.01) | 213 (5751) |

**(ea-ep) – (sa-sp)** minimal cluster size for significance: 54 voxels

**ea-ep > sa-sp**

| 1 | < 1mm from right Cuneus | Right caudate, right rostrodorsal BA39 & BA40 | -49.5 | 52.5 | 58.5 | 4.007 (<.04) | 68 (1647) |

**ea-ep < sa-sp**

No significant clusters matching criteria

| Nr. | location of peak | extent | peak coordinates | | | peak Z-score (*p*) | size voxels (mm³) |
|---|---|---|---|---|---|---|---|
| | | | X | Y | Z | | |
| **ea-ep ∩ sa-sp** conjunction of ea-ep and sa-sp, no minimal cluster size | | | | | | | |
| | Location of internal center | | Center of mass | | | | |
| 1 | Right dACC | Right and left dACC, right medial BA9 | -4.5 | -25.5 | 28.5 | NA | 101 (2727) |
| 2 | Right lateral occipital cortex | Bilateral occipital cortex | -13.5 | 88.5 | 22.5 | NA | 95 (2565) |
| 3 | Left ventromedial putamen <1mm from left caudate | Left striatum (caudate, putamen, anterior cingulate) | 19.5 | -10.5 | -4.5 | NA | 76 (2052) |
| 4 | Right ventromedial putamen <1mm from right caudate | Right striatum (caudate, putamen) | -16.5 | -10.5 | -1.5 | NA | 47 (1269) |
| 5 | Left occipital cortex | Left occipital cortex | 7.5 | 97.5 | 13.5 | NA | 43 (1161) |

*Note*. Cluster peak location and extent. For conjunction analysis, internal center coordinates (as calculated through AFNIs iCenter function) are given. Regions accounting for less than 5% of a cluster are not included in the table. All coordinates in MNI-notation. NA: Not applicable; Nr.: Number of cluster.

### 4.2.2 ADDITIONAL EXPLORATORY ANALYSES

For each participant, average beta-estimates in the cluster identified in the contrast between the two incentive-conditions were calculated. A multiple regression model with burst-scores, domain-specific and -general risk-taking propensity and SVO-values was calculated. It does not explain a statistically significant amount of variance in the average contrast estimates ($F(6,29) = 1.21$, $p = .32$, $R = .200$, $R^2_{adjusted} = .035$). Only the burst-score in the social-incentive condition was significant at $p < .1$ ($\beta = 0.0027$, 95% CI [-0.0002, 0.0056], $\beta_i = 0.40$, $t(29) = 1.883$, $p = .070$). The smaller model therefore included only the social-incentive burst score as a predictor. The model explains a statistically significant amount of variance in the average contrast estimates ($F(1,37) = 8.51$, $p = .006$, $R = .187$, $R^2_{adjusted} = .165$, $\beta = 0.0028$, 95% CI [0.0009, 0.0048], $\beta_i = 0.43$).

### 4.2.3 INFLUENCES OF SARS-COV-2 PANDEMIC ON FMRI RESULTS

No significant differences in the beta-weights of the main parametric regressors of interest were found between participants from before and during the pandemic.

# Chapter 5: Discussion

This work investigates the impact of different incentives on participants' risk-taking behavior and their respective neural responses. On the behavioral level, participants were less risk-seeking and had longer response times if incentives were social compared to financial. Both significant differences and commonalities in the neural correlates between the two conditions were found. The commonalities outline a domain-general risk-taking network similar to the findings of the meta-analysis. Significant differences between the conditions were found in the inferior parietal lobule. It seems unlikely that the onset of the SARS-CoV-2 pandemic during the data collection influenced results to a considerable degree.

## 5.1 Extent of Influences of the SARS-CoV-2 Pandemic

Based on prior literature, an influence of the onset of the pandemic on behavioral data was possible. Self-selection bias might have influenced the sample selection (Bish & Mitchie, 2010; Wise et al., 2020). Furthermore, risk-taking propensity might have decreased due to the pandemic's adverse financial and health effects (cf. Malmendier & Nagel, 2011; Cohn et al., 2015; Decker & Schmitz, 2016).

None of the analyses conducted to investigate possible effects of the pandemic on behavior, self-description, and self-selection bias found a significant effect. On the descriptive level, scores on the GRiPS were slightly higher during the pandemic compared to before its onset. Furthermore, risk-taking with financial incentives was slightly decreased during the pandemic (cf. figure 7

and 8). However, both effects were not significant and should, at most, be seen as a starting point for further investigations.

The present behavioral findings indicate that no large systematic differences between the participants from before and during the pandemic were measurable. However, they cannot be used to rule out any effects of the pandemic on risk-taking. The sample size is relatively small and the two statistical tests used had a power of .18 and .25 to uncover effects of a medium size for the self-report scales and the behavioral data, respectively. Wise and colleagues (2020) report a significant but small correlation of $r = .2$ between perceived risk of infection and willingness to participate in social distancing in the early days of the pandemic. Cohn and colleagues (2015) describe small immediate effects of financial losses on financial risk-taking propensity ($OR =$ 1.65, cf. Chen et al., 2010). Decker and Schmitz (2016) found a very small effect of health shocks on risk-taking propensity ($d = -.11$, cf. Gignac & Szodorai, 2016). All these measures can not be directly translated to the study at hand. They can, however, serve as an estimate of likely effect sizes of pandemic-related effects on risk-taking behavior. Based on them, the sample used in this study was too small to reliably measure an effect of the estimated size.

The comparison between participants measured before and during the pandemic could not discern between self-selection bias and changes in risk-taking propensity at the individual level. It could even result in null findings in case both effects existed and were of a similar magnitude. To circumvent this effect, participants from before the pandemic were contacted again, and sixteen participants completed the GRiPS and DOSPERT again. While no

significant effects were found, the analysis suffers from the same problem of low sample size as the other analyses.

The fMRI analyses revealed no differences in the contrasts of interest between the participants from before and during the pandemic. There is a broad agreement that the effects of surgical mask wearing on oxygen levels in the brain on task-related changes in brain oxygenation should be minimal, although the details are highly disputed (Scholkmann et al., 2021; Fisher et al., 2021). Taking into consideration the ethical aspect of providing participants with a safe environment during measurements, the present results encourage mask wearing during fMRI measurements in a pandemic context.

Concerning the primary study, no effects impeding a combined analysis of data collected before and during the pandemic were found. Thus, the data from all participants were used for all analyses discussed in the following paragraphs.

## 5.2 Discussion of Behavioral Results

Participants took longer to respond to active balloons compared to passive balloons, indicating that additional processing took place in the active condition (Kyllonen & Zu, 2016). Furthermore, response times were slower for trials with social incentives compared to financial incentives. Zhang and colleagues (2019) calculated a similar analysis on response times in a task where participants took risks for themselves and others. They did not find differences in response times between risk-taking for oneself and others in the win domain. The effect of the incentive domain on response times can be seen as an indicator that the present design succeeded in creating clearly

distinguishable incentives and showed an effect beyond that of studies on self-other differences in risk-taking.

In active trials, participants were more risk-seeking for financial incentives than social incentives. On average, approximately 10% fewer balloons exploded in social trials ($burst_{soc}$ = 35% ($SD$ = 8%-points), $burst_{fin}$ = 39% ($SD$ = 9%-points)). A study on risk-taking for oneself and others (Zhang et al., 2019) did not find similar effects. Sun and colleagues (2020) found differences in the risk-taking propensity between decisions for oneself and others, albeit in opposing directions, depending on the variance of gambles. In high variance gambles, such as the inflation of an already large balloon, they found decreased risk-taking propensity when making decisions for others. Their findings are comparable to those of the this study - the lower burst scores in the social incentive condition indicate that participants chose the safe option (payout) earlier. However, other variables should be considered in the behavioral analysis. For instance, not all participants reported being equally motivated by both types of rewards. A large enough sample size to estimate a model encompassing more relevant variables would be required to adequately delineate behavioral effects.

## 5.3 Discussion of fMRI Results

The contrast between active and passive risk-taking within the financial incentive condition resembles analyses conducted by previous studies (e.g. Lei et al., 2017, Rao et al., 2018). It can thus be understood as a loose conceptual replication of these prior studies and can be used to validate the design. It will therfore be discussed first. In the following paragraphs, the contrast within the

social condition is briefly discussed before focusing on the differences and commonalities between social and financial incentives.

### 5.3.1 Risk-taking with financial incentives

Active compared to passive risk-taking with financial incentives elicited stronger brain activation correlates in multiple regions. Beta estimates in the bilateral striatum, insula, dACC, and OC were higher in active risk-taking. Based on the prior meta-analysis, a similar pattern was expected. However, unlike in the meta-analysis, the present study found no activation in the right dlPFC and midbrain. Instead, clusters in the OC were found that have no comparable finding in the meta-analysis data.

A probable source of this discrepancy in findings are differences in the task design of the present study and most primary studies of the meta-analysis. One such difference is the usage of a passive risk-taking task for contrasting. Some previous studies implemented similar paradigms (e.g. Lei et al., 2017; Rao et al., 2018), but the use of different contrast conditions is more widespread (cf. meta-analysis; Poudel et al., 2020; Wu et al., 2021). Accordingly, differences in findings between the present analysis of neural correlates of risk-taking with financial incentives and the meta-analysis are likely related to this difference in approaches.

Right dlPFC activation has previously been linked to error awareness (e.g., Harty et al., 2014). As argued above, a link between right dlPFC activation and a learning component is likely (cf. meta-analysis). In the present study, explosion probabilities were the same in the active and the passive condition. Learning of probabilities and error awareness can thus be equally present

under both conditions. Voloh and colleagues (2015) propose that the dACC is recruited for strategy monitoring and that the dlPFC initiates strategy changes. This role of the dlPFC is coherent with present findings if strategies are understood as spanning multiple trials. Observations made during passive trials could still lead to a change of strategy on a neuronal level, even though this change would only manifest on the behavioral level in the subsequent active trial. Contrary to this explanation, Rao and colleagues (2008) investigated a similar contrast between active and passive risk-taking in the BART and found differences between the two conditions in the left and right dlPFC. The present study has a larger sample size (39 subjects compared to 14) and profits from the numerous advances in fMRI methodology since Rao and colleagues (2008) published their work, so it is likely to be more reliable. However, the exact origin of discrepancies in dlPFC-findings remain unclear. Subjects could be interviewed on their perception of passive risk-taking trials in future studies to delineate the role of the dlPFC more precisely.

Findings in the OC are likely affected by attention and not direct visual input. The relationship between balloon size (directly linked to risk of explosion) and the parametric regressors is the same in active and passive conditions. While balloon colors changed between conditions so participants could distinguish them effortlessly, the colors were counterbalanced over participants. The activation in the OC is likely affected by attention. Attention focused on visual stimuli changes the related activation patterns of primary visual areas (Song et al., 2011; Hembrook-Short et al., 2019). Participants probably paid closer attention to the actual balloon size in the active condition where they had to make a choice compared to the passive one, thus upregulating neural

activation and BOLD-signal in the relevant primary sensory areas (Green et al., 2017).

### 5.3.2 Risk-taking with social incentives

As detailed in the methods, the results within the social incentive condition are not discussed in detail on their own, but mostly in comparison to those in the financial condition. The contrast of active and passive risk-taking within the social condition revealed three clusters where beta-estimates were higher in the passive condition - one in the left IPL and two in the left IFG. While these are not found in the financial incentive condition, the contrast between the financial and social incentive conditions shows no significant difference in these regions. Indeed, a similar cluster in the left IPL is found in the financial condition when an uncorrected threshold of $p < .001$ is applied to the data. However, it only consists of 21 voxels and thus does not pass cluster thresholding, determined to be at 55 voxels for an FDR below five percent. Similar findings from the financial and social incentive exist for most other differences between the two analyses - significant differences between active and passive risk-taking from within one domain exist in the other, only right below the significance threshold.

These observations stress the importance to not only compare significant results of two contrast analyses, but to instead compare the underlying effect sizes and variances statistically. Furthermore, it highlights how hard cutoffs implemented through statistical thresholding in fMRI-analysis carry the risk of information loss and impede the comparison of results between studies (cf. Chen et al., 2017). An approach with finer-grained measures such as different

confidence levels derived from Bayesian statistics would suffer less from this problem.

### 5.3.3 Differences between financial and social incentives

Contrasting incentive conditions resulted in a single cluster in the inferior parietal lobule (IPL), where activations related to active risk-taking were higher in the financial compared to the social condition. Large parts of the cluster are located in BA40, specifically in its caudal (A40c, comprises 42% of cluster) and rostrodorsal (A40rd, comprises 25% of cluster) part. These areas are sometimes referred to as PFm and PFt, respectively (cf. Caspers et al., 2013; Fan et al., 2016; nomenclature based on the Economo-Koskinas area names, cf. Triarhou, 2007). The cluster comprises two peaks, one located in each of the two areas. The incentive-dependent activation found in the IPL is adjacent to one of the clusters of convergent findings of primary studies on risk-taking found in the meta-analysis.

Caspers and colleagues (2013) define seven subregions in the IPL that can be grouped into three larger regions based on receptor distributions: rostroventral, intermediate, and caudate IPL. A40rd lies in the rostral part of the IPL. Caspers and colleagues (2013) associate the region with action observation and imitation (based on works by Molenberghs et al., 2009; Van Overwalle & Baetens, 2009; Caspers et al., 2010). A40c is located in the intermediate part of the IPL (Caspers et al., 2013). The region was previously associated with switching between choice options (Boormann et al., 2009).

More recently, Nummsen and colleagues (2021) used ROI analyses to analyze IPL function in tasks on attention, lexical decisions, and social cognition. They

employed three different analysis techniques and converged on the same findings: both left and right IPL can, functionally, be separated in an anterior and posterior part. The coupling of function and architecture is less consistent in heteromodal brain regions like the IPL compared to, e.g., primary cortices (Braga & Leech, 2015). This decoupling can explain the difference in functional (Numsen et al., 2021) and cytoarchitectural topography (Caspers et al., 2013). In the functional topography of Nummsen and colleagues (2021), the differences in activation depending on the incentive in the present study are located at the border of anterior and posterior IPL, linked to attention relocation and social cognition respectively. It is, however, likely that both regions play a broader role in cognition as they were linked to the processing of stimuli and tasks in various domains (Caspers et al., 2013; Nummsen et al., 2021).

Functional localization in heteromodal regions varies between (Dubois et al., 2019; Fehr et al., 2019; Gilmore et al., 2021) and within subjects (Boukhdhir et al., 2021). Indeed, neural activation patterns in the parietal cortex are known to be highly individual: Gilmore and colleagues (2021) point to a history of findings of individuality in the lateral parietal cortex based on the works by Mueller and colleagues (2013) and Laumann and colleagues (2015). The parts of the IPL where activation differed based on the incentive in the present study form part of the parietal memory network (PMN) first described by Gilmore and colleagues (2015). The PMN was later found to consist of various separate regions differing in their location between individuals (Gilmore et al., 2019, Gilmore et al., 2021). Heterogeneity in inferior parietal cortex topography is also reported in risk-taking tasks. Rao and colleagues (2018) analyzed genetic contributions to variations in the neural correlates of risk-taking in a sample of

111 pairs of twins. They implemented the BART similarly to the present study with an active and a passive condition, and found genetic influences on neural activation patterns in the IPL and SPL during active risk-taking. Based on these findings, it can be hypothesized that heterogeneity in functional topography in the IPL might correlate with inter-and intraindividual differences between and within incentive domains.

Different from the expectation based on part of the previous literature, no differences in activation between the incentive conditions were found in the striatum or insula. Gu and colleagues (2019) use an ALE meta-analysis to investigate prior findings on differences between social and financial reward anticipation. They find a shared network being active irrespective of the reward type, including the striatum and the aINS. Gu and colleagues (2019) argue that their findings align with the common-currency hypothesis (Berridge & Kringelbach, 2013) that the representation of value and motivational processes are at least partially incentive-type independent. The present data support this hypothesis and hint at this common valuation network being similar in reward anticipation and reward-related risk-taking processes.

### 5.3.4 COMMONALITIES OF FINANCIAL AND SOCIAL INCENTIVES

Findings of commonality between the two incentive conditions were similar to the findings in the financial reward condition and thus to the general network identified in the meta-analysis. Overlaps in activation were found bilaterally in the striatum, dACC, primary visual areas, and the left insular cortex.

Activation in the dACC was, as hypothesized, independent of the incentive. Prior research has linked dACC involvement to strategy adaption and

implementation (Kolling et al., 2016, Kolling & O'Reilly, 2018, Voloh et al., 2015), a task seemingly independent of the incentive involved. Furthermore, no dlPFC involvement was found in either the social or financial incentive condition, and as such, no overlap was found either. As discussed above for the contrast within the financial incentive condition, this likely occurred due to effects of the passive condition and seemingly independent of the incentive.

One of the major differences between the network found in both incentive domains and the network identified in the meta-analysis is the right aINS. Activation of the right insula was linked to risk-taking in the meta-analysis and the financial incentive condition. However, no activation of the right aINS was observed in the social incentive condition. This is similar to findings by Gu and colleagues (2019), who investigated differences and commonalities in neural activation patterns between social and financial reward anticipation with an ALE meta-analysis. Like the present analysis, they found no overlap of brain activation related to both incentive types in the right aINS.

The present study used a passive risk-taking task for contrasting to minimize the effect that differences between social and financial reward anticipation have on the findings. Rewards were the same in the passive and active conditions. As such, the large overlap of the present findings and the incentive-independent reward-anticipation network identified by Gu and colleagues (2019) is noteworthy. The left aINS and striatal regions, both part of this network, were consistently stronger involved in active than passive risk-taking. Accordingly, their activation not only tracks value in the present study but does so more strongly when decisions have to be made based on it. Similarly, activation in the OC was common to both conditions. As in the financial

condition, this was likely caused by participants paying closer attention to the actual visual stimuli in the active condition (Green et al., 2017).

In summary, an incentive-independent risk-taking network could be identified that includes the left aINS, parts of the left and right striatum, and the dACC. Such a network fits the common currency hypothesis (Berridge & Kringelbach, 2013).

### 5.3.5 ADDITIONAL EXPLORATORY ANALYSES

Based on the above identified cluster of differences between social and financial incentives in the IPL, average beta-estimates for that contrast and cluster were calculated for each participant. An exploratory regression model with the beta-estimates as criterion and six predictors based on questionnaires and behavioral data found a single significant predictor of beta-estimates in the IPL-cluster: Higher social risk-taking propensity in the BART is related to higher beta-estimates in the between-incentives contrast. As mentioned above, posterior IPL-activation has been linked to social cognition (Numssen et al., 2021). Furthermore, Ethofer and colleagues (2019) find the right IPL to be involved in the processing of situations where others behave socially accepting towards a participants. Based on the present findings and the prior literature, the differences found in the main analysis in the IPL seem more likely to be an effect specific to the addition of the social incentive.

However, results from these additional analyses are highly exploratory. No hypotheses were formulated beforehand, and statistical thresholds were deliberately more liberal than usual (p < .1). While these liberal thresholds partly counteract the high probability of type II errors resulting from the small

sample size, the sample size itself constrains attempts at generalization from the present findings (Poldrack et al., 2017; Chen et al., 2022). Even though they should not be interpreted on their own, the findings of the exploratory analysis constitute a first cue to the exact implication of the IPL-cluster and provide a starting point for future studies.

## 5.4 Limitations and Outlook

*Task-design*

In the present study, inflating a balloon yielded a fixed reward in both the social and the financial incentive conditions. However, this fixed amount, in combination with an increasing probability of explosion and a larger bank as the balloon grew, leads to a diminishing of the expected value (EV) with each inflation (compare figure 12). The change in EV results in a "tipping point": risk-taking is adaptive before and maladaptive after a specific balloon size.

While the option to differentiate between adaptive and maladaptive risk-taking would allow for specific analyses otherwise not feasible (cf. Dean et al., 2011), it poses a problem for the present analysis. The regressors used for fMRI analysis do not capture the qualitative difference between beneficial and detrimental risk-taking. It is thus unknown if or how such a qualitative difference might have influenced the results. Participants behaved differently depending on the incentive. Accordingly, it cannot be ruled out that differences between the incentive conditions result from a difference in perception of advantageous and detrimental risk-taking. Future research could use a similar design to focus on these differences specifically.

**Figure 12.**

*Expected value for different balloon sizes within the financial incentive condition*
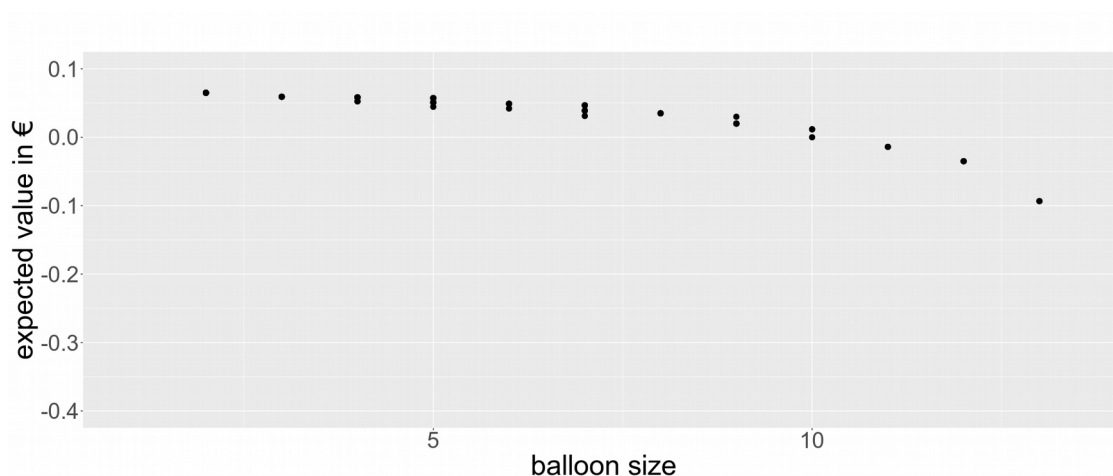


*Note.* For some sizes, different expected values are possible, due to the balloons growing by different amounts with each inflation. Above a size of ten, further inflations have a negative expected value. Expected values for the social conditions were exactly the same, only with gift-bags instead of euros. Figure cropped at a balloon size of 14. Expected value continues to drop exponentially and the smaller scale required to display low values diminishes visibility of the tipping point where EV becomes negative.

An inherent limitation of the BART is that explosion probabilities have to be learned by participants (Schonberg et al., 2010). The present study tried to minimize participants' heterogeneity in education and age, two variables known to influence findings in the BART through learning (Dean et al., 2011; Mata et al., 2011; Mamerow et al., 2016), but a considerable variance in participants' ability to learn the probabilities is likely (Bull et al., 2015). In the fMRI analysis, the actual probability of an explosion was used for the parametric regressors of risk. However, a self-report questionnaire conducted after the measurement revealed notable differences between participants'

expectations and actual probabilities. Most participants reported subjective explosion probabilities that increased mostly linearly with balloon size, while the actual probabilities increased exponentially, as figure 1 in the appendix illustrates. This could just be an artefact due to the misperception of exponential growth (Wagenaar & Sagaria, 1975), a bias also demonstrated in highly educated samples as this one (Schonger & Sele, 2021). However, using the reported probabilities as regressors in the regression model for fMRI analysis might lead to better-fitting regressors or at least a better understanding of exponential growth misperception. While this regression model is not part of this thesis, it is planned as a future exploratory analysis.

*Statistical power, replicability and sample size*

This study used an exploratory whole-brain approach. Previous literature supports the present findings, but false positives cannot be excluded. Direct replications in fMRI research are rare (Turner et al., 2018). However, future studies on a similar topic that would allow for replicating the present analyses should do so. In the above meta-analysis, a notable amount of the 114 studies excluded because no relevant contrast was reported collected all necessary data to calculate a contrast relevant for the meta-analysis but did not do so. Especially studies comparing an experimental and a control group often did not report the results from the control group alone. A more detailed analysis of existing data sets and the communication of all resulting findings of future studies, at least as supplements, are likely to benefit neuroscientific research. One step further, the publication of primary data would allow combining multiple data sets. Thus, more detailed meta-analyses and the application of modern methods to older data sets would be possible. However, such a

publication of primary data would risk infringing on data protection, as structural MRI data can also be used to circumvent anonymization (Theyers et al., 2021). While defacing can mitigate some risks, it would still be possible to link data from different experiments based on defaced structural MRI data (ibid.).

The sample size of the current study is relatively small, as is the resulting statistical power, even for within-participant analyses (Poldrack et al., 2017). The relatively high number of trials (average of 74 inflation events per participant and category) increases the statistical power of the within-participant analyses (Chen et al., 2021, 2022). However, the sample size is too small to allow for a correlation of external variables such as self-reports or behavior with brain activation on a whole-brain basis (Poldrack et al., 2017; Turner et al., 2018; Grady et al., 2021; Chen et al., 2022). Such analyses would be a valuable tool to investigate the neuronal basis of inter-individual differences in risk-taking propensity. The exploratory analysis of beta-estimates of the between-incentives contrast in the IPL-cluster provides a first cue that IPL activation might be related to social incentives specifically. However, due to its exploratory nature and small sample size, it should not be interpreted on its own.

This study used incentives belonging to only two different domains and can thus not depict a domain-general account of risk-taking. However, the two incentive conditions were explicitly designed as similar as possible. Future studies on risk-taking with social and financial incentives could use a design where incentives differ more strongly. Furthermore, social and financial risk-taking are only two of many domains - health risks are essential for

policymakers and might have worse outcomes and higher costs than either financial or social risks on the individual and the societal level. Additionally, behavioral research showed that participants perform worse in a risk-taking task if ,e.g., odors, food, or electric shocks are used as affect-rich outcomes (von Helversen et al., 2020; Rosati & Hare, 2016; Sunstein & Zeckhauser, 2011). Investigating the neuroscientific underpinnings of such effects could further improve our understanding of the differences between adaptive and maladaptive risk-taking.

*Interindividual differences in brain topography*

Besides a general call for larger samples in group analyses (Poldrack et al., 2017; Turner et al., 2018; Grady et al., 2021; Chen et al., 2022), neuroscientific research in the past few years has increasingly focused on individuality in brain topography (Fehr et al., 2019; Dubois et al., 2019; Gilmore et al., 2021). In behavioral research on decision-making, a similar movement exists. Regenwetter and colleagues (2022) criticize an overly simplistic inference from summary statistics to the individual level, with a concurrent call for a stronger focus on the individual instead of the group. The average choice behavior might not reflect any single individual's behavior (Chen et al., 2020). In behavioral research, hierarchical statistical models could be one way to solve the apparent dichotomy between group-level analyses and a focus on the individual (Scheibehenne, 2022). In fMRI research, newly developed methods might fill a similar role. For resting-state and task-based connectivity data, precision fMRI (Laumann et al., 2015; Gordon et al., 2017; Gilmore et al., 2021) promises a high enough resolution to identify inter-individual differences (Gordon et al., 2020). Additionally, Bayesian multilevel modeling (BML, Chen,

Burkner, et al., 2019; Chen, Xiao, et al., 2019) could advance investigations of intersubject correlation in naturalistic fMRI studies (Chen, Xiao, et al., 2019) and brain-behavior correlations in task-based designs with higher precision and less data loss compared to previous methods (Chen et al., 2021).

*Future research directions*

A repeatedly stated aim of neuroscientific research on human risk-taking is the identification of neural correlates of excessive risk-taking in patients (e.g., Macoveanu et al., 2016; Rao et al., 2018) and other at-risk groups, such as young adults (e.g., Yu et al., 2016; Perino et al., 2019). It has been shown that individual differences in network architecture correlate with behavior (Smith et al., 2021). Based on the present study, IPL activation is linked to domain specificity in risk-taking and, as discussed above, considerable heterogeneity in the functional topography of this activation is probable. Future studies should leverage the new possibilities of precision fMRI and BML-approaches to determine if a link between functional topography and risk-taking propensity can be established.

Future studies on risk-taking should consider how they incentivize participants' behavior. While a network of brain regions was identified in the present study that was active independently of whether incentives were social or financial, findings in IPL activation differed in the present study. Based on the exploratory analyses, the difference in brain activation related to the different incentives in the IPL seems to be driven by the social incentive condition. It is, however, unclear if there is a unique component to risk-taking with social incentives, or if it is rather a more general component of risk-processing that is only absent if incentives are financial. On the one hand, it

has previously been argued that financial incentives take a special role, as they can be translated to other domains (Rosati & Hare, 2016). On the other hand, social situations were shown to change participants behavior in risk-taking tasks (Gardner & Steinberg, 2005; Reniers et al., 2017). A future study focusing on the IPL, for example via ROI-analyses, could compare the correlates of risk-taking with social, monetary, and a third incentive domain. A plausible option for a third incentive could be the use of odors akin to the work of von Helversen and colleagues (2020). Results would help to discern if financial or social incentives are unique in their level of IPL-activation. Such studies also promise to further illuminate the boundaries of the domain-general risk-taking network identified here.

Due to the heterogeneity in the topography of heteromodal cortices such as the IPL (c.f., Dubois et al., 2019; Gilmore et al., 2021), the standard approach of voxelwise comparison across subjects might prove inadequate to further examine the details of risk-related activation in the IPL. One way around such problems would be a combined approach of resting-state and task-based analyses akin to the work by Gilmore and colleagues (2019). Extensive resting-state analyses can reveal individual network structures. These network structures can be linked to task-based activation and thus be compared between participants. Comparing the extent and topography of the identified networks with behavioral and self-report measures could unveil possible links between individual functional topography and risk-preference. Furthermore, using these individual ROIs as a basis for correlational analysis of task-based activations and external measures could result in a better signal-to-noise ratio, as it would take topographic heterogeneity in account.

Another way to broaden the understanding of neural correlates of risk-taking would be to investigate decisions with incentives from multiple domains. Real-life decisions often involve the weighting of incentives from various domains. An example is the decision to drive faster to ensure that nobody is upset because one is coming late - weighing a health risk for social risk. Future research on risk-taking or reward-anticipation in different domains should also focus on the role of the right aINS. In the present study and in the work by Gu and colleagues (2019), activation in the right aINS was found to be at least partly dependent on the reward domain, but the underlying reasons are still unclear.

*Implications of findings*

The present findings stress the importance of studying risk-taking with non-financial incentives. It implicates that risk-taking with social and financial incentives differs in risk-taking propensity and neuronal activation patterns. Besides this specific point, the broader implication is that findings from one incentive domain can not necessarily be translated to others. Investigating differences in incentives and domain promises to yield further insight into the details of human risk-taking. General behavior- and brain activation patterns are well researched, but the importance of incentives and, likely, the importance of other context details remains under-explored.

Policy-makers and clinical psychologists are interested in risk-taking in a context where incentives are often non-financial. An example of the former group is young adults who drive fast or take drugs and are likely not motivated by financial incentives. For the latter group, risk-taking in patients with mental illness is linked to several negative symptoms such as aggression or response

disinhibition (c.f., Reddy et al., 2014). When trying to adapt results from laboratory studies to the real-world, differences in incentives and context have to be taken into account.

Policy-makers trying to incentivize prosocial behavior often pursue changes in behavior that are not directly related to financial incentives. Limiting drug use, promoting careful driving, and increasing vaccination rates are all areas where the potential target group takes risks with social and health incentives. Concerning driving behavior, Bingham and colleagues (2016) observed social effects on driving behavior in young adults, as did Simons-Morton and colleagues (2019). Regarding vaccines, Tram and colleagues (2022) found, among other factors, social ("Other people need it more right now") and health ("Plan to wait and see if it is save") concerns responsible for vaccine hesitancy during the early vaccination periods in the SARS-CoV-2 pandemic in the USA. For both examples, the effect of financial incentives on behavior was studied. In "pay-how-you-drive" insurance schemes, risky-driver are identified through continuous measurements of driving behavior. Such drivers have to pay a premium on their insurance. "Pay-how-you-drive" schemes were shown to decrease risky driving, albeit, to the author's knowledge, studies were conducted in the general population and not specific at-risk groups so far (Tselentis et al., 2017). Financial incentives were shown to increase vaccination adherence before the SARS-CoV-2 pandemic (cf. Higgins et al., 2021). A survey on SARS-CoV-2 vaccine hesitancy in Germany found that a financial incentive of 50€ would likely increase vaccine adherence by 2.2 percentage points (Klüver et al., 2021). However, the prospect of getting exemptions from pandemic restrictions had the strongest effect on vaccine adherence in young adults, while older adults were most strongly influenced by the option to get

their vaccination at a local doctor instead of a vaccination center. Of all three incentives, the financial one had the lowest effect.

The literature outlined above highlights the complexity that interventions in risk-taking face once they are applied to the real world. While studies on the effects of interventions in the real world, such as the work by Tselentis and colleagues (2017) on insurance schemes, help clarify real-world effects, laboratory studies allow to separate the different components and study them in isolation. Laboratory studies on the neural correlates of risk-taking offer further possibilities. First, uncovering differences and convergences in the neural correlates of risk-taking for other incentive types promises a better understanding of domain-specificity. A more complete model of the interactions between risk-taking and incentive domains could inform future interventions in excessive risk-taking in areas where incentives are non-financial. Second, better information on the same neuronal networks involved in risk-taking and their dependence on incentives could lead to a better understanding of changes in risk-taking propensity in mental illness.

# Chapter 6: Conclusion

A common network of brain regions activated when taking risks with financial and social risks was identified. It includes the bilateral striatum, the dACC, and the left insular cortex. Overlaps between this network and the domain-general valuation network identified by Gu and colleagues (2019) lead to the conclusion that it might generalize to risk-taking with incentives from other domains besides financial and social. The existence of this network supports the idea of a domain-general risk-taking propensity, as proposed by various authors (e.g., Mata et al., 2018; Zhang et al., 2019).

The link between domain-general risk-taking propensity and exhibited risk-taking in each domain is likely moderated by differences in the perception and valuation of stimuli from different domains. These intra-individual differences dependent on the incentive are connected to activation of the right IPL, at least for risk-taking with social and financial incentives. Based on previous work on heterogeneity in functional topography in the IPL (Laumann et al., 2015; Gordon et al., 2017; Gilmore et al., 2021), it is also a probable source of inter-individual differences in risk-taking propensity.

Research on the neural correlates of human risk-taking has converged on a few regions reliably identified across participants in prior studies (cf. Poudel et al., 2020; Wu et al., 2021). The present thesis is a first step in generalizing these findings to other incentive domains. Based on it, two promising roads to a better understanding of risk-taking can be made out. First, the domain-general risk-taking network proposed here could be tested by investigating the neural correlates of risk-taking with incentives from other domains such as health.

Second, BML or precision fMRI studies on IPL involvement in risk-taking might uncover neural correlates of excessive risk-taking that could lead to a better understanding of altered risk-taking in affected patients.

# Chapter 7: References and Further Material

## 7.1 References

### 7.1.1 References in Text

Afif, A., Minotti, L., Kahane, P., & Hoffmann, D. (2010). Anatomofunctional organization of the insular cortex: a study using intracerebral electrical stimulation in epileptic patients. *Epilepsia, 51(11)*, 2305-2315.

Aklin, W. M., Lejuez, C. W., Zvolensky, M. J., Kahler, C. W., & Gwadz, M. (2005). Evaluation of behavioral measures of risk-taking propensity with inner city adolescents. *Behaviour Research and Therapy, 43(2)*, 215-228.

American Psychiatric Association. (2013). Diagnostic and statistical manual of mental disorders (5th ed.).

Arsalidou, M., Vijayarajah, S., & Sharaev, M. (2020). Basal ganglia lateralization in different types of reward. *Brain Imaging and Behavior, 14*(6), 2618-2646.

Ashenhurst, J. R., Jentsch, J. D., & Ray, L. A. (2011). Risk-taking and alcohol use disorders symptomatology in a sample of problem drinkers. *Experimental and clinical psychopharmacology, 19*(5), 361.

Baddeley, A. (2003). Working memory: looking back and looking forward. *Nature reviews neuroscience, 4(10)*, 829-839.

Balleine, B. W., Delgado, M. R., & Hikosaka, O. (2007). The role of the dorsal striatum in reward and decision-making. *Journal of Neuroscience, 27*(31), 8161-8165.

Bechara, A., Damasio, A. R., Damasio, H., & Anderson, S. W. (1994). Insensitivity to future consequences following damage to human prefrontal cortex. *Cognition, 50*(1-3), 7-15.

Berridge, K. C., & Kringelbach, M. L. (2013). Neuroscience of affect: brain mechanisms of pleasure and displeasure. *Current opinion in neurobiology, 23*(3), 294-303.

Best, R., & Charness, N. (2015). Age differences in the effect of framing on risky choice: A meta-analysis. *Psychology and aging, 30*(3), 688.

Bingham, C. R., Simons-Morton, B. G., Pradhan, A. K., Li, K., Almani, F., Falk, E. B., ... & Albert, P. S. (2016). Peer passenger norms and pressure: experimental effects on simulated driving among teenage males. *Transportation research part F: traffic psychology and behaviour, 41*, 124-137.

Bish, A., & Michie, S. (2010). Demographic and attitudinal determinants of protective behaviours during a pandemic: A review. *British journal of health psychology, 15*(4), 797-824.

Bjork, J. M., Momenan, R., Smith, A. R., & Hommer, D. W. (2008). Reduced posterior mesofrontal cortex activation by risky rewards in substance-dependent patients. *Drug and alcohol dependence, 95*(1-2), 115-128.

Bjork, J. M., Smith, A. R., Danube, C. L., & Hommer, D. W. (2007). Developmental differences in posterior mesofrontal cortex recruitment by risky rewards. *Journal of Neuroscience, 27*(18), 4839-4849.

Blais, A. R., & Weber, E. U. (2006). A domain-specific risk-taking (DOSPERT) scale for adult populations. *Judgment and Decision making, 1*(1), 33-47.

Boorman, E. D., Behrens, T. E., Woolrich, M. W., & Rushworth, M. F. (2009). How green is the grass on the other side? Frontopolar cortex and the evidence in favor of alternative courses of action. *Neuron, 62*(5), 733-743.

Boukhdhir, A., Zhang, Y., Mignotte, M., & Bellec, P. (2021). Unraveling reproducible dynamic states of individual brain functional parcellation. *Network Neuroscience, 5(*1), 28-55.

Boyer, T. W. (2006). The development of risk-taking: A multi-perspective review. *Developmental Review, 26*(3), 291-345.

Braga, R. M., & Leech, R. (2015). Echoes of the brain: local-scale representation of whole-brain functional networks within transmodal cortex. *The Neuroscientist, 21*(5), 540-551.

Brainard, D. H. (1997). The psychophysics toolbox. *Spatial vision, 10*(4), 433-436.

Bran, A., & Vaidis, D. C. (2019). Assessing risk-taking: what to measure and how to measure it. *Journal of Risk Research, 23*(4), 490-503.

Brevers, D., Bechara, A., Hermoye, L., Divano, L., Kornreich, C., Verbanck, P., & Noël, X. (2015). Comfort for uncertainty in pathological gamblers: A fMRI study. *Behavioural Brain Research, 278*, 262-270.

Bridges, D., Pitiot, A., MacAskill, M. R., & Peirce, J. W. (2020). The timing mega-study: comparing a range of experiment generators, both lab-based and online. *PeerJ, 8*, e9414.

Brigadoi, S., Moro, S. B., Falchi, R., Cutini, S., & Dell'Acqua, R. (2018). On pacing trials while scanning brain hemodynamics: the case of the SNARC effect. *Psychonomic Bulletin & Review, 25*(6), 2267-2273.

Buckert, M., Schwieren, C., Kudielka, B. M., & Fiebach, C. J. (2014). Acute stress affects risk taking but not ambiguity aversion. *Frontiers in neuroscience, 8(*82), 1-11.

Bull, P. N., Tippett, L. J., & Addis, D. R. (2015). Decision making in healthy participants on the Iowa Gambling Task: new insights from an operant approach. *Frontiers in Psychology,* 391.

Caspers, S., Zilles, K., Laird, A. R., & Eickhoff, S. B. (2010). ALE meta-analysis of action observation and imitation in the human brain. *NeuroImage, 50*(3), 1148-1167.

Caspers, S., Schleicher, A., Bacha-Trams, M., Palomero-Gallagher, N., Amunts, K., & Zilles, K. (2013). Organization of the human inferior parietal lobule based on receptor architectonics. *Cerebral Cortex, 23*(3), 615-628.

Chan, N. C., Li, K., & Hirsh, J. (2020). Peripheral oxygen saturation in older persons wearing nonmedical face masks in community settings. *JAMA, 324*(22), 2323-2324.

Chandrakumar, D., Feuerriegel, D., Bode, S., Grech, M., & Keage, H. A. (2018). Event-related potentials in relation to risk-taking: a systematic review. *Frontiers in Behavioral Neuroscience, 12*, 111.

Chen, H., Cohen, P., & Chen, S. (2010). How big is a big odds ratio? Interpreting the magnitudes of odds ratios in epidemiological studies. *Communications in Statistics—simulation and Computation, 39*(4), 860-864.

Chen, G., Taylor, P. A., & Cox, R. W. (2017). Is the statistic value all we should care about in neuroimaging?. *NeuroImage, 147*, 952-959.

Chen, G., Bürkner, P. C., Taylor, P. A., Li, Z., Yin, L., Glen, D. R., ... & Pessoa, L. (2019). An integrative Bayesian approach to matrix-based analysis in neuroimaging. *Human brain mapping, 40*(14), 4072-4090.

Chen, G., Xiao, Y., Taylor, P. A., Rajendra, J. K., Riggins, T., Geng, F., ... & Cox, R. W. (2019). Handling multiplicity in neuroimaging through Bayesian lenses with multilevel modeling. *Neuroinformatics, 17*(4), 515-545.

Chen, G., Padmala, S., Chen, Y., Taylor, P. A., Cox, R. W., & Pessoa, L. (2021). To pool or not to pool: Can we ignore cross-trial variability in FMRI?. *NeuroImage, 225*, 117496.

Chen, G., Pine, D. S., Brotman, M. A., Smith, A. R., Cox, R. W., Taylor, P. A., & Haller, S. P. (2022). Hyperbolic trade-off: the importance of balancing trial and subject sample sizes in neuroimaging. *NeuroImage, 247*, 118786.

Clark, L., Studer, B., Bruss, J., Tranel, D., & Bechara, A. (2014). Damage to insula abolishes cognitive distortions during simulated gambling. *Proceedings of the National Academy of Sciences, 111*(16), 6098-6103.

Cohn, A., Engelmann, J., Fehr, E., & Maréchal, M. A. (2015). Evidence for countercyclical risk aversion: An experiment with financial professionals. *American Economic Review, 105*(2), 860-85.

Congdon, E., Bato, A. A., Schonberg, T., Mumford, J. A., Karlsgodt, K. H., Sabb, F. W., ... & Poldrack, R. A. (2013). Differences in neural activation as a function of risk-taking task parameters. *Frontiers in neuroscience, 7*, 173.

Cox, R. W. (1996). AFNI: software for analysis and visualization of functional magnetic resonance neuroimages. *Computers and Biomedical research, 29*(3), 162-173.

Cox, R. W., & Hyde, J. S. (1997). Software tools for analysis and visualization of fMRI data. *NMR in Biomedicine 10*(4-5), 171-178.

Cox, R. W., & Glen, D. R. (2013). Nonlinear warping in AFNI. Poster presented at the 19th Annual Meeting of the Organization for Human Brain Mapping.

Cox, R. W., Chen, G., Glen, D. R., Reynolds, R. C., & Taylor, P. A. (2017). fMRI clustering and false-positive rates. *Proceedings of the National Academy of Sciences, 114*(17), E3370-E3371.

Cox, R. W., Chen, G., Glen, D. R., Reynolds, R. C., & Taylor, P. A. (2017). FMRI clustering in AFNI: false-positive rates redux. *Brain connectivity, 7(3)*, 152-171.

De Groot, K., & Thurik, R. (2018). Disentangling risk and uncertainty: When risk-taking measures are not about risk. *Frontiers in Psychology, 9*, 2194.

Decker, S., & Schmitz, H. (2016). Health shocks and risk aversion. *Journal of health economics, 50*, 156-170.

Distefano, A., Jackson, F., Levinson, A. R., Infantolino, Z. P., Jarcho, J. M., & Nelson, B. D. (2018). A comparison of the electrocortical response to monetary and social reward. *Social, Cognitive and Affective Neuroscience, 13*(3), 247-255.

Dubois, J., & Adolphs, R. (2016). Building a science of individual differences from fMRI. *Trends in cognitive sciences, 20*(6), 425-443.

Dunn, B. D., Dalgleish, T., & Lawrence, A. D. (2006). The somatic marker hypothesis: A critical evaluation. *Neuroscience & Biobehavioral Reviews, 30*(2), 239-271.

Eickhoff, S. B., Laird, A. R., Grefkes, C., Wang, L. E., Zilles, K., & Fox, P. T. (2009). Coordinate-based activation likelihood estimation meta-analysis of neuroimaging data: A random-effects approach based on empirical estimates of spatial uncertainty. *Human brain mapping, 30*(9), 2907-2926.

Eickhoff, S. B., Bzdok, D., Laird, A. R., Kurth, F., & Fox, P. T. (2012). Activation likelihood estimation meta-analysis revisited. *NeuroImage, 59*(3), 2349-2361.

Eickhoff, S. B., Laird, A. R., Fox, P. T., Bzdok, D., Hensel, L. (2016). Functional segregation of the human dorsomedial prefrontal cortex. *Cerebral Cortex 26*, 304–321.

Ethofer, T., Stegmaier, S., Koch, K., Reinl, M., Kreifelts, B., Schwarz, L., ... & Wildgruber, D. (2020). Are you laughing at me? Neural correlates of social intent attribution to auditory and visual laughter. *Human Brain Mapping, 41*(2), 353-361.

Fan, L., Li, H., Zhuo, J., Zhang, Y., Wang, J., Chen, L., ... & Jiang, T. (2016). The human brainnetome atlas: a new brain atlas based on connectional architecture. *Cerebral cortex, 26*(8), 3508-3526.

Faul, F., Erdfelder, E., Buchner, A., & Lang, A.-G. (2009). Statistical power analyses using G*Power 3.1: Tests for correlation and regression analyses. *Behavior Research Methods, 41*, 1149-1160.

Feinberg, D. A., & Setsompop, K. (2013). Ultra-fast MRI of the human brain with simultaneous multi-slice imaging. *Journal of magnetic resonance, 229,* 90-100.

Ferbinteanu, J. (2019). Memory systems 2018–Towards a new paradigm. *Neurobiology of learning and memory, 157*, 61-78.

Fiore, V. G., & Gu, X. (2022). Similar network compositions, but distinct neural dynamics underlying belief updating in environments with and without explicit outcomes. *NeuroImage, 247*, 118821.

Fischhoff, B., & Broomell, S. B. (2020). Judgment and decision making. *Annual Review of Psychology, 71*(1), 331-355.

Flores, A., Münte, T. F., & Doñamayor, N. (2015). Event-related EEG responses to anticipation and delivery of monetary and social reward. *Biological psychology, 109*, 10-19.

Fonov, V., Evans, A. C., Botteron, K., Almli, C. R., McKinstry, R. C., Collins, D. L., & Brain Development Cooperative Group. (2011). Unbiased average age-appropriate atlases for pediatric studies. *NeuroImage, 54*(1), 313-327.

Friedl, A., Pondorfer, A., & Schmidt, U. (2020). Gender differences in social risk taking. *Journal of Economic Psychology, 77*, 102182.

Fukunaga, R., Brown, J. W., & Bogg, T. (2012). Decision making in the Balloon Analogue Risk Task (BART): anterior cingulate cortex signals loss aversion

but not the infrequency of risky choices. *Cognitive, Affective, & Behavioral Neuroscience, 12*(3), 479-490.

Fukunaga, R., Purcell, J. R., & Brown, J. W. (2018). Discriminating formal representations of risk in anterior cingulate cortex and inferior frontal gyrus. *Frontiers in Neuroscience, 12*, 553.

Gardner, M., & Steinberg, L. (2005). Peer influence on risk taking, risk preference, and risky decision making in adolescence and adulthood: an experimental study. *Developmental psychology, 41*(4), 625.

Gasquoine, P. G. (2014). Contributions of the insula to cognition and emotion. *Neuropsychology review, 24*(2), 77-87.

Gignac, G. E., & Szodorai, E. T. (2016). Effect size guidelines for individual differences researchers. *Personality and individual differences, 102*, 74-78.

Gilman, J. M., Smith, A. R., Ramchandani, V. A., Momenan, R., & Hommer, D. W. (2012). The effect of intravenous alcohol on the neural correlates of risky decision making in healthy social drinkers. *Addiction biology, 17*(2), 465-478.

Gilmore, A. W., Nelson, S. M., & McDermott, K. B. (2015). A parietal memory network revealed by multiple MRI methods. *Trends in cognitive sciences, 19*(9), 534-543.

Gilmore, A. W., Nelson, S. M., Laumann, T. O., Gordon, E. M., Berg, J. J., Greene, D. J., ... & McDermott, K. B. (2019). High-fidelity mapping of repetition-related changes in the parietal memory network. *NeuroImage, 199*, 427-439.

Gilmore, A. W., Nelson, S. M., & McDermott, K. B. (2021). Precision functional mapping of human memory systems. *Current Opinion in Behavioral Sciences, 40*, 52-57.

Glen, D. R., Taylor, P. A., Buchsbaum, B. R., Cox, R. W., & Reynolds, R. C. (2020). Beware (surprisingly common) left-right flips in your MRI data: an efficient and robust method to check MRI dataset consistency using AFNI. *Frontiers in neuroinformatics, 18*.

Gordon, E. M., Laumann, T. O., Gilmore, A. W., Newbold, D. J., Greene, D. J., Berg, J. J., ... & Dosenbach, N. U. (2017). Precision functional mapping of individual human brains. *Neuron, 95*(4), 791-807.

Gordon, E. M., Laumann, T. O., Marek, S., Raut, R. V., Gratton, C., Newbold, D. J., ... & Nelson, S. M. (2020). Default-mode network streams for coupling to language and control systems. *Proceedings of the National Academy of Sciences, 117*(29), 17308-17319.

Gowin, J. L., Mackey, S., & Paulus, M. P. (2013). Altered risk-related processing in substance users: imbalance of pain and gain. *Drug and alcohol dependence, 132*(1-2), 13-21.

Grady, C. L., Rieck, J. R., Nichol, D., Rodrigue, K. M., & Kennedy, K. M. (2021). Influence of sample size and analytic approach on stability and interpretation of brain-behavior correlations in task-related fMRI data. *Human Brain Mapping, 42*(1), 204-219.

Green, J. J., Boehler, C. N., Roberts, K. C., Chen, L. C., Krebs, R. M., Song, A. W., & Woldorff, M. G. (2017). Cortical and subcortical coordination of visual spatial attention revealed by simultaneous EEG–fMRI recording. *Journal of Neuroscience, 37*(33), 7803-7810.

Gu, R., Huang, W., Camilleri, J., Xu, P., Wei, P., Eickhoff, S. B., & Feng, C. (2019). Love is analogous to money in human brain: Coordinate-based and functional connectivity meta-analyses of social and monetary reward anticipation. *Neuroscience & Biobehavioral Reviews, 100*, 108-128.

Haddad, A. D., Harrison, F., Norman, T., & Lau, J. Y. (2014). Adolescent and adult risk-taking in virtual social contexts. *Frontiers in psychology, 5*, 1476.

Harty, S., Robertson, I. H., Miniussi, C., Sheehy, O. C., Devine, C. A., McCreery, S., & O'Connell, R. G. (2014). Transcranial direct current stimulation over right dorsolateral prefrontal cortex enhances error awareness in older age. *Journal of Neuroscience, 34*(10), 3646-3652.

Harwell, M. R., Rubinstein, E. N., Hayes, W. S., & Olds, C. C. (1992). Summarizing Monte Carlo results in methodological research: The one-and

two-factor fixed effects ANOVA cases. *Journal of educational statistics, 17*(4), 315-339.

Hembrook-Short, J. R., Mock, V. L., Usrey, W. M., & Briggs, F. (2019). Attention enhances the efficacy of communication in V1 local circuits. *Journal of Neuroscience, 39*(6), 1066-1076.

Hertrich, I., Dietrich, S., Blum, C., & Ackermann, H. (2021). The role of the dorsolateral prefrontal cortex for speech and language processing. *Frontiers in Human Neuroscience, 15*, 217.

Higgins, S. T., Klemperer, E. M., & Coleman, S. R. (2021). Looking to the empirical literature on the potential for financial incentives to enhance adherence with COVID-19 vaccination. *Preventive medicine, 145*, 106421.

Holroyd, C. B., & Verguts, T. (2021). The best laid plans: computational principles of anterior cingulate cortex. *Trends in Cognitive Sciences, 25*(4), 316-329.

Hövermann, A., & Kohlrausch, B. (2020). Soziale Ungleichheit und Einkommenseinbußen in der Corona-Krise–Befunde einer Erwerbstätigenbefragung. *WSI Mitteilungen, 6*, 485-492.

Hulvershorn, L. A., Hummer, T. A., Fukunaga, R., Leibenluft, E., Finn, P., Cyders, M. A., ... & Brown, J. (2015). Neural activation during risky decision-making in youth at high risk for substance use disorders. *Psychiatry Research: Neuroimaging, 233*(2), 102-111.

Hunt, M. K., Hopko, D. R., Bare, R., Lejuez, C. W., & Robinson, E. V. (2005). Construct validity of the balloon analog risk task (BART) associations with psychopathy and impulsivity. Assessment, 12(4), 416-428.

Hwang, K., Bertolero, M. A., Liu, W. B., & D'Esposito, M. (2017). The human thalamus is an integrative hub for functional brain networks. *Journal of Neuroscience, 37*(23), 5594-5607.

Jauhar, S., Fortea, L., Solanes, A., Albajes-Eizagirre, A., McKenna, P. J., & Radua, J. (2021). Brain activations associated with anticipation and delivery of monetary reward: A systematic review and meta-analysis of fMRI studies. *PloS one, 16*(8), e0255292.

Josef, A. K., Richter, D., Samanez-Larkin, G. R., Wagner, G. G., Hertwig, R., & Mata, R. (2016). Stability and change in risk-taking propensity across the adult life span. *Journal of Personality and Social Psychology, 111*(3), 430-450.

Kann, L., McManus, T., Harris, W. A., Shanklin, S. L., Flint, K. H., Queen, B., Lowry, R., Chyen, D., Whittle, L., Thornton, J. & Lim, C. (2018). Youth risk behavior surveillance—United States, 2017. *MMWR Surveillance Summaries, 67*(8), 1.

Karlsson, M. P., Tervo, D. G., & Karpova, A. Y. (2012). Network resets in medial prefrontal cortex mark the onset of behavioral uncertainty. *Science, 338*(6103), 135-139.

Klüver, H., Hartmann, F., Humphreys, M., Geissler, F., & Giesecke, J. (2021). Incentives can spur COVID-19 vaccination uptake. *Proceedings of the National Academy of Sciences, 118*(36), e2109543118.

Knight, F. H. (1921). Risk, uncertainty and profit, reprint: 1971. Library of Economics and Liberty.

Kohno, M., Ghahremani, D. G., Morales, A. M., Robertson, C. L., Ishibashi, K., Morgan, A. T., ... & London, E. D. (2015). Risk-taking behavior: dopamine D2/D3 receptors, feedback, and frontolimbic activity. *Cerebral cortex, 25*(1), 236-245.

Kolling, N., Behrens, T.E., Mars, R.B. & Rushworth, M.F. Neural mechanisms of foraging. *Science 336,* 95–98 (2012).

Kolling, N., Wittmann, M. K., Behrens, T. E., Boorman, E. D., Mars, R. B., & Rushworth, M. F. (2016). Value, search, persistence and model updating in anterior cingulate cortex. *Nature neuroscience, 19*(10), 1280-1285.

Kolling, N., & O'Reilly, J. X. (2018). State-change decisions and dorsomedial prefrontal cortex: The importance of time. *Current Opinion in Behavioral Sciences, 22*, 152-160.

Krain, A. L., Wilson, A. M., Arbuckle, R., Castellanos, F. X., & Milham, M. P. (2006). Distinct neural mechanisms of risk and ambiguity: a meta-analysis of decision-making. *NeuroImage, 32*(1), 477-484.

Kray, L., & Gonzalez, R. (1999). Differential weighting in choice versus advice: I'll do this, you do that. *Journal of Behavioral Decision Making, 12*(3), 207-218.

Kurth, F., Eickhoff, S. B., Schleicher, A., Hoemke, L., Zilles, K., & Amunts, K. (2010). Cytoarchitecture and probabilistic maps of the human posterior insular cortex. *Cerebral cortex, 20*(6), 1448-1461.

Kurth, F., Zilles, K., Fox, P. T., Laird, A. R., & Eickhoff, S. B. (2010). A link between the systems: functional differentiation and integration within the human insula revealed by meta-analysis. *Brain Structure and Function, 214*(5), 519-534.

Kurzban, R., Duckworth, A., Kable, J. W., & Myers, J. (2013). An opportunity cost model of subjective effort and task performance. *Behavioral and brain sciences, 36*(6), 661-679.

Kyllonen, P. C., & Zu, J. (2016). Use of response time for measuring cognitive ability. *Journal of Intelligence, 4*(4), 14.

Laird, A. R., Eickhoff, S. B., Kurth, F., Fox, P. M., Uecker, A. M., Turner, J. A., ... & Fox, P. T. (2009). ALE meta-analysis workflows via the brainmap database: progress towards a probabilistic functional brain atlas. *Frontiers in neuroinformatics, 3*, 23.

Laird, A. R., Fox, P. M., Price, C. J., Glahn, D. C., Uecker, A. M., Lancaster, J. L., Turkeltaub, P. E., Kochunov, P. & Fox, P. T. (2005). ALE meta-analysis: Controlling the false discovery rate and performing statistical contrasts. *Human brain mapping, 25*(1), 155-164.

Laird, A. R., Robinson, J. L., McMillan, K. M., Tordesillas-Gutiérrez, D., Moran, S. T., Gonzales, S. M., ... & Lancaster, J. L. (2010). Comparison of the disparity between Talairach and MNI coordinates in functional neuroimaging data: validation of the Lancaster transform. *NeuroImage, 51*(2), 677-683.

Lancaster, J. L., Tordesillas-Gutiérrez, D., Martinez, M., Salinas, F., Evans, A., Zilles, K., ... & Fox, P. T. (2007). Bias between MNI and Talairach coordinates analyzed using the ICBM-152 brain template. *Human brain mapping, 28*(11), 1194-1205.

Lau, B., & Glimcher, P. W. (2008). Value representations in the primate striatum during matching behavior. *Neuron, 58*(3), 451-463.

Laumann, T. O., Gordon, E. M., Adeyemo, B., Snyder, A. Z., Joo, S. J., Chen, M. Y., ... & Petersen, S. E. (2015). Functional system and areal organization of a highly sampled individual human brain. *Neuron, 87*(3), 657-670.

Lauriola, M., Panno, A., Levin, I. P., & Lejuez, C. W. (2014). Individual differences in risky decision making: A meta-analysis of sensation seeking and impulsivity with the balloon analogue risk task. *Journal of Behavioral Decision Making, 27*(1), 20-36.

Law, C. S., Lan, P. S., & Glover, G. H. (2021). Effect of wearing a face mask on fMRI BOLD contrast. *NeuroImage, 229*, 117752.

Lei, Y., Wang, L., Chen, P., Li, Y., Han, W., Ge, M., Yang, L., Chen, S., Hu, W., Wu, X. & Yang, Z. (2017) Neural correlates of increased risk-taking propensity in sleep-deprived people along with a changing risk level. *Brain Imaging Behav. 11*(6), 1910-1921.

Lejuez, C. W., Read, J. P., Kahler, C. W., Richards, J. B., Ramsey, S. E., Stuart, G. L., Strong, D. R. & Brown, R. A. (2002). Evaluation of a behavioral measure of risk taking: the Balloon Analogue Risk Task (BART). *Journal of Experimental Psychology: Applied, 8*(2), 75-84.

Levin, I. P., & Hart, S. S. (2003). Risk preferences in young children: Early evidence of individual differences in reaction to potential gains and losses. *Journal of Behavioral Decision Making, 16*(5), 397-413.

Levy, I. (2017). Neuroanatomical substrates for risk behavior. *The Neuroscientist, 23*(3), 275-286.

Li, X., Morgan, P. S., Ashburner, J., Smith, J., & Rorden, C. (2016). The first step for neuroimaging data analysis: DICOM to NIfTI conversion. *Journal of neuroscience methods, 264*, 47-56.

Lipshitz, R., & Strauss, O. (1997). Coping with uncertainty: A naturalistic decision-making analysis. *Organizational Behavior and Human Decision Processes, 69*(2), 149-163.

Liu, X., Hairston, J., Schrier, M., & Fan, J. (2011). Common and distinct networks underlying reward valence and processing stages: a meta-analysis of functional neuroimaging studies. *Neuroscience & Biobehavioral Reviews, 35*(5), 1219-1236.

Lix, L. M., Keselman, J. C., & Keselman, H. J. (1996). Consequences of assumption violations revisited: A quantitative review of alternatives to the one-way analysis of variance F test. *Review of educational research, 66(*4), 579-619.

Macoveanu, J., Miskowiak, K., Kessing, L. V., Vinberg, M., & Siebner, H. R. (2016). Healthy co-twins of patients with affective disorders show reduced risk-related activation of the insula during a monetary gambling task. *Journal of Psychiatry and Neuroscience, 41*(1), 38-47.

Malmendier, U., & Nagel, S. (2011). Depression babies: do macroeconomic experiences affect risk taking?. *The quarterly journal of economics, 126*(1), 373-416.

Mamerow, L., Frey, R., & Mata, R. (2016). Risk taking across the life span: A comparison of self-report and behavioral measures of risk taking. *Psychology and Aging, 31*(7), 711.

Mata, R., Josef, A. K., Samanez-Larkin, G. R., & Hertwig, R. (2011). Age differences in risky choice: a meta-analysis. *Annals of the New York Academy of Sciences, 1235*, 18-19.

Mata, R., Frey, R., Richter, D., Schupp, J., & Hertwig, R. (2018). Risk preference: A view from psychology. *Journal of Economic Perspectives, 32*(2), 155-72.

Miedl, S. F., Fehr, T., Meyer, G., & Herrmann, M. (2010). Neurobiological correlates of problem gambling in a quasi-realistic blackjack scenario as revealed by fMRI. *Neuroimaging, 181*(3), 165-173.

Mishra, S. (2014). Decision-making under risk: Integrating perspectives from biology, economics, and psychology. *Personality and Social Psychology Review, 18*(3), 280-307.

Mohr, P. N., Biele, G., & Heekeren, H. R. (2010). Neural processing of risk. *Journal of Neuroscience, 30*(19), 6613-6619.

Molenberghs, P., Cunnington, R., & Mattingley, J. B. (2009). Is the mirror neuron system involved in imitation? A short review and meta-analysis. *Neuroscience & biobehavioral reviews, 33*(7), 975-980.

Mueller, S., Wang, D., Fox, M. D., Yeo, B. T., Sepulcre, J., Sabuncu, M. R., ... & Liu, H. (2013). Individual variability in functional connectivity architecture of the human brain. *Neuron, 77*(3), 586-595.

Murphy, K., & Garavan, H. (2004). An empirical investigation into the number of subjects required for an event-related fMRI study. *NeuroImage, 22*(2), 879-885.

Murphy, R. O., Ackermann, K. A., & Handgraaf, M. (2011). Measuring social value orientation. *Judgment and Decision making, 6*(8), 771-781.

Ngetich, R., Zhou, J., Zhang, J., Jin, Z., & Li, L. (2020). Assessing the effects of continuous theta burst stimulation over the dorsolateral prefrontal cortex on human cognition: a systematic review. *Frontiers in integrative neuroscience, 35*.

Nicolaou, N., & Shane, S. (2019). Common genetic effects on risk-taking preferences and choices. *Journal of Risk and Uncertainty, 59*(3), 261-279.

Numssen, O., Bzdok, D., & Hartwigsen, G. (2021). Functional specialization within the inferior parietal lobes across cognitive domains. *elife, 10*.

Oehrn, C. R., Hanslmayr, S., Fell, J., Deuker, L., Kremers, N. A., Do Lam, A. T., ... & Axmacher, N. (2014). Neural communication patterns underlying conflict detection, resolution, and adaptation. *Journal of Neuroscience, 34*(31), 10438-10452.

Ogawa, A., Ueshima, A., Inukai, K., & Kameda, T. (2018). Deciding for others as a neutral party recruits risk-neutral perspective-taking: Model-based behavioral and fMRI experiments. *Scientific reports, 8*(1), 1-10.

Page, M. J., McKenzie, J. E., Bossuyt, P. M., Boutron, I., Hoffmann, T. C., Mulrow, C. D., ... & Moher, D. (2021). The PRISMA 2020 statement: an

updated guideline for reporting systematic reviews. *International Journal of Surgery, 88*, 105906.

Panikratova, Y. R., Vlasova, R. M., Akhutina, T. V., Korneev, A. A., Sinitsyn, V. E., & Pechenkova, E. V. (2020). Functional connectivity of the dorsolateral prefrontal cortex contributes to different components of executive functions. *International Journal of Psychophysiology, 151*, 70-79.

Paulus, M. P., & Frank, L. R. (2006). Anterior cingulate activity modulates nonlinear decision weight function of uncertain prospects. *NeuroImage, 30*(2), 668-677.

Pelli, D. G. (1997). The VideoToolbox software for visual psychophysics: Transforming numbers into movies. *Spatial vision, 1*0, 437-442.

Perino, M. T., Guassi Moreira, J. F., McCormick, E. M., & Telzer, E. H. (2019). Apples to apples? Neural correlates of emotion regulation differences between high-and low-risk adolescents. *Social cognitive and affective neuroscience, 14*(8), 827-836.

Pletzer, B., & Ortner, T. M. (2016). Neuroimaging supports behavioral personality assessment: Overlapping activations during reflective and impulsive risk taking. *Biological psychology, 119*, 46-53.

Poldrack, R. A., Baker, C. I., Durnez, J., Gorgolewski, K. J., Matthews, P. M., Munafò, M. R., ... & Yarkoni, T. (2017). Scanning the horizon: towards transparent and reproducible neuroimaging research. *Nature reviews neuroscience, 18*(2), 115-126.

Poldrack, R. A., Mumford, J. A., & Nichols, T. E. (2011). Handbook of functional MRI data analysis. Cambridge University Press.

Pollak, Y., Poni, B., Gershy, N., & Aran, A. (2020). The role of parental monitoring in mediating the link between adolescent ADHD symptoms and risk-taking behavior. *Journal of attention disorders, 24*(8), 1141-1147.

Poudel, R., Riedel, M. C., Salo, T., Flannery, J. S., Hill-Bowen, L. D., Eickhoff, S. B., Larid, A. R. & Sutherland, M. T. (2020). Common and distinct brain activity associated with risky and ambiguous decision-making. *Drug and alcohol dependence, 209*, 107884.

Rademacher, L., Krach, S., Kohls, G., Irmak, A., Gründer, G., & Spreckelmeyer, K. N. (2010). Dissociation of neural networks for anticipation and consumption of monetary and social rewards. *NeuroImage, 49*(4), 3276-3285.

Rao, H., Korczykowski, M., Pluta, J., Hoang, A., & Detre, J. A. (2008). Neural correlates of voluntary and involuntary risk taking in the human brain: an fMRI Study of the Balloon Analog Risk Task (BART). *NeuroImage, 42*(2), 902-910.

Rao, L. L., Zhou, Y., Zheng, D., Yang, L. Q., & Li, S. (2018). Genetic contribution to variation in risk taking: a functional MRI twin study of the balloon analogue risk task. *Psychological Science, 29*(10), 1679-1691.

Reddy, L. F., Lee, J., Davis, M. C., Altshuler, L., Glahn, D. C., Miklowitz, D. J., & Green, M. F. (2014). Impulsivity and risk taking in bipolar disorder and schizophrenia. *Neuropsychopharmacology, 39*(2), 456-463.

Regenwetter, M., Robinson, M. M., & Wang, C. (2022). Are you an exception to your favorite decision theory? Behavioral decision research is a linda problem!. *Decision, 9*(2), 91–111.

Reniers, R. L., Beavan, A., Keogan, L., Furneaux, A., Mayhew, S., & Wood, S. J. (2017). Is it all in the reward? Peers influence risk-taking behaviour in young adulthood. *British Journal of Psychology, 108*(2), 276-295.

Robinson, J. L., Laird, A. R., Glahn, D. C., Blangero, J., Sanghera, M. K., Pessoa, L., ... & Fox, P. T. (2012). The functional connectivity of the human caudate: an application of meta-analytic connectivity modeling with behavioral filtering. *NeuroImage, 60*(1), 117-129.

Rosati, A. G., & Hare, B. (2016). Reward currency modulates human risk preferences. *Evolution and Human Behavior, 37*(2), 159-168.

Saad, Z. S., Glen, D. R., Chen, G., Beauchamp, M. S., Desai, R., & Cox, R. W. (2009). A new method for improving functional-to-structural MRI alignment using local Pearson correlation. *NeuroImage, 44*(3), 839-848.

Scheibehenne, B. (2022). Experimenter meets correlator: Comment on Regenwetter et al. (2022). *Decision, 9*(2), 121–123.

Schmider, E., Ziegler, M., Danay, E., Beyer, L., & Bühner, M. (2010). Is it really robust? Reinvestigating the robustness of ANOVA against violations of the normal distribution assumption. *Methodology, 6*(4), 147.

Schmitz, F., Manske, K., Preckel, F., & Wilhelm, O. (2016). The multiple faces of risk-taking. *European Journal of Psychological Assessment* (2016).

Scholkmann, F., Fischer, J. B., Frisk, L. K., Delgado-Mederos, R., Mayos, M., Highton, D., ... & Durduran, T. (2021). Influence of study design on effects of mask wearing on fMRI BOLD contrast and systemic physiology—A comment on Law et al.(2021). *NeuroImage, 244*, 118549.

Schonberg, T., Fox, C. R., & Poldrack, R. A. (2010). Mind the gap: bridging economic and naturalistic risk-taking with cognitive neuroscience. *Trends in cognitive sciences, 1*5(1), 11-19.

Schonberg, T., Fox, C. R., Mumford, J. A., Congdon, E., Trepel, C., & Poldrack, R. A. (2012). Decreasing ventromedial prefrontal cortex activity during sequential risk-taking: an fMRI investigation of the balloon analog risk task. *Frontiers in neuroscience, 6*, 80.

Schonger, M., & Sele, D. (2021). Intuition and exponential growth: bias and the roles of parameterization and complexity. *Mathematische Semesterberichte, 68*(2), 221-235.

Seeber, M., Cantonas, L. M., Hoevels, M., Sesia, T., Visser-Vandewalle, V., & Michel, C. M. (2019). Subcortical electrophysiological activity is detectable with high-density EEG source imaging. *Nature communications, 10*(1), 1-7.

Seikel, J. A. T., & Seikel, J. A. T. (2018). An attentional view of right hemisphere dysfunction. *Clinical Archives of Communication Disorders, 3*(1), 76-88.

Sevi, B., & Shook, N. J. (2021). The relation between disgust sensitivity and risk-taking propensity: A domain specific approach. *Judgment & Decision Making, 16*(4).

Shenhav, A., Botvinick, M. M., & Cohen, J. D. (2013). The expected value of control: an integrative theory of anterior cingulate cortex function. *Neuron, 79*(2), 217-240.

Sherman, L., Steinberg, L., & Chein, J. (2018). Connecting brain responsivity and real-world risk taking: Strengths and limitations of current methodological approaches. *Developmental Cognitive Neuroscience, 33,* 27-41.

Sherman, S. M. (2016). Thalamus plays a central role in ongoing cortical functioning. *Nature neuroscience, 19*(4), 533-541.

Shima, K., Isoda, M., Mushiake, H., & Tanji, J. (2007). Categorization of behavioural sequences in the prefrontal cortex. *Nature, 445*(7125), 315-318.

Shou, Y., De Silva, H. S., & Olney, J. (2022). Attitudes toward ambiguous situations resemble the domain-specificity of attitudes toward risk. *Personality and Individual Differences, 195*, 111667.

Simons-Morton, B. G., Bingham, C. R., Li, K., Zhu, C., Buckley, L., Falk, E. B., & Shope, J. T. (2019). The effect of teenage passengers on simulated risky driving among teenagers: A randomized trial. *Frontiers in psychology, 10*, 923.

Skeel, R. L., Pilarski, C., Pytlak, K., & Neudecker, J. (2008). Personality and performance-based measures in the prediction of alcohol use. *Psychology of Addictive Behaviors, 22*(3), 402.

Smith, D. M., Perez, D. C., Porter, A., Dworetsky, A., & Gratton, C. (2021). Light through the fog: using precision fMRI data to disentangle the neural substrates of cognitive control. *Current Opinion in Behavioral Sciences, 40*, 19-26.

Smith, E. H., Horga, G., Yates, M. J., Mikell, C. B., Banks, G. P., Pathak, Y. J., ... & Sheth, S. A. (2019). Widespread temporal coding of cognitive control in the human prefrontal cortex. *Nature neuroscience, 22*(11), 1883-1891.

Solomou, I., & Constantinidou, F. (2020). Prevalence and predictors of anxiety and depression symptoms during the COVID-19 pandemic and compliance with precautionary measures: age and sex matter. *International journal of environmental research and public health, 17*(14), 4924.

Song, J. H., Rowland, J., McPeek, R. M., & Wade, A. R. (2011). Attentional modulation of fMRI responses in human V1 is consistent with distinct spatial maps for chromatically defined orientation and contrast. *Journal of Neuroscience, 31*(36), 12900-12905.

Stone, E. R., Yates, A. J., & Caruthers, A. S. (2002). Risk Taking in Decision Making for Others Versus the Self 1. *Journal of Applied Social Psychology, 32*(9), 1797-1824.

Stone, E. R., YoonSun, C., Bruine de Bruin, W., & Mandel, D. R. (2013). I can take the risk, but you should be safe: Self-other differences in situations involving physical safety. *Judgment and Decision making, 8*(3), 250-267.

Strigo, Irina A., and Arthur D. Craig. "Interoception, homeostatic emotions and sympathovagal balance." *Philosophical Transactions of the Royal Society B: Biological Sciences 371*.1708 (2016): 20160010.

Sun, Q., Jiang, T., Zhang, J., Wu, Q., Zhao, L., & Hu, F. (2020). Riskier for me or for others? The role of domain and probability in self-other differences, in risky decision-making. *The Journal of General Psychology, 147*(2), 169-185.

Sunstein, C. R., & Zeckhauser, R. (2011). Overreaction to fearsome risks. *Environmental and Resource Economics, 48*(3), 435-449.

Talairach, J. (1967). Atlas of stereotaxic anatomy of the telencephalon: anatomo-radiological studies. Masson.

Talairach, J., Tournoux, P. (1988) Co-planar stereotaxic atlas of the human brain: 3-Dimensional proportional system: An approach to cerebral imaging. Thieme Medical Publishers, Inc., New York.

Tamimi, A., Dahbour, S., Al-Btush, A., Al-Qudah, A., Masri, A., Al-Ghanem, S., ... & Tamimi, I. (2022). Facemask wearing does not impact neuro-electrical brain activity. *Scientific Reports, 12*(1), 1-8.

Theyers, A. E., Zamyadi, M., O'Reilly, M., Bartha, R., Symons, S., MacQueen, G. M., ... & Arnott, S. R. (2021). Multisite comparison of MRI defacing software across multiple cohorts. *Frontiers in psychiatry, 12*, 617997.

Tram, K. H., Saeed, S., Bradley, C., Fox, B., Eshun-Wilson, I., Mody, A., & Geng, E. (2022). Deliberation, Dissent, and Distrust: Understanding Distinct Drivers of Coronavirus Disease 2019 Vaccine Hesitancy in the United States. *Clinical infectious diseases, 74*(8), 1429-1441.

Triarhou, L. C. (2007). The Economo-Koskinas atlas revisited: cytoarchitectonics and functional context. *Stereotactic and functional neurosurgery, 85*(5), 195-203.

Tselentis, D. I., Yannis, G., & Vlahogianni, E. I. (2017). Innovative motor insurance schemes: A review of current practices and emerging challenges. *Accident Analysis & Prevention, 98*, 139-148.

Turkeltaub, P. E., Eden, G. F., Jones, K. M., & Zeffiro, T. A. (2002). Meta-analysis of the functional neuroanatomy of single-word reading: method and validation. *NeuroImage, 16*(3), 765-780.

Turkeltaub, P. E., Eickhoff, S. B., Laird, A. R., Fox, M., Wiener, M., & Fox, P. (2012). Minimizing within-experiment and within-group effects in activation likelihood estimation meta-analyses. *Human brain mapping, 33*(1), 1-13.

Turner, B. O., Paul, E. J., Miller, M. B., & Barbey, A. K. (2018). Small sample sizes reduce the replicability of task-based fMRI studies. *Communications Biology, 1(*1), 1-10.

Uddin, L. Q., Nomi, J. S., Hébert-Seropian, B., Ghaziri, J., & Boucher, O. (2017). Structure and function of the human insula. *Journal of clinical neurophysiology, 34*(4), 300.

Ulrich, M., Keller, J., Hoenig, K., Waller, C., & Gron, G. (2014). Neural correlates of experimentally induced flow experiences. *NeuroImage, 86*, 194–202.

Venkatraman, V., Payne, J. W., Bettman, J. R., Luce, M. F., & Huettel, S. A. (2009). Separate neural mechanisms underlie choices and strategic preferences in risky decision making. *Neuron, 62*(4), 593-602.

Vermeer, A. B. L., Boksem, M. A., & Sanfey, A. G. (2014). Neural mechanisms underlying context-dependent shifts in risk preferences. NeuroImage, 103, 355-363.

Voloh, B., Valiante, T. A., Everling, S., & Womelsdorf, T. (2015). Theta–gamma coordination between anterior cingulate and prefrontal cortex indexes correct attention shifts. *Proceedings of the National Academy of Sciences, 112*(27), 8457-8462.

von Helversen, B., Coppin, G., & Scheibehenne, B. (2020). Money does not stink: Using unpleasant odors as stimulus material changes risky decision making. *Journal of Behavioral Decision Making, 33*(5), 593-605.

Von Siebenthal, Z., Boucher, O., Rouleau, I., Lassonde, M., Lepore, F., & Nguyen, D. K. (2017). Decision-making impairments following insular and medial temporal lobe resection for drug-resistant epilepsy. *Social cognitive and affective neuroscience, 12*(1), 128-137.

Vrtička, P., Sander, D., Anderson, B., Badoud, D., Eliez, S., & Debbané, M. (2014). Social feedback processing from early to late adolescence: influence of sex, age, and attachment style. *Brain and behavior, 4*(5), 703-720.

Wagenaar, W. A., & Sagaria, S. D. (1975). Misperception of exponential growth. *Perception & Psychophysics, 18*(6), 416-422.

Weber, E. U., Anderson, C. J., & Birnbaum, M. H. (1992). A theory of perceived risk and attractiveness. O*rganizational Behavior and Human Decision Processes, 52*(3), 492-523.

Williams, S. N., Armitage, C. J., Tampe, T., & Dienes, K. (2020). Public perceptions and experiences of social distancing and social isolation during the COVID-19 pandemic: A UK-based focus group study. *BMJ open, 10*(7), e039334.

Wise, T., Zbozinek, T. D., Michelini, G., Hagan, C. C., & Mobbs, D. (2020). Changes in risk perception and self-reported protective behaviour during the first week of the COVID-19 pandemic in the United States. *Royal Society open science, 7*(9), 200742.

Wu, S., Sun, S., Camilleri, J. A., Eickhoff, S. B., & Yu, R. (2021). Better the devil you know than the devil you don't: Neural processing of risk and ambiguity. *NeuroImage, 236*, 118109.

Xiong, Y., & Newman, S. (2021). Both activation and deactivation of functional networks support increased sentence processing costs. *NeuroImage, 225,* 117475.

Yu, J., Mamerow, L., Lei, X., Fang, L., & Mata, R. (2016). Altered value coding in the ventromedial prefrontal cortex in healthy older adults. *Frontiers in aging neuroscience, 8*, 210.

Zhang, D. C., Highhouse, S., & Nye, C. D. (2019). Development and validation of the general risk propensity scale (GRiPS). *Journal of Behavioral Decision Making, 32*(2), 152-167.

## 7.1.2 Studies included in the meta-analysis

Bjork, J. M., Momenan, R., Smith, A. R., & Hommer, D. W. (2008). Reduced posterior mesofrontal cortex activation by risky rewards in substance-dependent patients. *Drug and alcohol dependence, 95*(1-2), 115-128.

Bjork, J. M., Smith, A. R., Danube, C. L., & Hommer, D. W. (2007). Developmental differences in posterior mesofrontal cortex recruitment by risky rewards. *Journal of Neuroscience, 27*(18), 4839-4849.

Brevers, D., Bechara, A., Hermoye, L., Divano, L., Kornreich, C., Verbanck, P., & Noël, X. (2015). Comfort for uncertainty in pathological gamblers: A fMRI study. *Behavioural Brain Research, 278,* 262-270.

Campbell-Meiklejohn, D. K., Woolrich, M. W., Passingham, R. E., & Rogers, R. D. (2008). Knowing when to stop: the brain mechanisms of chasing losses. *Biological psychiatry, 63*(3), 293-300.

Cohen, M. X., Heller, A. S., & Ranganath, C. (2005). Functional connectivity with anterior cingulate and orbitofrontal cortices during decision-making. *Cognitive Brain Research, 23*(1), 61-70.

Congdon, E., Bato, A. A., Schonberg, T., Mumford, J. A., Karlsgodt, K. H., Sabb, F. W., ... & Poldrack, R. A. (2013). Differences in neural activation as a function of risk-taking task parameters. *Frontiers in neuroscience, 7*, 173.

Engelmann, J. B., & Tamir, D. (2009). Individual differences in risk preference predict neural responses during financial decision-making. *Brain research, 1290*, 28-51.

Fukunaga, R., Brown, J. W., & Bogg, T. (2012). Decision making in the Balloon Analogue Risk Task (BART): anterior cingulate cortex signals loss aversion

but not the infrequency of risky choices. *Cognitive, Affective, & Behavioral Neuroscience, 12*(3), 479-490.

Fukunaga, R., Purcell, J. R., & Brown, J. W. (2018). Discriminating formal representations of risk in anterior cingulate cortex and inferior frontal gyrus. *Frontiers in Neuroscience, 12*, 553.

Gilman, J. M., Smith, A. R., Ramchandani, V. A., Momenan, R., & Hommer, D. W. (2012). The effect of intravenous alcohol on the neural correlates of risky decision making in healthy social drinkers. *Addiction biology, 17*(2), 465-478.

Häusler, A. N., Kuhnen, C. M., Rudorf, S., & Weber, B. (2018). Preferences and beliefs about financial risk taking mediate the association between anterior insula activation and self-reported real-life stock trading. *Scientific reports, 8*(1), 1-13.

Kohno, M., Ghahremani, D. G., Morales, A. M., Robertson, C. L., Ishibashi, K., Morgan, A. T., ... & London, E. D. (2015). Risk-taking behavior: dopamine D2/D3 receptors, feedback, and frontolimbic activity. *Cerebral cortex, 25*(1), 236-245.

Lee, T. M., Leung, A. W., Fox, P. T., Gao, J. H., & Chan, C. C. (2008). Age-related differences in neural activities during risk taking as revealed by functional MRI. *Social cognitive and affective neuroscience, 3*(1), 7-15.

Li, X., Pan, Y., Fang, Z., Lei, H., Zhang, X., Shi, H., ... & Rao, H. (2020). Test-retest reliability of brain responses to risk-taking during the balloon analogue risk task. *NeuroImage, 209*, 116495.

Liu, L., Xue, G., Potenza, M. N., Zhang, J. T., Yao, Y. W., Xia, C. C., ... & Fang, X. Y. (2017). Dissociable neural processes during risky decision-making in individuals with Internet-gaming disorder. *NeuroImage, 14*, 741-749.

Vermeer, A. B. L., Boksem, M. A., & Sanfey, A. G. (2014). Neural mechanisms underlying context-dependent shifts in risk preferences. *NeuroImage, 103*, 355-363.

Macoveanu, J., Fisher, P. M., Madsen, M. K., Mc Mahon, B., Knudsen, G. M., & Siebner, H. R. (2016). Bright-light intervention induces a dose-dependent

increase in striatal response to risk in healthy volunteers. *NeuroImage, 139*, 37-43.

Macoveanu, J., Miskowiak, K., Kessing, L. V., Vinberg, M., & Siebner, H. R. (2016). Healthy co-twins of patients with affective disorders show reduced risk-related activation of the insula during a monetary gambling task. *Journal of Psychiatry and Neuroscience, 41*(1), 38-47.

Matthews, S. C., Simmons, A. N., Lane, S. D., & Paulus, M. P. (2004). Selective activation of the nucleus accumbens during risk-taking decision making. *Neuroreport, 15*(13), 2123-2127.

Meder, D., Haagensen, B. N., Hulme, O., Morville, T., Gelskov, S., Herz, D. M., ... & Siebner, H. R. (2016). Tuning the brake while raising the stake: network dynamics during sequential decision-making. *Journal of neuroscience, 36*(19), 5417-5426.

Miedl, S. F., Fehr, T., Meyer, G., & Herrmann, M. (2010). Neurobiological correlates of problem gambling in a quasi-realistic blackjack scenario as revealed by fMRI. Psychiatry Research: *Neuroimaging, 181(*3), 165-173.

Paulus, M. P., Rogalsky, C., Simmons, A., Feinstein, J. S., & Stein, M. B. (2003). Increased activation in the right insula during risk-taking decision making is related to harm avoidance and neuroticism. *NeuroImage, 19*(4), 1439-1448.

Paulus, M. P., & Frank, L. R. (2006). Anterior cingulate activity modulates nonlinear decision weight function of uncertain prospects. *NeuroImage, 30*(2), 668-677.

Pletzer, B., & Ortner, T. M. (2016). Neuroimaging supports behavioral personality assessment: Overlapping activations during reflective and impulsive risk taking. *Biological psychology, 119*, 46-53.

Rao, H., Korczykowski, M., Pluta, J., Hoang, A., & Detre, J. A. (2008). Neural correlates of voluntary and involuntary risk taking in the human brain: an fMRI Study of the Balloon Analog Risk Task (BART). *NeuroImage, 42*(2), 902-910.

Roy, A. K., Gotimer, K., Kelly, A. C., Castellanos, F. X., Milham, M. P., & Ernst, M. (2011). Uncovering putative neural markers of risk avoidance. *Neuropsychologia, 49*(5), 937-944.

Schonberg, T., Fox, C. R., Mumford, J. A., Congdon, E., Trepel, C., & Poldrack, R. A. (2012). Decreasing ventromedial prefrontal cortex activity during sequential risk-taking: an fMRI investigation of the balloon analog risk task. *Frontiers in neuroscience, 6*, 80.

Smith, B. W., Mitchell, D. G., Hardin, M. G., Jazbec, S., Fridberg, D., Blair, R. J. R., & Ernst, M. (2009). Neural substrates of reward magnitude, probability, and risk during a wheel of fortune decision-making task. *NeuroImage, 44*(2), 600-609.

Symmonds, M., Wright, N. D., Bach, D. R., & Dolan, R. J. (2011). Deconstructing risk: Separable encoding of variance and skewness in the brain. *NeuroImage, 58*(4), 1139-1149.

Weber, B. J., & Huettel, S. A. (2008). The neural substrates of probabilistic and intertemporal decision making. *Brain research, 1234*, 104-115.

Wright, N. D., Symmonds, M., & Dolan, R. J. (2013). Distinct encoding of risk and value in economic choice between multiple risky options. *NeuroImage, 81*, 431-440.

Xue, G., Lu, Z., Levin, I. P., Weller, J. A., Li, X., & Bechara, A. (2009). Functional dissociations of risk and reward processing in the medial prefrontal cortex. *Cerebral cortex, 19*(5), 1019-1027.

Yu, J., Mamerow, L., Lei, X., Fang, L., & Mata, R. (2016). Altered value coding in the ventromedial prefrontal cortex in healthy older adults. *Frontiers in aging neuroscience, 8*, 210.

Zhang, X., Li, S., Liu, Y., Chen, X., Shang, X., Qi, F., ... & Chen, J. (2019). Gain–loss situation modulates neural responses to self–other decision making under risk. *Scientific reports, 9*(1), 1-9.

### 7.1.3 SOFTWARE

Eaton, J. W., Bateman, D., Hauberg, S. & Wehbring, R. (2017). GNU Octave version 4.2.1 manual: a high-level interactive language for numerical computations. URL https://www.gnu.org/software/octave/doc/v4.2.1/

Kleiner, M., Brainard, D., & Pelli, D. (2007). What's new in Psychtoolbox-3?. Perception, 36, ECVP Abstract Supplement.

R Core Team (2022). R: A language and environment for statistical computing. R Foundation for Statistical Computing, Vienna, Austria.

RStudio Team (2022). RStudio: Integrated Development Environment for R. RStudio, PBC, Boston, MA.

## 7.2 Lists of Tables and Figures

### 7.2.1 LIST OF TABLES

### 7.2.2 LIST OF FIGURES

## 7.3 Abbreviations

| Abbreviation | Full term |
| --- | --- |
| ACC | anterior cingulate cortex |
| ADHD | attention deficit hyperactivity disorder |
| aINS | anterior Insula |
| ALE | activation likelihood estimation (cf. Turkeltaub et al. 2002) |
| ANOVA | analysis of variance |
| BA | Brodmann Area |
| BART | balloon analogue risk task |
| BML | Bayesian multilevel modeling |
| BOLD | blood-oxygen-level-dependent |
| dACC | dorsal anterior cingulate cortex |
| dlPFC | dorsolateral prefrontal cortex |
| dmPFC | dorsomedial prefrontal cortex |
| DOSPERT | domain-specific risk-taking scale |
| EEG | electroencephalography |
| EPI | echo-planar imaging |
| ERP | event related potential |
| EV | expected value |
| fMRI | functional magnetic resonance imaging |
| GLT | general linear test |
| GRiPS | "general risk propensity scale |
| IFG | inferior frontal gyrus |
| IGT | Iowa Gambling Task (cf. Bechara et al. 1994) |
| IPL | inferior parietal lobule |
| ISI | inter stimulus interval |
| ITI | inter trial interval |
| mOFC | medial orbitofrontal cortex |
| MRI | magnetic resonance imaging |
| NAc | nucleus Accumbens |

| Abbreviation | Full term |
| --- | --- |
| OC | occipital cortex |
| PMN | parietal memory network |
| PRISMA | preferred reporting items for systematic reviews and meta-analyses (cf. Page et al. 2021) |
| ROI | region of interest |
| RSN | resting state network |
| SARS-CoV-2 | severe acute respiratory syndrome coronavirus type 2 |
| SPL | superior parietal lobule |
| STG | superior temporal gyrus |
| SVO-Scale | Social Value Orientation Scale (cf. Murphy et al., 2011) |
| TPJ | temporoparietal junction |
| TR | repetition time |

## 7.4 Revisions for Published Version

Page 75, line 19 and following:

"Functional MRI data were preprocessed as follows:[...] and defaced through AFNI[...]"

changed to:

"MRI data were preprocessed as follows: [...] and structural data were defaced through AFNI[...]".


Page 78, line 14:

"A symbolic GLM was calculated [...]."

changed to:

"A symbolic GLT was calculated [...]."

# Chapter 8: Appendix

## 8.1 Table 1 – All peaks identified for the ALE meta-analysis

| Study | year | Region | Talairach | | | MNI | | | effect size | | Nr | dir. |
|---|---|---|---|---|---|---|---|---|---|---|---|---|
| | | | X | Y | Z | X | Y | Z | t | z | | |
| Bjork et al. | 2008 | L posterior mesofrontal cortex | 4 | 11 | 44 | | | | 8.19 | | 4 | NR |
| Bjork et al. | 2008 | L inferior parietal lobule | 41 | -38 | 53 | | | | 7.45 | | 4 | NR |
| Bjork et al. | 2008 | L inferior parietal lobule | 26 | -49 | 39 | | | | 6.59 | | 4 | NR |
| Bjork et al. | 2008 | L middle temporal gyrus | -30 | -71 | 20 | | | | 5.68 | | 4 | NR |
| Bjork et al. | 2008 | R rniddle temporal gyrus | 38 | -53 | 0 | | | | 7.45 | | 4 | NR |
| Bjork et al. | 2008 | Dorsomesial cerebellum | 4 | -56 | -4 | | | | 7.21 | | 4 | NR |
| Bjork et al. | 2008 | L middle frontal gyrus | -38 | 26 | 29 | | | | 6.89 | | 4 | NR |
| Bjork et al. | 2008 | R middle frontal gyrus | 38 | 30 | 24 | | | | 7.14 | | 4 | NR |
| Bjork et al. | 2008 | R middle frontal gyrus | 30 | -4 | 58 | | | | 6.26 | | 4 | NR |
| Bjork et al. | 2008 | R posterior mesofrontal cortex | 11 | 4 | 58 | | | | 6.87 | | 4 | NR |
| Bjork et al. | 2008 | L insula | -30 | -15 | 20 | | | | 6.8 | | 4 | NR |
| Bjork et al. | 2008 | R superior occipital gyrus | 26 | -71 | 39 | | | | 6.77 | | 4 | NR |
| Bjork et al. | 2008 | L precentra l gyrus | -30 | -8 | 44 | | | | 6.23 | | 4 | NR |
| Bjork et al. | 2008 | R posterior cingulate | 4 | -34 | 24 | | | | 5.8 | | 4 | NR |
| Bjork et al. | 2008 | L superior parietal lobule | -15 | -60 | 53 | | | | 5.7 | | 4 | NR |
| Bjork et al. | 2008 | R precuneus | 8 | -75 | 48 | | | | 5.63 | | 4 | NR |
| Bjork et al. | 2008 | R superior frontal gyrus | 34 | 49 | 15 | | | | 5.27 | | 4 | NR |
| Bjork et al. | 2008 | L middle frontal gyrus | -34 | 34 | 20 | | | | 5.65 | | 5 | NR |
| Bjork et al. | 2008 | L middle frontal gyrus | -26 | 38 | 37 | | | | 5.57 | | 5 | NR |
| Bjork et al. | 2008 | R middle frontal gyrus | 19 | 0 | 53 | | | | 9.32 | | 5 | NR |
| Bjork et al. | 2008 | R middle frontal gyrus | 26 | 34 | 39 | | | | 6.9 | | 5 | NR |
| Bjork et al. | 2008 | R superior occipital gyrus | 27 | -68 | 39 | | | | 8.98 | | 5 | NR |
| Bjork et al. | 2008 | L putamen | -19 | 11 | 4 | | | | 8.63 | | 5 | NR |
| Bjork et al. | 2008 | R thalamus | 12 | -12 | 15 | | | | 8.53 | | 5 | NR |
| Bjork et al. | 2008 | L thalamus | -19 | -26 | 15 | | | | 8.35 | | 5 | NR |
| Bjork et al. | 2008 | L cuneus | -4 | -83 | 15 | | | | 8.18 | | 5 | NR |
| Bjork et al. | 2008 | L postcentral gyrus | -49 | -30 | 48 | | | | 7.77 | | 5 | NR |
| Bjork et al. | 2008 | L postcentral gyrus | -26 | -11 | 48 | | | | 7.5 | | 5 | NR |
| Bjork et al. | 2008 | L superior frontal gyrus | -11 | -4 | 63 | | | | 7.73 | | 5 | NR |
| Bjork et al. | 2008 | L posterior mesofrontal cortex | -4 | 4 | 44 | | | | 7.71 | | 5 | NR |
| Bjork et al. | 2008 | R substantia nigra | 11 | -19 | -4 | | | | 7.42 | | 5 | NR |
| Bjork et al. | 2008 | L anterior cingulate cortex | -4 | 19 | 24 | | | | 7.2 | | 5 | NR |
| Bjork et al. | 2008 | R inferior parietal lobule | 41 | -45 | 53 | | | | 7.15 | | 5 | NR |
| Bjork et al. | 2008 | Dorsomesial cerebellum | 0 | -60 | -4 | | | | 6.97 | | 5 | NR |
| Bjork et al. | 2008 | L middle occipital gyrus | -41 | -68 | -4 | | | | 6.7 | | 5 | NR |
| Bjork et al. | 2008 | L middle occipital gyrus | -30 | -75 | 24 | | | | 5.52 | | 5 | NR |
| Bjork et al. | 2008 | R middle occipital gyrus | 38 | -64 | 10 | | | | 5.61 | | 5 | NR |
| Bjork et al. | 2008 | L superior parietal lobule | -11 | -64 | 58 | | | | 6.53 | | 5 | NR |
| Bjork et al. | 2008 | R lingual gyrus | 19 | -53 | 4 | | | | 6.39 | | 5 | NR |
| Bjork et al. | 2008 | R lingual gyrus | 8 | -90 | -4 | | | | 5.62 | | 5 | NR |
| Bjork et al. | 2008 | L cuneus | -4 | -79 | 15 | | | | 7.37 | | 5 | NR |
| Bjork et al. | 2008 | R cuneus | 15 | 71 | 15 | | | | 7.51 | | 5 | NR |
| Bjork et al. | 2008 | L lingual gyrus | -11 | -56 | 5 | | | | 6 | | 5 | NR |
| Bjork et al. | 2008 | R lingual gyrus | 11 | -49 | 5 | | | | 5.48 | | 5 | NR |
| Brevers et al. | 2015 | L Precentral gyrus | | | | -37 | -27 | 56 | 4.9 | | 6 | neg |
| Brevers et al. | 2015 | L Superior temporal gyrus | | | | -64 | -23 | 14 | 6.07 | | 6 | neg |
| Brevers et al. | 2015 | L Posterior insular cortex | | | | -38 | -23 | 15 | 5.26 | | 6 | neg |
| Brevers et al. | 2015 | L Superior temporal gyrus | | | | -64 | -40 | 8 | 5.28 | | 6 | neg |
| Brevers et al. | 2015 | R middle frontal gyrus | | | | 30 | 54 | 3 | 5.2 | | 6 | neg |
| Campbell et al. | 2008 | L gyrus rectus (anterior peak) | | | | -6 | 50 | -16 | 4.15 | | 7 | pos |
| Campbell et al. | 2008 | L gryus rectus (posterior peak) | | | | -6 | 38 | -18 | 3.34 | | 7 | pos |

| Study | year | Region | Talairach | | | MNI | | | effect size | | Nr | dir. |
|---|---|---|---|---|---|---|---|---|---|---|---|---|
| | | | X | Y | Z | X | Y | Z | t | z | | |
| Bjork et al. | 2008 | L posterior mesofrontal cortex | 4 | 11 | 44 | | | | 8.19 | | 4 | NR |
| Bjork et al. | 2008 | L inferior parietal lobule | 41 | -38 | 53 | | | | 7.45 | | 4 | NR |
| Bjork et al. | 2008 | L inferior parietal lobule | 26 | -49 | 39 | | | | 6.59 | | 4 | NR |
| Bjork et al. | 2008 | L middle temporal gyrus | -30 | -71 | 20 | | | | 5.68 | | 4 | NR |
| Bjork et al. | 2008 | R rniddle temporal gyrus | 38 | -53 | 0 | | | | 7.45 | | 4 | NR |
| Bjork et al. | 2008 | Dorsomesial cerebellum | 4 | -56 | -4 | | | | 7.21 | | 4 | NR |
| Bjork et al. | 2008 | L middle frontal gyrus | -38 | 26 | 29 | | | | 6.89 | | 4 | NR |
| Bjork et al. | 2008 | R middle frontal gyrus | 38 | 30 | 24 | | | | 7.14 | | 4 | NR |
| Bjork et al. | 2008 | R middle frontal gyrus | 30 | -4 | 58 | | | | 6.26 | | 4 | NR |
| Bjork et al. | 2008 | R posterior mesofrontal cortex | 11 | 4 | 58 | | | | 6.87 | | 4 | NR |
| Bjork et al. | 2008 | L insula | -30 | -15 | 20 | | | | 6.8 | | 4 | NR |
| Bjork et al. | 2008 | R superior occipital gyrus | 26 | -71 | 39 | | | | 6.77 | | 4 | NR |
| Bjork et al. | 2008 | L precentra l gyrus | -30 | -8 | 44 | | | | 6.23 | | 4 | NR |
| Bjork et al. | 2008 | R posterior cingulate | 4 | -34 | 24 | | | | 5.8 | | 4 | NR |
| Bjork et al. | 2008 | L superior parietal lobule | -15 | -60 | 53 | | | | 5.7 | | 4 | NR |
| Bjork et al. | 2008 | R precuneus | 8 | -75 | 48 | | | | 5.63 | | 4 | NR |
| Bjork et al. | 2008 | R superior frontal gyrus | 34 | 49 | 15 | | | | 5.27 | | 4 | NR |
| Bjork et al. | 2008 | L middle frontal gyrus | -34 | 34 | 20 | | | | 5.65 | | 5 | NR |
| Bjork et al. | 2008 | L middle frontal gyrus | -26 | 38 | 37 | | | | 5.57 | | 5 | NR |
| Bjork et al. | 2008 | R middle frontal gyrus | 19 | 0 | 53 | | | | 9.32 | | 5 | NR |
| Bjork et al. | 2008 | R middle frontal gyrus | 26 | 34 | 39 | | | | 6.9 | | 5 | NR |
| Bjork et al. | 2008 | R superior occipital gyrus | 27 | -68 | 39 | | | | 8.98 | | 5 | NR |
| Bjork et al. | 2008 | L putamen | -19 | 11 | 4 | | | | 8.63 | | 5 | NR |
| Bjork et al. | 2008 | R thalamus | 12 | -12 | 15 | | | | 8.53 | | 5 | NR |
| Bjork et al. | 2008 | L thalamus | -19 | -26 | 15 | | | | 8.35 | | 5 | NR |
| Bjork et al. | 2008 | L cuneus | -4 | -83 | 15 | | | | 8.18 | | 5 | NR |
| Bjork et al. | 2008 | L postcentral gyrus | -49 | -30 | 48 | | | | 7.77 | | 5 | NR |
| Bjork et al. | 2008 | L postcentral gyrus | -26 | -11 | 48 | | | | 7.5 | | 5 | NR |
| Bjork et al. | 2008 | L superior frontal gyrus | -11 | -4 | 63 | | | | 7.73 | | 5 | NR |
| Bjork et al. | 2008 | L posterior mesofrontal cortex | -4 | 4 | 44 | | | | 7.71 | | 5 | NR |
| Bjork et al. | 2008 | R substantia nigra | 11 | -19 | -4 | | | | 7.42 | | 5 | NR |
| Bjork et al. | 2008 | L anterior cingulate cortex | -4 | 19 | 24 | | | | 7.2 | | 5 | NR |
| Bjork et al. | 2008 | R inferior parietal lobule | 41 | -45 | 53 | | | | 7.15 | | 5 | NR |
| Bjork et al. | 2008 | Dorsomesial cerebellum | 0 | -60 | -4 | | | | 6.97 | | 5 | NR |
| Bjork et al. | 2008 | L middle occipital gyrus | -41 | -68 | -4 | | | | 6.7 | | 5 | NR |
| Bjork et al. | 2008 | L middle occipital gyrus | -30 | -75 | 24 | | | | 5.52 | | 5 | NR |
| Bjork et al. | 2008 | R middle occipital gyrus | 38 | -64 | 10 | | | | 5.61 | | 5 | NR |
| Bjork et al. | 2008 | L superior parietal lobule | -11 | -64 | 58 | | | | 6.53 | | 5 | NR |
| Bjork et al. | 2008 | R lingual gyrus | 19 | -53 | 4 | | | | 6.39 | | 5 | NR |
| Bjork et al. | 2008 | R lingual gyrus | 8 | -90 | -4 | | | | 5.62 | | 5 | NR |
| Bjork et al. | 2008 | L cuneus | -4 | -79 | 15 | | | | 7.37 | | 5 | NR |
| Bjork et al. | 2008 | R cuneus | 15 | 71 | 15 | | | | 7.51 | | 5 | NR |
| Bjork et al. | 2008 | L lingual gyrus | -11 | -56 | 5 | | | | 6 | | 5 | NR |
| Bjork et al. | 2008 | R lingual gyrus | 11 | -49 | 5 | | | | 5.48 | | 5 | NR |
| Brevers et al. | 2015 | L Precentral gyrus | | | | -37 | -27 | 56 | 4.9 | | 6 | neg |
| Brevers et al. | 2015 | L Superior temporal gyrus | | | | -64 | -23 | 14 | 6.07 | | 6 | neg |
| Brevers et al. | 2015 | L Posterior insular cortex | | | | -38 | -23 | 15 | 5.26 | | 6 | neg |
| Brevers et al. | 2015 | L Superior temporal gyrus | | | | -64 | -40 | 8 | 5.28 | | 6 | neg |
| Brevers et al. | 2015 | R middle frontal gyrus | | | | 30 | 54 | 3 | 5.2 | | 6 | neg |
| Campbell et al. | 2008 | L gyrus rectus (anterior peak) | | | | -6 | 50 | -16 | 4.15 | | 7 | pos |
| Campbell et al. | 2008 | L gryus rectus (posterior peak) | | | | -6 | 38 | -18 | 3.34 | | 7 | pos |

Appendix: Table 1 – All peaks identified for the ALE meta-analysis

| Study | year | Region | Talairach | | | MNI | | | effect size | | Nr | dir. |
|---|---|---|---|---|---|---|---|---|---|---|---|---|
| | | | X | Y | Z | X | Y | Z | t | z | | |
| Campbell et al. | 2008 | B subgenual ACC | | | | -2 | 6 | -12 | 3.13 | | 7 | pos |
| Campbell et al. | 2008 | L parietal cortex, angular gyrus | | | | -54 | -70 | 26 | 3.82 | | 7 | pos |
| Campbell et al. | 2008 | B dorsal ACC | | | | -4 | 22 | 38 | 5.47 | | 7 | neg |
| Campbell et al. | 2008 | R anterior insula | | | | 36 | 18 | 0 | 5.42 | | 7 | neg |
| Campbell et al. | 2008 | R middle frontal gyrus | | | | 38 | 30 | 36 | 4.47 | | 7 | neg |
| Campbell et al. | 2008 | R middle frontal gyrus | | | | 40 | 8 | 52 | 4.46 | | 7 | neg |
| Campbell et al. | 2008 | L insula, anterior | | | | -32 | 20 | 2 | 4.69 | | 7 | neg |
| Campbell et al. | 2008 | B mid posterior CC | | | | 0 | -30 | 26 | 4.55 | | 7 | neg |
| Campbell et al. | 2008 | L caudate nucleus/putamen | | | | -18 | 18 | -4 | 3.65 | | 7 | neg |
| Campbell et al. | 2008 | R caudate nucleus/putamen | | | | 18 | 18 | -6 | 3.62 | | 7 | neg |
| Campbell et al. | 2008 | L inferior parietal gyrus | | | | 44 | -52 | 52 | 5.2 | | 7 | neg |
| Campbell et al. | 2008 | L inferior parietal gyrus | | | | -42 | -44 | 48 | 4.83 | | 7 | neg |
| Campbell et al. | 2008 | B occipital cortex, cuneus | | | | 8 | -74 | 6 | 4.57 | | 7 | neg |
| Campbell et al. | 2008 | B parietal cortex, precuneus | | | | 4 | -74 | 44 | 4.47 | | 7 | neg |
| Cohen et al. | 2005 | R orbital frontal | | | | 24 | 39 | -12 | 4.72 | | 8 | pos |
| Cohen et al. | 2005 | R Cingulate | | | | 7 | 43 | 23 | 4.48 | | 8 | pos |
| Cohen et al. | 2005 | R middle frontal | | | | 52 | 33 | 20 | 4.47 | | 8 | pos |
| Cohen et al. | 2005 | L inferior parietal lobule | | | | -63 | -33 | 51 | 4.98 | | 8 | pos |
| Cohen et al. | 2005 | L lateral temporal | | | | -51 | -54 | -20 | 5.23 | | 8 | pos |
| Congdon et al. | 2013 | B ACC to OC | | | | 2 | 22 | 38 | | 5.83 | 9 | pos |
| Congdon et al. | 2013 | R Post. PC | | | | 50 | -40 | 52 | | 3.93 | 9 | pos |
| Congdon et al. | 2013 | L Post. PC | | | | -40 | -42 | 48 | | 4.07 | 9 | pos |
| Engelmann et al. | 2009 | Superior frontal gyrus | 24.8 | 48 | 32.6 | | | | | 6.09 | 10 | pos |
| Engelmann et al. | 2009 | Superior frontal gyrus | 19.8 | 33.9 | 45.4 | | | | | 5.96 | 10 | pos |
| Engelmann et al. | 2009 | Anterior cingulate cortex | 11.6 | 33.5 | -0.5 | | | | | 6.16 | 10 | pos |
| Engelmann et al. | 2009 | Middle frontal gyrus | 29.7 | 32.4 | -13 | | | | | 9.95 | 10 | pos |
| Engelmann et al. | 2009 | Anterior cingulate cortex | 12 | 28.5 | 30.9 | | | | | 6.6 | 10 | pos |
| Engelmann et al. | 2009 | Anterior cingulate cortex | -4.1 | 26.8 | 28.5 | | | | | 9.42 | 10 | pos |
| Engelmann et al. | 2009 | Caudate nucleus | -13 | 9.8 | 10 | | | | | 6.01 | 10 | pos |
| Engelmann et al. | 2009 | Posterior orbital gyrus | 25.5 | 7.5 | -13 | | | | | 5.29 | 10 | pos |
| Engelmann et al. | 2009 | Caudate nucleus | -7.8 | 7.5 | 21.4 | | | | | 7.55 | 10 | pos |
| Engelmann et al. | 2009 | Superior frontal gyrus | 9.7 | 5.2 | 65.5 | | | | | 5.97 | 10 | pos |
| Engelmann et al. | 2009 | Supplementary motor | 0.6 | -0.6 | 68.5 | | | | | 7.51 | 10 | pos |
| Engelmann et al. | 2009 | Thalamus | 0.9 | -13 | 17.5 | | | | | 10.08 | 10 | pos |
| Engelmann et al. | 2009 | Brainstem (substantia nigra) | 1.5 | -17.1 | -4.7 | | | | | 6.14 | 10 | pos |
| Engelmann et al. | 2009 | Posterior cingulate cortex | 1.8 | -25 | 34.2 | | | | | 6.04 | 10 | pos |
| Engelmann et al. | 2009 | Parahippocampal gyrus | -17.1 | -35.1 | 4.3 | | | | | 6.61 | 10 | pos |
| Engelmann et al. | 2009 | Parahippocampal gyrus | 18.9 | -36 | 5.5 | | | | | 5.93 | 10 | pos |
| Engelmann et al. | 2009 | Cerebelum | 18.6 | -48 | -21 | | | | | 6.04 | 10 | pos |
| Engelmann et al. | 2009 | Fusiform gyrus | 24.4 | -48 | -14 | | | | | 6.63 | 10 | pos |
| Engelmann et al. | 2009 | Fusiform gyrus | -38 | -57.1 | -3 | | | | | 6.85 | 10 | pos |
| Engelmann et al. | 2009 | Precuneus | -17.4 | -66 | 39.4 | | | | | 6.06 | 10 | pos |
| Engelmann et al. | 2009 | Inferior occipital gyrus | 42 | -70 | -2.5 | | | | | 8.06 | 10 | pos |
| Engelmann et al. | 2009 | Cuneus | -17 | -71.5 | 18.5 | | | | | 5.52 | 10 | pos |
| Engelmann et al. | 2009 | Precuneus | -26 | -75 | 35.5 | | | | | 6.21 | 10 | pos |
| Engelmann et al. | 2009 | Middle occipital gyrus | 32.8 | -83 | 12.5 | | | | | 6.55 | 10 | pos |
| Engelmann et al. | 2009 | Middle occipital gyrus | -31.7 | -84 | 11.8 | | | | | 7.25 | 10 | pos |
| Fukunaga et al. | 2012 | R anterior cingulate | | | | 6 | 26 | 24 | 6.73 | | 11 | neg |
| Fukunaga et al. | 2012 | L inferior frontal gyrus | | | | -44 | 16 | -8 | 4.26 | | 11 | neg |
| Fukunaga et al. | 2012 | R inferior frontal gyrus | | | | 48 | 20 | -6 | 6.39 | | 11 | neg |
| Fukunaga et al. | 2012 | L ventromedial prefrontal cortex | | | | -12 | 36 | -18 | NA | | 11 | neg |

| Study | year | Region | Talairach | | | MNI | | | effect size | | Nr | dir. |
|---|---|---|---|---|---|---|---|---|---|---|---|---|
| | | | X | Y | Z | X | Y | Z | t | z | | |
| Fukunaga et al. | 2012 | L inferior frontal gyrus | | | | 40 | 18 | -4 | 7.61 | | 12 | pos |
| Fukunaga et al. | 2012 | R inferior frontal gyrus | | | | 40 | 18 | -6 | 7.47 | | 12 | pos |
| Fukunaga et al. | 2018 | R Angular/Supramarginal Gyrus | | | | 52 | -50 | 28 | 7.46 | | 13 | pos |
| Fukunaga et al. | 2018 | R Medial Frontal Gyrus | | | | 16 | 32 | 44 | 7.17 | | 13 | pos |
| Fukunaga et al. | 2018 | R middle frontal gyrus | | | | 42 | 18 | 46 | 6.75 | | 13 | pos |
| Fukunaga et al. | 2018 | L fusiform Gyrus | | | | -34 | -52 | -14 | 5.52 | | 13 | pos |
| Fukunaga et al. | 2018 | L inferior parietal lobule | | | | -52 | -36 | 40 | 4.96 | | 13 | pos |
| Fukunaga et al. | 2018 | L Insula | | | | -32 | 14 | -10 | 4.81 | | 13 | pos |
| Fukunaga et al. | 2018 | R parahippocampal gyrus | | | | 26 | -32 | -16 | 4.8 | | 13 | pos |
| Fukunaga et al. | 2018 | R inferior temporal gyrus | | | | 58 | -36 | -14 | 4.75 | | 13 | pos |
| Fukunaga et al. | 2018 | R lingual gyrus | | | | 12 | -84 | -8 | 6.54 | | 13 | neg |
| Fukunaga et al. | 2018 | R paracentral lobule | | | | 10 | -44 | 64 | 6.06 | | 13 | neg |
| Fukunaga et al. | 2018 | L mid-Cingulum | | | | 0 | -14 | 40 | 3.83 | | 13 | neg |
| Gilman et al. | 2012 | no activation found | NA | NA | NA | NA | NA | NA | NA | NA | 14 | NA |
| Haeusler et al. | 2018 | R Sensorymotor cortex | | | | 39 | -19 | 53 | 5.81 | | 15 | pos |
| Haeusler et al. | 2018 | L visual cortex | | | | -12 | -97 | 8 | 5.19 | | 15 | pos |
| Haeusler et al. | 2018 | L Sensorymotor cortex | | | | -36 | -22 | 62 | 5.63 | | 15 | neg |
| Kohno et al. | 2015 | B occipital cortex | | | | 2 | -84 | -6 | | 5.52 | 16 | pos? |
| Kohno et al. | 2015 | R Insula | | | | 32 | 24 | -2 | | 5.52 | 16 | pos? |
| Kohno et al. | 2015 | R Middle frontal gyrus | | | | 38 | 46 | 26 | | 4.52 | 16 | pos? |
| Kohno et al. | 2015 | R Orbital frontal cortex | | | | 30 | 22 | -12 | | 4.51 | 16 | pos? |
| Kohno et al. | 2015 | R inferior frontal gyrus | | | | 54 | 12 | 4 | | 3.55 | 16 | pos? |
| Kohno et al. | 2015 | B ACC | | | | 6 | 28 | 28 | | 4.57 | 16 | pos? |
| Kohno et al. | 2015 | Brainstem | | | | 6 | -24 | -8 | | 3.75 | 16 | pos? |
| Kohno et al. | 2015 | Thalamus | | | | 4 | -2 | 0 | | 3.75 | 16 | pos? |
| Kohno et al. | 2015 | B Precuneus | | | | -14 | -58 | 18 | | 4.05 | 17 | pos? |
| Kohno et al. | 2015 | L postcentral gyrus | | | | -28 | -32 | 66 | | 4.03 | 17 | pos? |
| Kohno et al. | 2015 | R Caudate | | | | 10 | 22 | 2 | | 3.34 | 17 | pos? |
| Kohno et al. | 2015 | Subcallosal cortex | | | | 2 | 18 | -6 | | 3.33 | 17 | pos? |
| Kohno et al. | 2015 | B Nucleus accumbens | | | | 12 | 8 | -8 | | 3.4 | 17 | pos? |
| Lee et al. | 2008 | L Superior temporal gyrus | | | | -40 | -6 | -14 | 5.73 | | 18 | pos |
| Lee et al. | 2008 | L parahippocampal grus | | | | -26 | -28 | 20 | 5.68 | | 18 | pos |
| Lee et al. | 2008 | R cerebellum | | | | -28 | -44 | -8 | 5.71 | | 18 | pos |
| Li et al. | 2020 | B ACC/MFC | | | | 8 | 2 | 42 | | 5.04 | 44 | pos |
| Li et al. | 2020 | L DLPFC | | | | -34 | 44 | 30 | | 4.01 | 44 | pos |
| Li et al. | 2020 | R DLPFC | | | | 38 | 52 | 22 | | 4.24 | 44 | pos |
| Li et al. | 2020 | R Thalamus | | | | 5 | -24 | -6 | | 5.5 | 44 | pos |
| Li et al. | 2020 | L Thalamus | | | | -2 | -23 | -10 | | 5.61 | 44 | pos |
| Li et al. | 2020 | L striatum | | | | -12 | -22 | -2 | | 5.89 | 44 | pos |
| Li et al. | 2020 | R striatum | | | | 14 | -21 | 0 | | 5.84 | 44 | pos |
| Li et al. | 2020 | L Insula | | | | -38 | -20 | -2 | | 5.06 | 44 | pos |
| Li et al. | 2020 | R Insula | | | | 32 | -19 | -2 | | 5.5 | 44 | pos |
| Li et al. | 2020 | L occipital | | | | -22 | -18 | 2 | | 5.86 | 44 | pos |
| Li et al. | 2020 | R occipital | | | | 20 | -17 | -2 | | 5.85 | 44 | pos |
| Liu et al. | 2017 | B precentral gyrus | | | | -51 | 9 | 33 | 5.28 | | 19 | pos |
| Liu et al. | 2017 | B dmPFC | | | | 6 | 21 | 42 | 4.98 | | 19 | pos |
| Losecaat et al. | 2014 | R Fusiform gyrus | | | | 27 | -70 | -8 | | 7.53 | 20 | pos |
| Losecaat et al. | 2014 | R anterior insula | | | | 31 | 25 | -5 | | 6.53 | 20 | pos |
| Losecaat et al. | 2014 | L anterior insula | | | | -33 | 21 | -5 | | 5.67 | 20 | pos |
| Losecaat et al. | 2014 | L Globus Pallidus | | | | -8 | 7 | -1 | | 5.61 | 20 | pos |
| Losecaat et al. | 2014 | R Caudate | | | | 10 | 11 | -1 | | 5.38 | 20 | pos |

| Study | year | Region | Talairach X | Y | Z | MNI X | Y | Z | effect size t | z | Nr | dir. |
|---|---|---|---|---|---|---|---|---|---|---|---|---|
| Losecaat et al. | 2014 | L midbrain | | | | -5 | -28 | -5 | | 5.11 | 20 | pos |
| Losecaat et al. | 2014 | L IFG/dlpfc | | | | -40 | 7 | 24 | | 5.04 | 20 | pos |
| Losecaat et al. | 2014 | L superior parietal lobule | | | | -29 | -53 | 48 | | 4.98 | 20 | pos |
| Losecaat et al. | 2014 | R dmPFC/ACC | | | | 6 | 35 | 38 | | 4.9 | 20 | pos |
| Losecaat et al. | 2014 | R ACC | | | | 10 | 39 | 10 | | 4.83 | 20 | pos |
| Losecaat et al. | 2014 | R lateral parietal lobe | | | | 45 | -67 | 27 | | 5.58 | 20 | neg |
| Losecaat et al. | 2014 | l lateral OC | | | | -43 | -77 | 31 | | 5.11 | 20 | neg |
| Macoveanu et al. 1 | 2016 | R Ventral Striatum | | | | 12 | 8 | -10 | | 8 | 21 | pos |
| Macoveanu et al. 1 | 2016 | L Ventral Striatum | | | | -16 | 4 | -10 | | 8 | 21 | pos |
| Macoveanu et al. 1 | 2016 | R Midbrain | | | | 14 | 6 | -10 | | 7 | 21 | pos |
| Macoveanu et al. 1 | 2016 | L Amygdala | | | | -16 | 2 | 12 | | 6 | 21 | pos |
| Macoveanu et al. 1 | 2016 | Posterior cingulate cortex | | | | 4 | -8 | 30 | | 5.9 | 21 | pos |
| Macoveanu et al. 1 | 2016 | Anterior cingulate cortex | | | | -2 | 14 | 28 | | 5 | 21 | pos |
| Macoveanu et al. 1 | 2016 | L hippocampus | | | | -12 | 0 | -14 | | 5.5 | 21 | pos |
| Macoveanu et al. 1 | 2016 | R hippocampus | | | | 18 | -20 | -14 | | 5.4 | 21 | pos |
| Macoveanu et al. 1 | 2016 | R Thalamus | | | | 4 | -12 | 6 | | 5.3 | 21 | pos |
| Macoveanu et al. 1 | 2016 | L Thalamus | | | | -24 | -30 | 4 | | 5.2 | 21 | pos |
| Macoveanu et al. 1 | 2016 | L insula | | | | -30 | 14 | -4 | | 5 | 21 | pos |
| Macoveanu et al. 1 | 2016 | R insula | | | | 32 | 24 | -6 | | 4.1 | 21 | pos |
| Macoveanu et al. 1 | 2016 | L Middle frontal sulcus | | | | -34 | 22 | 30 | | 5 | 21 | pos |
| Macoveanu et al. 1 | 2016 | R middle frontal sulcus | | | | 32 | 50 | 26 | | 4.3 | 21 | pos |
| Macoveanu et al. 2 | 2016 | L Ventral Striatum | | | | -16 | 6 | -8 | | 8 | 22 | pos |
| Macoveanu et al. 2 | 2016 | R Ventral Striatum | | | | 16 | 10 | -8 | | 8 | 22 | pos |
| Macoveanu et al. 2 | 2016 | Thalamus | | | | 8 | -22 | -4 | | 8 | 22 | pos |
| Macoveanu et al. 2 | 2016 | L Anterior insula | | | | -28 | 16 | -6 | | 6.68 | 22 | pos |
| Macoveanu et al. 2 | 2016 | R anterior insula | | | | 32 | 22 | -10 | | 5.45 | 22 | pos |
| Macoveanu et al. 2 | 2016 | L dmPFC | | | | -6 | 34 | 30 | | 6.93 | 22 | pos |
| Macoveanu et al. 2 | 2016 | L middle occipital cortex | | | | -34 | -76 | 36 | | 6.93 | 22 | pos |
| Macoveanu et al. 2 | 2016 | R middle occipital cortex | | | | -44 | -76 | 18 | | 6.16 | 22 | pos |
| Macoveanu et al. 2 | 2016 | R cerebellum | | | | 8 | -62 | 22 | | 6.35 | 22 | pos |
| Macoveanu et al. 2 | 2016 | L cerebellum | | | | -8 | -58 | -20 | | 4.48 | 22 | pos |
| Macoveanu et al. 2 | 2016 | L posterior cingulate | | | | -6 | -32 | 30 | | 6.25 | 22 | pos |
| Macoveanu et al. 2 | 2016 | R posterior cingulate | | | | 10 | -36 | 30 | | 5.44 | 22 | pos |
| Macoveanu et al. 2 | 2016 | L Precuneus | | | | -12 | -68 | 32 | | 6.2 | 22 | pos |
| Macoveanu et al. 2 | 2016 | R precuneus | | | | 16 | -64 | 48 | | 5.88 | 22 | pos |
| Macoveanu et al. 2 | 2016 | L Middle temporal cortex | | | | -54 | -50 | 12 | | 5.95 | 22 | pos |
| Macoveanu et al. 2 | 2016 | L Middle frontal cortex | | | | -22 | 28 | 50 | | 5.61 | 22 | pos |
| Macoveanu et al. 2 | 2016 | L inferior frontal cortex | | | | -46 | 8 | 18 | | 5.56 | 22 | pos |
| Macoveanu et al. 2 | 2016 | L lateral orbitofrontal cortex | | | | -42 | 48 | 0 | | 5.32 | 22 | pos |
| Matthews et al. | 2004 | L Superior temporal gyrus | -47 | -55 | 27 | | | | | | 23 | neg |
| Matthews et al. | 2004 | R middle temporal gyrus | 35 | -61 | 31 | | | | | | 23 | neg |
| Matthews et al. | 2004 | L inferior frontal gyrus | -63 | 12 | 24 | | | | | | 23 | neg |
| Matthews et al. | 2004 | R Medial Frontal Gyrus | 17 | 47 | 10 | | | | | | 23 | pos |
| Matthews et al. | 2004 | L nucleus accumbens | -14 | 8 | 4 | | | | | | 23 | pos |
| Matthews et al. | 2004 | R caudate | 23 | -36 | 15 | | | | | | 23 | pos |
| Matthews et al. | 2004 | L middle occipital cortex | -30 | -83 | -2 | | | | | | 23 | pos |
| Meder et al. | 2016 | R ventral striatum | | | | 14 | 10 | -4 | | 5.99 | 24 | pos |
| Meder et al. | 2016 | L Ventral Striatum | | | | -12 | 4 | -2 | | 5.22 | 24 | pos |
| Meder et al. | 2016 | r Pre-SMA | | | | 6 | 16 | 52 | | 5.9 | 24 | pos |
| Meder et al. | 2016 | r dorsal ACC | | | | 6 | 26 | 38 | | 5.64 | 24 | pos |
| Meder et al. | 2016 | r v3 | | | | 48 | -62 | -20 | | 4.73 | 24 | pos |

| Study | year | Region | Talairach | | | MNI | | | effect size | | Nr | dir. |
|---|---|---|---|---|---|---|---|---|---|---|---|---|
| | | | X | Y | Z | X | Y | Z | t | z | | |
| Meder et al. | 2016 | l v3 | | | | -22 | -100 | 0 | | 5.37 | 24 | pos |
| Meder et al. | 2016 | R inferior frontal gyrus | | | | 42 | 24 | 6 | | 5.24 | 24 | pos |
| Meder et al. | 2016 | L inferior frontal gyrus | | | | -32 | 22 | -10 | | 5.29 | 24 | pos |
| Meder et al. | 2016 | R inferior parietal cortex | | | | 32 | -54 | 52 | | 5.1 | 24 | pos |
| Meder et al. | 2016 | L inferior parietal cortex | | | | -46 | -36 | 42 | | 4.24 | 24 | pos |
| Meder et al. | 2016 | R thalamus | | | | 8 | -16 | -14 | | 5.08 | 24 | pos |
| Meder et al. | 2016 | R dlPFC | | | | 32 | 52 | 26 | | 4.87 | 24 | pos |
| Meder et al. | 2016 | L dlPFC | | | | -34 | 56 | 20 | | 4.68 | 24 | pos |
| Meder et al. | 2016 | l subthalamic nucleus | | | | -6 | -14 | -12 | | 4.67 | 24 | pos |
| Meder et al. | 2016 | r subthalamic nucleus | | | | 8 | -16 | -12 | | 4.96 | 24 | pos |
| Meder et al. | 2016 | L inferior parietal cortex | | | | -40 | -82 | 38 | | 5.15 | 24 | neg |
| Meder et al. | 2016 | L Precuneus | | | | -4 | -60 | 20 | | 3.81 | 24 | neg |
| Miedel et al. | 2010 | L Superior Frontal Gyrus | -2 | 7 | 57 | | | | 3.98 | | 25 | neg |
| Miedel et al. | 2010 | R Precentral Gyrus | 20 | -16 | 63 | | | | 3.84 | | 25 | neg |
| Miedel et al. | 2010 | R Postcentral Gyrus | 42 | -18 | 25 | | | | 3.88 | | 25 | neg |
| Miedel et al. | 2010 | R Superior Temporal Gyrus | 67 | -21 | 8 | | | | 4.77 | | 25 | neg |
| Miedel et al. | 2010 | R Superior Temporal Gyrus | 53 | -13 | 6 | | | | 4.49 | | 25 | neg |
| Miedel et al. | 2010 | R Superior Temporal Gyrus | 59 | -31 | 9 | | | | 4 | | 25 | neg |
| Miedel et al. | 2010 | R Superior Temporal Gyrus | 44 | -29 | 9 | | | | 3.68 | | 25 | neg |
| Miedel et al. | 2010 | R Superior Temporal Gyrus | 28 | -45 | -3 | | | | 3.69 | | 25 | neg |
| Miedel et al. | 2010 | L Thalamus | -6 | -23 | 10 | | | | 4.12 | | 25 | neg |
| Miedel et al. | 2010 | R Thalamus | 6 | -23 | 10 | | | | 3.75 | | 25 | neg |
| Miedel et al. | 2010 | R Insula | 42 | -28 | 18 | | | | 3.77 | | 25 | neg |
| Paulus et al. | 2003 | R Insula | 32 | 18 | 7 | | | | | | 26 | pos? |
| Paulus et al. | 2003 | L Cuneus | 7 | -74 | 32 | | | | | | 26 | pos? |
| Paulus et al. | 2003 | L Precuneus | -17 | -70 | 40 | | | | | | 26 | pos? |
| Paulus et al. | 2003 | R Precuneus | 10 | -65 | 27 | | | | | | 26 | pos? |
| Paulus et al. | 2003 | R middle frontal gyrus | 37 | 7 | 33 | | | | | | 26 | pos? |
| Paulus et al. | 2006 | R Precuneus | 14 | -78 | 43 | | | | 4.49 | | 27 | neg |
| Paulus et al. | 2006 | L Cingulate Gyrus | -2 | 5 | 41 | | | | 4.36 | | 27 | neg |
| Paulus et al. | 2006 | R Insula | 42 | 3 | 6 | | | | 4.81 | | 27 | neg |
| Paulus et al. | 2006 | L Middle frontal gyrus | -39 | 31 | 28 | | | | 3.97 | | 27 | neg |
| Paulus et al. | 2006 | R Middle occipital gyrus | 36 | -77 | 13 | | | | 4.32 | | 27 | neg |
| Paulus et al. | 2006 | L Precuneus | -23 | -76 | 42 | | | | 3.82 | | 27 | neg |
| Paulus et al. | 2006 | L Superior parietal lobule | -26 | -59 | 55 | | | | 3.97 | | 27 | neg |
| Paulus et al. | 2006 | L Insula | -40 | 8 | 2 | | | | 5.58 | | 27 | neg |
| Paulus et al. | 2006 | L Thalamus | -3 | 0 | 4 | | | | 4.41 | | 27 | neg |
| Paulus et al. | 2006 | R Postcentral gyrus | 54 | -22 | 16 | | | | 6.59 | | 27 | neg |
| Paulus et al. | 2006 | R inferior parietal lobule | 42 | -55 | 36 | | | | 4.71 | | 27 | neg |
| Paulus et al. | 2006 | L middle frontal gyrus | -21 | 20 | 38 | | | | 4.71 | | 27 | neg |
| Paulus et al. | 2006 | R superior temporal gyrus | 56 | 17 | -10 | | | | 3.46 | | 27 | neg |
| Paulus et al. | 2006 | L precentral gyrus | -47 | -9 | 10 | | | | 5.21 | | 27 | neg |
| Paulus et al. | 2006 | L caudate | -5 | 0 | 21 | | | | 3.94 | | 27 | neg |
| Pletzer et al. | 2016 | B Caudate | | | | -9 | 5 | -2 | 6.66 | | 28 | pos |
| Pletzer et al. | 2016 | B Caudate | | | | 9 | 8 | 1 | 6.35 | | 28 | pos |
| Pletzer et al. | 2016 | L Insula | | | | -30 | 26 | -2 | 5.64 | | 28 | pos |
| Pletzer et al. | 2016 | R Insula | | | | 33 | 29 | -5 | 5.64 | | 28 | pos |
| Pletzer et al. | 2016 | L Insula | | | | -30 | 23 | -11 | 6.64 | | 29 | pos |
| Pletzer et al. | 2016 | B ACC SMA | | | | -3 | 35 | 28 | 7.08 | | 29 | pos |
| Rao et al. | 2008 | R Insula | | | | 38 | 10 | -2 | | 6.28 | 30 | pos |
| Rao et al. | 2008 | L. Insula | | | | -34 | 17 | -6 | | 6.23 | 30 | pos |

| Study | year | Region | Talairach | | | MNI | | | effect size | | | |
|---|---|---|---|---|---|---|---|---|---|---|---|---|
| | | | X | Y | Z | X | Y | Z | t | z | Nr | dir. |
| Rao et al. | 2008 | B ACC | | | | 0 | 12 | 42 | 5.83 | | 30 | pos |
| Rao et al. | 2008 | L. Striatum | | | | -10 | 2 | 4 | 5.76 | | 30 | pos |
| Rao et al. | 2008 | R. Striatum | | | | 14 | 2 | -2 | 5.18 | | 30 | pos |
| Rao et al. | 2008 | R. Midbrain | | | | 6 | -16 | -2 | 5 | | 30 | pos |
| Rao et al. | 2008 | L . Midbrain | | | | -6 | -12 | -4 | 4.29 | | 30 | pos |
| Rao et al. | 2008 | L. Fusiform | | | | -22 | -54 | -4 | 5.88 | | 30 | pos |
| Rao et al. | 2008 | R occipital | | | | 30 | -76 | 24 | 5.28 | | 30 | pos |
| Rao et al. | 2008 | R fusifurm | | | | 30 | -52 | -16 | 5.09 | | 30 | pos |
| Rao et al. | 2008 | L. occipital | | | | -28 | -80 | 20 | 4.53 | | 30 | pos |
| Rao et al. | 2008 | R. parietal | | | | 30 | -46 | 46 | 4.22 | | 30 | pos |
| Rao et al. | 2008 | L.DLPFC | | | | -34 | 46 | 16 | 4.21 | | 30 | pos |
| Rao et al. | 2008 | L. parietal | | | | -52 | -36 | 38 | 4 | | 30 | pos |
| Rao et al. | 2008 | R. DLPFC | | | | 30 | 36 | 20 | 3.74 | | 30 | pos |
| Rao et al. | 2008 | R ACC | | | | 12 | 18 | 38 | 6.09 | | 31 | pos |
| Rao et al. | 2008 | L striatum | | | | -8 | 0 | 4 | 5.64 | | 31 | pos |
| Rao et al. | 2008 | R insula | | | | 36 | 16 | 0 | 5.453 | | 31 | pos |
| Rao et al. | 2008 | L Insula | | | | -28 | 18 | 6 | 5.16 | | 31 | pos |
| Rao et al. | 2008 | R striatum | | | | 12 | 4 | 4 | 5.12 | | 31 | pos |
| Rao et al. | 2008 | R DLPFC | | | | 32 | 46 | 26 | 3.79 | | 31 | pos |
| Rao et al. | 2008 | L DLPFC | | | | -32 | 46 | 22 | 3.31 | | 31 | pos |
| Roy et al. | 2011 | Precuneus | | | | 24 | -60 | 52 | 6.22 | | 32 | pos |
| Roy et al. | 2011 | Precuneus | | | | 24 | -66 | 58 | 5.56 | | 32 | pos |
| Roy et al. | 2011 | Precuneus | | | | 24 | -66 | 48 | 5.31 | | 32 | pos |
| Roy et al. | 2011 | SPL | | | | 24 | -60 | 60 | 5.8 | | 32 | pos |
| Roy et al. | 2011 | Fusiform gyrus | | | | 22 | -92 | -10 | 5.14 | | 32 | pos |
| Roy et al. | 2011 | MIddle occipital gyrus | | | | 38 | -88 | 4 | 5.12 | | 32 | pos |
| Roy et al. | 2011 | Lateral occipital gyrus | | | | -26 | -90 | 2 | 6.04 | | 32 | pos |
| Roy et al. | 2011 | Middle occipital gyrus | | | | -24 | -96 | 10 | 5.09 | | 32 | pos |
| Roy et al. | 2011 | Cuneus | | | | -20 | -96 | 4 | 5.51 | | 32 | pos |
| Roy et al. | 2011 | Cuneus | | | | -24 | -84 | 14 | 5.2 | | 32 | pos |
| Roy et al. | 2011 | Precuneus | | | | -26 | -78 | 24 | 5.15 | | 32 | pos |
| Roy et al. | 2011 | Lingual Gyrus | | | | -16 | -98 | 0 | 5.24 | | 32 | pos |
| Roy et al. | 2011 | Caudate | | | | -8 | 6 | -4 | 4.96 | | 32 | pos |
| Roy et al. | 2011 | Caudate | | | | 14 | 14 | 0 | 4.59 | | 32 | pos |
| Roy et al. | 2011 | Caudate | | | | 10 | 8 | 2 | 4.5 | | 32 | pos |
| Roy et al. | 2011 | Caudate | | | | 12 | 6 | -4 | 4.42 | | 32 | pos |
| Roy et al. | 2011 | Caudate | | | | 8 | 8 | -2 | 4.42 | | 32 | pos |
| Roy et al. | 2011 | Brainstem | | | | 8 | -28 | -12 | 4.12 | | 32 | pos |
| Roy et al. | 2011 | cingulate gyrus | | | | 4 | 22 | 44 | 5.24 | | 32 | pos |
| Roy et al. | 2011 | cingulate gyrus | | | | -4 | 30 | 30 | 4.46 | | 32 | pos |
| Roy et al. | 2011 | cingulate gyrus | | | | 4 | 38 | 24 | 3.37 | | 32 | pos |
| Roy et al. | 2011 | medial frontal gyrus | | | | 4 | 30 | 38 | 5.1 | | 32 | pos |
| Roy et al. | 2011 | medial frontal gyrus | | | | -6 | 12 | 50 | 3.87 | | 32 | pos |
| Roy et al. | 2011 | precentral gyrus | | | | -24 | -6 | 52 | 4.65 | | 32 | pos |
| Roy et al. | 2011 | precentral gyrus | | | | -36 | -4 | 60 | 3.61 | | 32 | pos |
| Roy et al. | 2011 | precentral gyrus | | | | -38 | -6 | 50 | 3.55 | | 32 | pos |
| Roy et al. | 2011 | precentral gyrus | | | | -38 | -10 | 52 | 3.51 | | 32 | pos |
| Roy et al. | 2011 | Middle frontal gyrus | | | | -32 | 0 | 64 | 4.12 | | 32 | pos |
| Roy et al. | 2011 | Middle frontal gyrus | | | | -28 | 0 | 60 | 4.07 | | 32 | pos |
| Roy et al. | 2011 | Middle frontal gyrus | | | | 30 | 0 | 56 | 4.38 | | 32 | pos |
| Roy et al. | 2011 | medial frontal gyrus | | | | 22 | -4 | 52 | 4.29 | | 32 | pos |

| Study | year | Region | Talairach | | | MNI | | | effect size | | Nr | dir. |
|---|---|---|---|---|---|---|---|---|---|---|---|---|
| | | | X | Y | Z | X | Y | Z | t | z | | |
| Roy et al. | 2011 | cingulate gyrus | | | | 24 | 4 | 42 | | 3.33 | 32 | pos |
| Roy et al. | 2011 | cingulate gyrus | | | | 24 | 8 | 46 | | 3.27 | 32 | pos |
| Roy et al. | 2011 | Middle frontal gyrus | | | | 48 | 32 | 30 | | 4.14 | 32 | pos |
| Roy et al. | 2011 | Middle frontal gyrus | | | | 44 | 34 | 22 | | 3.96 | 32 | pos |
| Roy et al. | 2011 | Middle frontal gyrus | | | | 40 | 32 | 28 | | 3.88 | 32 | pos |
| Roy et al. | 2011 | Middle frontal gyrus | | | | 40 | 26 | 46 | | 3.22 | 32 | pos |
| Roy et al. | 2011 | Middle frontal gyrus | | | | 36 | 22 | 54 | | 3.08 | 32 | pos |
| Roy et al. | 2011 | Superior frontal gyrus | | | | 36 | 24 | 50 | | 3.03 | 32 | pos |
| Roy et al. | 2011 | insula | | | | 30 | 24 | 0 | | 4.1 | 32 | pos |
| Roy et al. | 2011 | insula | | | | 32 | 22 | 6 | | 3.46 | 32 | pos |
| Roy et al. | 2011 | insula | | | | 32 | 24 | -4 | | 3.98 | 32 | pos |
| Roy et al. | 2011 | insula | | | | 36 | 18 | -4 | | 3.96 | 32 | pos |
| Roy et al. | 2011 | inferior frontal gyrus | | | | 46 | 20 | 8 | | 3.25 | 32 | pos |
| Roy et al. | 2011 | frontal pole | | | | 36 | 60 | 12 | | 3.94 | 32 | pos |
| Roy et al. | 2011 | frontal pole | | | | 36 | 54 | 4 | | 3.65 | 32 | pos |
| Roy et al. | 2011 | frontal pole | | | | 40 | 58 | -10 | | 3.5 | 32 | pos |
| Roy et al. | 2011 | frontal pole | | | | 46 | 52 | 10 | | 3.16 | 32 | pos |
| Roy et al. | 2011 | Middle frontal gyrus | | | | -52 | 20 | 34 | | 4.01 | 32 | pos |
| Roy et al. | 2011 | Middle frontal gyrus | | | | -50 | 24 | 22 | | 3.62 | 32 | pos |
| Roy et al. | 2011 | precentral gyrus | | | | -52 | 0 | 36 | | 3.02 | 32 | pos |
| Roy et al. | 2011 | middle temporal gyrus | | | | 64 | -44 | 4 | | 4.99 | 32 | neg |
| Roy et al. | 2011 | middle temporal gyrus | | | | 62 | -50 | 2 | | 4.84 | 32 | neg |
| Roy et al. | 2011 | middle temporal gyrus | | | | 60 | -56 | 6 | | 4.8 | 32 | neg |
| Roy et al. | 2011 | middle temporal gyrus | | | | 66 | -48 | 6 | | 4.75 | 32 | neg |
| Roy et al. | 2011 | angular gyrus | | | | 54 | -54 | 18 | | 4.66 | 32 | neg |
| Roy et al. | 2011 | inferior parietal lobe | | | | 64 | -34 | 28 | | 4.96 | 32 | neg |
| Roy et al. | 2011 | inferior parietal lobe | | | | -64 | -30 | 24 | | 5.2 | 32 | neg |
| Roy et al. | 2011 | inferior parietal lobe | | | | -64 | -38 | 32 | | 4.93 | 32 | neg |
| Roy et al. | 2011 | inferior parietal lobe | | | | -62 | -42 | 34 | | 5.19 | 32 | neg |
| Roy et al. | 2011 | middle temporal gyrus | | | | -62 | -56 | 2 | | 4.52 | 32 | neg |
| Roy et al. | 2011 | middle temporal gyrus | | | | -64 | -52 | 8 | | 4.51 | 32 | neg |
| Roy et al. | 2011 | middle temporal gyrus | | | | -62 | -54 | -8 | | 4.45 | 32 | neg |
| Roy et al. | 2011 | cuneus | | | | 6 | -88 | 22 | | 5 | 32 | neg |
| Roy et al. | 2011 | cuneus | | | | 6 | -90 | 18 | | 4.89 | 32 | neg |
| Roy et al. | 2011 | precuneus | | | | -4 | -48 | 40 | | 4.41 | 32 | neg |
| Roy et al. | 2011 | precuneus | | | | -4 | -50 | 34 | | 4.26 | 32 | neg |
| Roy et al. | 2011 | precuneus | | | | -4 | -60 | 10 | | 4.6 | 32 | neg |
| Roy et al. | 2011 | cingulate gyrus | | | | -14 | -38 | 38 | | 4.05 | 32 | neg |
| Roy et al. | 2011 | precentral gyrus | | | | -58 | 8 | 6 | | 4.16 | 32 | neg |
| Roy et al. | 2011 | precentral gyrus | | | | -56 | 8 | 10 | | 4.02 | 32 | neg |
| Roy et al. | 2011 | precentral gyrus | | | | -52 | 2 | 8 | | 3.06 | 32 | neg |
| Schonberg et al. | 2012 | R anterior insula | | | | 32 | 20 | 2 | | 4.06 | 33 | pos |
| Schonberg et al. | 2012 | L anterior insula | | | | -30 | 14 | -8 | | 3.9 | 33 | pos |
| Schonberg et al. | 2012 | B dorsal ACC | | | | 6 | 8 | 46 | | 3.55 | 33 | pos |
| Schonberg et al. | 2012 | B intra calcarine | | | | 2 | -78 | 0 | | 4.11 | 33 | pos |
| Schonberg et al. | 2012 | R frontal pole | | | | 36 | 44 | 26 | | 3.31 | 33 | pos |
| Schonberg et al. | 2012 | vmPFC | | | | 4 | 20 | -16 | | 4.25 | 33 | neg |
| Schonberg et al. | 2012 | L lateral OFC | | | | -36 | 18 | -34 | | 3.66 | 33 | neg |
| Schonberg et al. | 2012 | R temporal pole | | | | 34 | 14 | -36 | | 3.33 | 33 | neg |
| Smith et al. | 2009 | cingulate gyrus | -4 | 22 | 44 | | | | | | 34 | pos |
| Smith et al. | 2009 | intraparietal lobule | -55 | -46 | 40 | | | | | | 34 | pos |

| Study | year | Region | Talairach X | Y | Z | MNI X | Y | Z | effect size t | z | Nr | dir. |
|---|---|---|---|---|---|---|---|---|---|---|---|---|
| Symmonds et al. | 2011 | L Ventral Striatum | | | | -6 | 8 | -4 | | 4.59 | 35 | pos |
| Symmonds et al. | 2011 | R Ventral Striatum | | | | 18 | 22 | -2 | | 4.4 | 35 | pos |
| Symmonds et al. | 2011 | R Middle Frontal Gyrus | | | | 20 | 40 | -14 | | 4.43 | 35 | pos |
| Symmonds et al. | 2011 | L Occipital Lobe/BA17 | | | | -14 | -94 | -8 | | 4.34 | 35 | pos |
| Symmonds et al. | 2011 | L Occipital Lobe | | | | -26 | -84 | -8 | | 4.3 | 35 | pos |
| Symmonds et al. | 2011 | L Occipital Lobe/BA18 | | | | -8 | -78 | -4 | | 4.02 | 35 | pos |
| Symmonds et al. | 2011 | L Superior Parietal Lobe | | | | -12 | -70 | 40 | | 4.2 | 35 | pos |
| Symmonds et al. | 2011 | L Superior Parietal Lobe | | | | -20 | -60 | 52 | | 3.42 | 35 | pos |
| Symmonds et al. | 2011 | L Precuneus | | | | -16 | -60 | 26 | | 3.03 | 35 | pos |
| Symmonds et al. | 2011 | R Superior Parietal Lobe | | | | 26 | -60 | 54 | | 4.03 | 35 | pos |
| Symmonds et al. | 2011 | R Parietal Lobe/Precuneus | | | | 20 | -62 | 32 | | 4.02 | 35 | pos |
| Symmonds et al. | 2011 | R Mid-occipital gyrus | | | | 30 | -68 | 30 | | 3.97 | 35 | pos |
| Symmonds et al. | 2011 | R posterior parietal | | | | 32 | -60 | 50 | | 3.71 | 36 | pos |
| Symmonds et al. | 2011 | R posterior parietal | | | | 28 | -46 | 46 | | 3.66 | 36 | pos |
| Symmonds et al. | 2011 | R posterior parietal | | | | 16 | -62 | 48 | | 3.59 | 36 | pos |
| Weber et al. | 2008 | L insula | | | | -40 | 6 | 6 | | 2.82 | 37 | pos |
| Weber et al. | 2008 | L posterior cingulate | | | | -8 | -56 | 18 | | 3.31 | 37 | pos |
| Weber et al. | 2008 | B ACC | | | | 2 | 32 | 10 | | 2.77 | 37 | pos |
| Weber et al. | 2008 | B ACC | | | | 2 | 34 | 0 | | 2.84 | 37 | pos |
| Weber et al. | 2008 | R Medial Frontal Gyrus | | | | 10 | 60 | 14 | | 3.31 | 37 | pos |
| Weber et al. | 2008 | R caudate | | | | 10 | 8 | -2 | | 3.07 | 37 | pos |
| Weber et al. | 2008 | R Postcentral gyrus | | | | 38 | -46 | 64 | | 2.95 | 37 | pos |
| Weber et al. | 2008 | R superior temporal gyrus | | | | 50 | 8 | -6 | | 2.85 | 37 | pos |
| Weber et al. | 2008 | R inferior frontal gyrus | | | | 58 | 38 | 0 | | 3.17 | 37 | pos |
| Weber et al. | 2008 | R middle frontal | | | | 36 | 6 | 52 | | 2.8 | 37 | neg |
| Wright et al. | 2012 | R caudate | | | | 15 | 17 | 10 | 5.65 | | 38 | pos |
| Wright et al. | 2012 | R caudate | | | | 0 | -1 | 16 | 4.02 | | 38 | pos |
| Wright et al. | 2012 | R caudate | | | | 6 | -13 | 25 | 3.86 | | 38 | pos |
| Wright et al. | 2012 | R inferior parietal lobule | | | | 51 | -34 | 49 | 4.62 | | 38 | pos |
| Wright et al. | 2012 | R inferior parietal lobule | | | | 45 | -43 | 46 | 4.39 | | 38 | pos |
| Wright et al. | 2012 | R precuneus | | | | 21 | -73 | 43 | 4.06 | | 38 | pos |
| Wright et al. | 2012 | R superior medial gyrus | | | | 9 | 32 | 40 | 4.15 | | 38 | pos |
| Wright et al. | 2012 | R superior medial gyrus | | | | 24 | 14 | 46 | 4 | | 38 | pos |
| Wright et al. | 2012 | L superior medial gyrus | | | | 3 | 38 | 31 | 4.15 | | 38 | pos |
| Wright et al. | 2013 | R Precuneus | | | | 21 | -72 | 40 | | 4.2 | 39 | pos |
| Wright et al. | 2013 | R superior parietal lobule | | | | 21 | -55 | 55 | | 4.1 | 39 | pos |
| Wright et al. | 2013 | R Angular gyrus | | | | 42 | -70 | 37 | | 4 | 39 | pos |
| Wright et al. | 2013 | B MCC | | | | -6 | 17 | 37 | | 4.2 | 39 | pos |
| Wright et al. | 2013 | B dmPFC | | | | 15 | 62 | 22 | | 4.1 | 39 | pos |
| Wright et al. | 2013 | B dmPFC | | | | 9 | 50 | 31 | | 3.9 | 39 | pos |
| Wright et al. | 2013 | R anterior insula | | | | 51 | 17 | 1 | | 4.1 | 39 | pos |
| Wright et al. | 2013 | R anterior insula | | | | 42 | 23 | 1 | | 3.8 | 39 | pos |
| Wright et al. | 2013 | R mid temporal gyrus | | | | 54 | 2 | -23 | | 3.3 | 39 | pos |
| Wright et al. | 2013 | B Cerebellum | | | | 3 | -49 | -8 | | 4.1 | 39 | pos |
| Wright et al. | 2013 | L middle orbital gyr | | | | -48 | -79 | 7 | | 3.9 | 39 | pos |
| Wright et al. | 2013 | R inferior temporal gyrus | | | | 51 | -58 | -5 | | 3.8 | 39 | pos |
| Wright et al. | 2013 | R cerebellum | | | | 12 | -61 | -47 | | 4.6 | 39 | pos |
| Wright et al. | 2013 | R cerebellum | | | | 6 | -55 | -41 | | 4.5 | 39 | pos |
| Wright et al. | 2013 | R cerebellum | | | | -6 | -49 | -44 | | 3.7 | 39 | pos |
| Wright et al. | 2013 | L cerebellum | | | | -27 | -58 | -44 | | 4.3 | 39 | pos |
| Wright et al. | 2013 | L cerebellum | | | | -30 | -67 | -38 | | 3.9 | 39 | pos |

| Study | year | Region | Talairach | | | MNI | | | effect size | | Nr | dir. |
|---|---|---|---|---|---|---|---|---|---|---|---|---|
| | | | X | Y | Z | X | Y | Z | t | z | | |
| Wright et al. | 2013 | L cerebellum | | | | -30 | -46 | -38 | | 3.7 | 39 | pos |
| Xue et al. | 2009 | dmPFC | | | | 4 | 48 | 26 | | 3.59 | 40 | pos? |
| Xue et al. | 2009 | dmPFC | | | | 2 | 52 | 30 | | 3.57 | 40 | pos? |
| Xue et al. | 2009 | dmPFC | | | | 4 | 50 | 12 | | 3.2 | 40 | pos? |
| Xue et al. | 2009 | Thalamus | | | | -2 | -2 | 4 | | 3.29 | 40 | pos? |
| Xue et al. | 2009 | right sm | | | | 54 | -42 | 34 | | 3.2 | 40 | pos? |
| Xue et al. | 2009 | right sm | | | | 54 | -50 | 46 | | 3.08 | 40 | pos? |
| Yu et al. | 2016 | R Insula | | | | 39 | 21 | 6 | 6.08 | | 41 | pos |
| Yu et al. | 2016 | L Insula | | | | -39 | 15 | 0 | 5.29 | | 41 | pos |
| Yu et al. | 2016 | R Thalamus | | | | 6 | -24 | 9 | 5.53 | | 41 | pos |
| Yu et al. | 2016 | R Cingulate | | | | 9 | 30 | 30 | 6.28 | | 41 | pos |
| Yu et al. | 2016 | L Postcentral | | | | -66 | -18 | 27 | 7.3 | | 41 | neg |
| Yu et al. | 2016 | R Fusiform | | | | 39 | -6 | -33 | 4.89 | | 41 | neg |
| Yu et al. | 2016 | L middle frontal gyrus | | | | -21 | 18 | 48 | 4.45 | | 41 | neg |
| Yu et al. | 2016 | vmPFC | | | | -12 | 33 | -15 | 5.51 | | 41 | neg |
| Yu et al. | 2016 | lnsula | | | | 39 | 18 | 3 | 10.28 | | 42 | pos |
| Yu et al. | 2016 | lnsula | | | | -33 | 21 | 3 | 8.66 | | 42 | pos |
| Yu et al. | 2016 | Superior frontal gyrus | | | | 30 | 57 | 15 | 7.12 | | 42 | pos |
| Yu et al. | 2016 | Middle frontal gyrus | | | | -33 | 54 | 9 | 5.05 | | 42 | pos |
| Yu et al. | 2016 | cinuglate | | | | 9 | 27 | 30 | 9.94 | | 42 | pos |
| Yu et al. | 2016 | calcarine | | | | 18 | -96 | -3 | 6.82 | | 42 | pos |
| Yu et al. | 2016 | Middle occipital gyru s | | | | -18 | -96 | -3 | 7.06 | | 42 | pos |
| Yu et al. | 2016 | parietal lobe | | | | 21 | -78 | 39 | 11.4 | | 42 | neg |
| Yu et al. | 2016 | vmPFC | | | | 36 | 42 | -18 | 7.27 | | 42 | neg |
| Zhang et al. | 2019 | anterior insula | | | | 30 | 21 | -8 | 9.11 | | 43 | pos |
| Zhang et al. | 2019 | precentral gyrus | | | | 45 | 0 | 45 | 8.49 | | 43 | pos |
| Zhang et al. | 2019 | caudate | | | | 9 | 9 | 3 | 8.48 | | 43 | pos |
| Zhang et al. | 2019 | anterior insula | | | | -27 | 21 | -3 | 8.28 | | 43 | pos |
| Zhang et al. | 2019 | middle occipital | | | | 27 | -90 | 3 | 7.93 | | 43 | pos |
| Zhang et al. | 2019 | middle occipital | | | | -27 | -90 | -3 | 7.15 | | 43 | pos |
| Zhang et al. | 2019 | precentral gyrus | | | | -48 | 0 | 39 | 7.04 | | 43 | pos |
| Zhang et al. | 2019 | DMPFC | | | | 3 | 45 | 33 | 6.32 | | 43 | pos |
| Zhang et al. | 2019 | ACC | | | | -3 | 39 | 27 | 5.98 | | 43 | pos |
| Zhang et al. | 2019 | inferior parietal lobule | | | | -27 | -51 | 48 | 5.98 | | 43 | pos |
| Zhang et al. | 2019 | L inferior temporal gyrus | | | | -54 | -12 | -27 | 7.79 | | 43 | neg |
| Zhang et al. | 2019 | L Middle orbital gyrus | | | | -3 | 48 | -12 | 7.13 | | 43 | neg |
| Zhang et al. | 2019 | L middle frontal gyrus | | | | -33 | 9 | 60 | 7.12 | | 43 | neg |
| Zhang et al. | 2019 | L superior temporal gyrus | | | | -63 | -27 | 9 | 6.67 | | 43 | neg |
| Zhang et al. | 2019 | L precuneus | | | | -9 | -57 | 21 | 6.11 | | 43 | neg |
| Zhang et al. | 2019 | R middle temporal gyrus | | | | 60 | -3 | -21 | 6.05 | | 43 | neg |

*Note.* Regions are taken from the primary studies, using their notation. Denotations of hemisphere (R, L, and B – right, left and both, respectively) were unified for simplicity, but only added where reported by primary studies. Full citations of all studies can be found in section two of the references. X,Y and Z columns report coordinates in the respective reference frames (Talairach and MNI). Coordinates in Talairach space were converted to MNI space before any further analyses were conducted. Effect sizes and coordinates are reported in the same way the primary studies did. Effect sizes were rounded to two decimal places. "NR" denotes the number of the experiment and can be used to differentiate multiple experiments from the same authors and year. Column "dir." denotes the direction of the effect, standardized as explained in the main text. pos?: likely positive direction (cf. main text). NA: Not applicable. NR: Not reported.

# Document 1 – Ethics vote and SARS-CoV-2 documents

## 8.1.1 DOCUMENT 1A – APPROVAL OF THE ETHICS COMMITTEE

Universität Bremen

EINGEGANGEN
05. Juli 2019

✉ Universität Bremen • Referat 06 • Postfach 33 04 40 • 28334 Bremen

Herrn
Niels Doehring
Department of Neuropsychology and
Behavioral Neurobiology
Cognium R0310

Im Hause

**Ethikkommission**

Der Vorsitzende:
Prof. Dr. Benedikt Buchner

Geschäftsführung:
Miriam Ahrenholz

Bibliothekstraße 1
VWG - Raum 2190
28359 Bremen

Telefon      (0421) 218-60216
FAX          (0421) 218-60210
E-Mail        ahrenholz@uni-
bremen.de

25.06.2019

Aktenzeichen:          Ihre Nachricht vom:          Unser Zeichen:
2019-14                                            06-3

**Ihr Vorhaben: „*Neural Correlates of Risk Taking in Social and Economic Contexts - an fMRI study*"**

Sehr geehrter Herr Doehring,
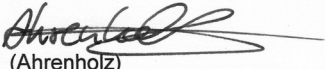
die Ethikkommission der Universität Bremen hat auf ihrer Sitzung am 18. Juni 2019 festgestellt, dass aus ihrer Sicht keine ethischen Bedenken gegen die Durchführung des o. g. Forschungsvorhabens bestehen, wenn folgende Auflagen erfüllt werden:

- Vernichtung der Fragebögen bei Vorliegen von Ausschlusskriterien oder Abbruch.
- Auf S. 18 des Antrags unter „Datenverarbeitung/Gewährleistung der Anonymität" ist im letzten Satz des Abschnittes das Wort „anonymisiert" durch eine verständliche Erläuterung zu ersetzen.

Bitte beachten Sie folgende Hinweise:

Änderungen des Forschungsvorhabens sowie alle schwerwiegenden oder unerwarteten unerwünschten Ereignisse vor oder während der Durchführung des Forschungsvorhabens, die die Sicherheit der Teilnehmer oder die Durchführung des Forschungsvorhabens beeinträchtigen, sind der Ethikkommission unverzüglich bekannt zu geben.

Mit freundlichen Grüßen,
Im Auftrag

(Ahrenholz)

## 8.1.2 Document 1B – Hygiene concept for fMRI studies during SARS-CoV-2

**„Kontrollierter und kontaktarmer Lehr- und Forschungsbetrieb" am FB 11 zur stufenweise Benutzung der Räumlichkeiten und Labore unter SARS-CoV-2 Bedingungen**

**Allgemeine Rahmenbedingungen:**

1. Sofern arbeitsrechtlich und arbeitstechnisch möglich und inhaltlich begründbar sollte weiterhin im „Home-Office" mit einer regelhaften Anbindung an die Arbeitsgruppe gearbeitet werden können.
2. Für diejenigen Personen, die für die Erledigung der Dienstpflichten betriebsnotwendige Arbeiten in den Räumlichkeiten ihrer AG wahrnehmen müssen, ist dies unter Berücksichtigung und Umsetzung der nachfolgenden Szenarien und Maßnahmen möglich.
3. Für die Begründung, Ausarbeitung und Einhaltung der speziellen Bedingungen für das Arbeiten und Betreten von Räumlichkeiten und Labore des FB11 sind die AG-Leiter*innen verantwortlich. Diese haben den Zugang zu dokumentieren und Personen so rechtzeitig der Fachbereichsverwaltung zu benennen, dass Zugangslisten für den darauf folgenden Monat erstellt werden können.

**Allgemeine Grundvoraussetzungen zur Benutzung der Räumlichkeiten und Labore des FB 11 entsprechend den RKI-Handreichungen (gilt für alle u.a. Szenarien):**

- Es sollte eine Entfernung zu anderen von min. 1,5 bis 2m gewährleistet sein; befinden sich mehrere Personen in einem Raum gilt ein Richtwert von 12m$^2$ pro Person in einem Raum.
- Risikogruppen: Personen, die zu Risikogruppen gehören (Diabetes, Immunschwäche, Immunsuppression, Schwangere), müssen besonders vorsichtig sein.
- Desinfektion: Waschen oder desinfizieren Sie Ihre Hände häufig; desinfizieren Sie Geräte, die Sie direkt an andere übergeben.
- Husten oder niesen Sie in den Ellenbogen, nicht in Ihre Hände.
- Das Tragen einfacher Gesichts(Nasen-Mund-Schutz)-Masken wird empfohlen, wenn Sie mit anderen Personen im selben Raum oder außerhalb Ihres Büroraums arbeiten müssen.
- Wenn Sie die geringsten Symptome einer Erkältung oder Fieber haben, bleiben Sie zu Hause.
- Es gilt ein generelles Zutrittsverbot für Personen mit COVID-19- Symptomen oder COVID-19-Erkrankte und für Personen mit bekanntem direkten oder indirekten Kontakt (z.B. Angehörige) zu COVID-19-Erkrankten.
- Eine Arbeitsplanung mit regelmäßigen Zutrittszeiten und im Schichtbetrieb ist zu bevorzugen.

**Rahmenbedingungen für unterschiedliche Szenarien der Gebäudenutzung am FB11:**

**1. Arbeit in Büroräumen mit überwiegender Verwaltungstätigkeit ohne weiteren Personenkontakt**

- Die Mitarbeiter*innen der Verwaltung des FB11 arbeiten ausschließlich allein in ihren Büroräumen.
- Zu keinem Zeitpunkt sind mehr als zwei Personen der Verwaltungsleitung anwesend, idealiter in der Form, dass nie zwei Personen mit gleicher Verwaltungstätigkeit anwesend sein müssen.
- Mitarbeiter*innen mit gleicher Funktion kommen alternierend ins Büro sofern dies sachlich oder anlassbezogen begründbar ist und arbeiten anderweitig, wenn genehmigt, im „Home-Office".

**2. Arbeit in Büroräumen mit weiterem Personenkontakt zur Ausübung der Diensttätigkeiten in Forschung und Lehre**

- Es ist eine Belegung von Büroräumen durch nur eine Person (ggf. im Schichtbetrieb) sicherzustellen.
- Persönliche Treffen (Face-to-face contacts) können stattfinden, wenn zwingend notwendig und Abstandsgebot und Tragen von Gesichts(Nasen-Mund-Schutz)-Masken eingehalten werden.
- Büros oder Arbeitsräume müssen regelmäßig gelüftet werden, insbesondere nach Besprechungen und wenn ein Arbeitsplatz im Schichtbetrieb geteilt wird.
- Kein Zutritt für Studierende, externe Besucher*innen und Studienteilnehmer*innen.
- Es gilt eine dringende Empfehlung für das Tragen von Gesichts(Nasen-Mund-Schutz)-Masken außerhalb allein genutzter Büros oder Arbeitsräume.

3. **Arbeit in Labor- oder Arbeitsräumen <u>ohne</u> zwingendem Kontakt zu Personen außerhalb der eigenen AG (bspw. Messungen an nicht-infektiösen Gegenständen oder am Phantom im MRT)**
   - Es arbeitet i.d.R. nur eine Person im Labor- oder Scannerraum oder am EEG-Gerät, aus Sicherheitsgründen darf sich max. eine zweite Person im Konsolen- oder EEG-Raum aufhalten.
   - Es sollte nur ein Mess-Slot pro Tag und AG realisiert werden.
   - Es wird empfohlen, Einmalhandschuhe zu tragen.
   - Nach jeder Messung müssen die benutzen Gerätschaften desinfiziert werden (auch Armaturen, bspw. im WC oder Klingelknöpfe und Handgriffe).
   - Neben einer erweiterten Grundhygiene durch das Reinigungspersonal / Dez. 4 werden zusätzlich täglich und regelmäßig nach jedem Experiment die Oberflächen, Tastaturen etc. in geeigneter und betriebssicherer Weise desinfiziert.

4. **Arbeit in Labor- oder Arbeitsräumen <u>mit</u> zwingendem Kontakt zu Personen außerhalb der eigenen AG (bspw. Messungen oder Gewinnung von Biomaterialien) <u>zusätzlich</u> zu den unter 3. genannten Maßnahmen**
   - Grundsätzlich gilt eine Pflicht zum Tragen von Gesichts(Nasen-Mund-Schutz)-Masken während des gesamten Untersuchungszeitraums und des Aufenthalts im Gebäude. OP-Masken, sofern sie ausreichend zur Verfügung gestellt werden, sollten bevorzugt werden.
   - Zusätzlich ist eine hygienische Händedesinfektion vor und nach Untersuchung obligatorisch; es wird empfohlen, Einmalhandschuhe zu tragen. Es sollen Sterilium-(Isopropanol) Spender installiert werden.
   - Der Zeitraum des Körperkontakts bei Probandenmessungen ist so kurz wie möglich zu halten (bspw. bei Überprüfung auf Metallteile am Körper, beim Positionieren der Probanden im Scanner, beim Anbringen/Gelen der Elektroden im EEG).
   - Für Blutentnahmen/-untersuchungen gelten die Bestimmungen für den Umgang mit potenziell infektiösen Materialien. Sofern Studien zu SARS-CoV-2 Antikörper durchgeführt werden, wird sich an Blutentnahme - und Verarbeitungsprotokollen des RKI orientiert.
   - Alle benutzten nicht Einmal-/ bzw. Wegwerfmaterialien (Handtücher) werden in einem Wäschesack isoliert und danach per Kochwäsche 90 °C gewaschen.
   - Neben der zu untersuchenden Person darf sich (abgesehen von Notsituationen) nur eine weitere Person im selben Raum unter genereller Einhaltung der Abstandsregel aufhalten. Für Lehrzwecke ist ggfls. eine Videoübertragung in Räumlichkeiten, die den Kautelen für Hygiene und physikalischem Abstand genügen, in Erwägung zu ziehen.

5. **Arbeit in Gruppen im PC-Labor des Cogniums ausschließlich für Lehrzwecke.**
   - Grundsätzlich sollten alle Möglichkeiten der online Lehre ausgeschöpft werden, bevor Präsenzveranstaltungen im PC-Labor des Cognium abgehalten werden.
   - Ansonsten gelten die Rahmenbedingungen und Hygienerichtlinien, wie sie vom ZMML für die Prüfungen im Testcenter definiert werden.


Ich erkläre hiermit, dass ich die o.g. Rahmenbedingungen zum „Kontrollierten und kontaktarmen Lehr- und Forschungsbetrieb" zur Kenntnis genommen habe und die Verantwortung für die Umsetzung in meinem Arbeitsbereich sicherstellen und dokumentieren werde.
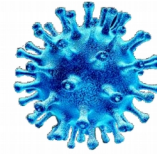

Bremen, den




(Unterschrift Mitarbeiter*in)          /          Arbeitsbereich

## 8.1.3 Document 1C – Additional consent form during SARS-CoV-2

### Erweiterte Information und Einwilligung für MRT-Proband*innen im Kontext COVID-19

Sehr geehrte Untersuchungsteilnehmerin, sehr geehrter Untersuchungsteilnehmer,

nach einem Notbetrieb und jetzt zunehmender Öffnung von Forschung, Lehre und Verwaltung an der Universität Bremen, werden auch die Forschungsarbeiten am Magnetresonanztomografen wieder aufgenommen. Für diese Untersuchungen gelten besondere Arbeitsschutz- und Hygiene-standards, die über die üblichen Maßnahmen an der Universität hinausgehen und über die wir Sie nachfolgend ausführlich informieren.

Neben den allgemeinen Rahmenbedingungen für einen „Kontrollierten und kontaktarmen Lehr- und Forschungsbetrieb" und einer erweiterten Grundhygiene haben wir zusätzliche Sicherheits-standards etabliert, die zu einem Infektionsschutz von Proband*innen und unseren Mit-arbeiter*innen beitragen:

1. Im gesamten Aufenthaltsbereich des Cogniums und MRT-Pavillons gilt für Proband*innen und Mitarbeiter*innen unserer Arbeitsbereiche Maskenpflicht. Für einen zusätzlichen Fremd- und Selbstschutz werden Ihnen vor Betreten des MRT-Pavillons medizinische Mund-Nasen-Masken zugeteilt, die Sie während des gesamten Untersuchungsverlaufes tragen werden. Alle Mit-arbeiter*innen sind zum Fremdschutz mit thermofixierten PET Filtermedien ausgestattet.

2. Am Eingang des MRT-Pavillons sowie an mehreren Stationen des Innenbereichs sind Sterilium-spender zur Händedesinfektion aufgestellt. Sie werden gebeten, vor und nach Betreten des Gebäudes Ihre Hände gründlich zu desinfizieren.

3. Die Mitarbeiter*innen tragen während des gesamten Untersuchungsablaufs Einmal-handschuhe. Diese werden Ihnen auf Wunsch ebenso zur Verfügung gestellt.

4. Neben Ihnen wird während des gesamten Untersuchungsablaufs der/die Untersuchungs-leiter/in im MRT-Trakt und Konsolenraum anwesend sein, sowie aus Sicherheitsgründen und mit gebotenem Sicherheitsabstand maximal drei weitere Person im gesamten Gebäude.

5. Um Kreuzungswege und Kontaktzonen zu beschränken, werden Sie an verschiedenen Orten zu den Untersuchungsräumen ein- und ausgelassen.

6. Sämtliche Kontaktoberflächen im MRT-Scanner und im Konsolenraum (Monitore, Tastaturen, Mäuse, …) ebenso wie Armaturen (Türgriffe) werden nach Untersuchung oberflächendes-infiziert.

7. Alle Einmalartikel (Ohrstöpsel, Papierlagen, …) werden nach Untersuchung vernichtet, benutzte Decken einer Kochwäsche zugeführt.

8. Zurzeit finden pro Tag max. zwei Untersuchungen mit Proband*innen im MRT-Scanner statt.

Mit Ihrer nachfolgenden Unterschrift bestätigen Sie, dass Sie von den o.g. Sicherheitsstandards Kenntnis genommen haben und diese auch einhalten werden. Sie erklären sich bereit, an der im Informationsblatt beschriebenen freiwilligen Untersuchung im Rahmen der oben genannten Beding-ungen teilzunehmen.

_____          _____          _____
Ort, Datum               Unterschrift Untersuchungsteilnehmer/in          Unterschrift Untersucher/in

## 8.2 Document 2 – Participant information and questionnaires

Note: Questionnaires public available and based on third sources (DOSPERT, GRiPS, SVO) are not reproduced here.

### 8.2.1 DOCUMENT 2A – PARTICIPANT INFORMATION ON FMRI AND MRI

SEHR GEEHRTE UNTERSUCHUNGSTEILNEHMERIN,
SEHR GEEHRTER UNTERSUCHUNGSTEILNEHMER,

vielen Dank für Ihr Interesse an dieser Studie, bei der die Aktivität im Gehirn während Entscheidungen gemessen werden soll. Wir möchten Sie zunächst über den Ablauf informieren, um Ihnen einen Überblick über die geplanten Messungen zu ermöglichen und Ihnen das Ziel der Untersuchungen zu erklären.
Die Untersuchungen werden mit einem Magnetresonanztomographen (kurz MRT) durchgeführt, der uns Messungen der Durchblutung im Gehirn schmerzfrei und ohne zusätzliche Gabe von Medikamenten ermöglicht.

**Ziele und Ablauf der Untersuchung**

In dieser Studie soll die Aktivität des Gehirns während Entscheidungsprozessen untersucht werden. Die Art der Aufgabe wird Ihnen vor der Messung ausführlich vom Versuchsleiter erklärt. In dieser Studie wird eine Reihe von Aufgaben gestellt, bei denen mit Hilfe zweier Tasten darüber entschieden werden soll, ob ein Ballon weiter aufgeblasen wird.
Insgesamt wird die Messung im MRT-Scanner ca. 50 Minuten dauern.

**Was ist eine Magnetresonanztomographie?**

Im Rahmen der Studie ist eine funktionelle Magnetresonanztomographie des Gehirns vorgesehen. Mit Hilfe dieser Methode ist es möglich, die Durchblutung in Ihrem Gehirn zu messen und daraus Rückschlüsse auf die bei der Aufgabe beteiligten Bereiche zu ziehen. Hierbei treffen Radiowellen, die in dem Magnetfeld erzeugt worden sind, auf den Körper, der Signale zurückschickt. Diese Echosignale werden von speziellen Antennen aufgefangen und in einem Computer ausgewertet. Ein Kontrastmittel ist **nicht** erforderlich. Es werden **keine** Röntgenstrahlen eingesetzt.

**Wie läuft die Untersuchung ab?**

Vor der Untersuchung werden Sie vom Untersuchungsleiter ausführlich über die für den Tag geplanten Messungen und Ziele informiert. Auch im Verlauf der Untersuchung werden Sie vom Untersucher jederzeit gehört. **Sie haben das Recht, ohne Angabe von Gründen jederzeit die Teilnahme an der Messung abzulehnen bzw. abzubrechen.**
Für die Untersuchung legen Sie sich auf eine Liege, wo Ihr Kopf in einer Kopfspule positioniert wird. Anschließend werden Sie langsam in die Öffnung des Magnetresonanztomographen geschoben. Dort befinden Sie sich während der gesamten Untersuchung. Während der Messungen sind sehr laute Klopfgeräusche zu hören, die völlig normal sind und von den schnell geschalteten Magnetfeldgradienten verursacht werden. Um Ihrem Gehör nicht zu schaden, müssen Sie einen geeigneten Hörschutz (Ohrstöpsel oder Schallschutzhörer) tragen. Für die Qualität der Messungen ist es wichtig, während der Untersuchung möglichst ruhig liegen zu bleiben. Um dies zu erleichtern, werden Kopf, Arme und Beine mit Polstern und anderen Hilfsmitteln schmerzfrei und bequem gelagert. Die Aufgaben, die Sie während der Untersuchung bearbeiten sollen, werden Ihnen über einen an der Kopfspule angebrachten Spiegel dargeboten.

**Mögliche Risiken der Methode:**

Im Magnet des Magnetresonanztomographen herrscht mit 3Tesla (T) ein Magnetfeld, das in etwa 62.500-mal stärker als das Erdmagnetfeld in Mitteleuropa ist. Dieser Magnet wird nie

ausgeschaltet und zieht mit sehr starker Kraft alle magnetischen und magnetisierbaren Gegenstände an, welche in seine Nähe geraten. Die größte Gefahr geht von Unfällen mit solchen Gegenständen aus, die angezogen werden und mit sehr großer Geschwindigkeit in den Magneten fliegen und anschließend an ihm „festkleben". Deshalb wird mit größter Sorgfalt darauf geachtet, dass keine magnetischen oder magnetisierbaren Gegenstände in die Nähe des Magneten geraten. Der Magnetresonanztomograph hält alle für die Sicherheit des Betriebes und insbesondere die Sicherheit der Probanden/Patienten erforderlichen Grenzwerte ein. Er wurde vom TÜV einer Sicherheitsprüfung unterzogen und wird darüber hinaus in den vorgeschriebenen Intervallen überprüft. Dennoch müssen folgende Punkte beachtet werden.

1. **Magnetische und magnetisierbare Gegenstände dürfen nicht in den Messraum gelangen.**
   Auf Gegenstände, die Eisen oder Nickel enthalten, wie z.B. Messer, Schraubenzieher, Kugelschreiber, Münzen, Haarspangen, etc., wird im Bereich des Magneten eine starke Anziehungskraft ausgeübt. Dadurch werden die Gegenstände mit großer Geschwindigkeit in den Magneten gezogen und können Personen gegebenenfalls lebensgefährlich verletzten. Metallkörper (Metallplatten etc.) und andere Fremdkörper wie Geschossteile können ebenfalls ferromagnetisch sein und durch magnetische Kräfte ihre Position im Körper verändern, die dann innere Verletzungen hervorrufen. Kleine Metallsplitter im Auge können durch magnetische Kräfte bewegt oder gedreht werden und das Auge verletzen.

2. Personen mit Chochlea-Implantaten, Defibrillatoren oder Pumpensystemen dürfen nicht einem starken Magnetfeld ausgesetzt werden, da es auch in diesen Fällen zu Risiken durch magnetische Kräfte kommen kann.

3. **Personen mit Herzschrittmachern dürfen nicht an Untersuchungen teilnehmen.**
   Herzschrittmacher können im Magnetfeld ihre Funktionsfähigkeit verlieren. Zumindest ist es sehr wahrscheinlich, dass diese in einen Grundzustand („Reset") versetzt werden.

4. Bei der Messung mit dem Magnetresonanztomographen kommt es zur Abstrahlung von hochfrequenter elektromagnetischer Strahlung, wie sie z.B. bei Radiosendern und Funktelefonen auftritt. Dies kann zu einer geringfügigen Erwärmung des untersuchten Gewebes führen, wird aber sowohl geräte- als auch steuerungstechnisch kontrolliert.

5. **Bei allen Messungen müssen entweder schallabsorbierende Kopfhörer oder Lärmschutzstopfen getragen werden, die wir zur Verfügung stellen.** Das Schalten der Magnetfeldgradienten führt in Teilen des Gradientensystems zu mechanischen Verformungen, die Geräusche mit Lautstärken über 100 dB erzeugen können. Bei Einhaltung dieser Vorsichtsmaßnahmen kann eine Schädigung des Hörsystems ausgeschlossen werden.

6. Manche Menschen erleben enge Räume als bedrohlich. Sie berichten über Unwohlsein z.B. in Fahrstühlen oder in großen Menschenansammlungen. Obwohl diese Angstgefühle meist über die Anamnese ausgeschlossen werden können, ist ein erstmaliges Auftreten während der Messung im Magnetresonanztomographen möglich. Der Untersucher ist bei der Messung anwesend; bei dem Auftreten von Symptomen kann der Proband über Sprechkontakt bzw. über eine Notklingel jederzeit auf sich aufmerksam machen, so dass eine rasche Intervention bei Symptomen gewährleistet ist.

**Datenverarbeitung/Gewährleistung der Anonymität**

Jeder teilnehmenden Versuchsperson wird ein Code, der aus einer fortlaufenden Liste entnommen wird, zugeordnet. Dieser Code hat keinen Bezug zur Person. Die Zuordnung der Codes zu den Teilnehmenden ist nur den Versuchsleitern zugänglich und wird nach Ablauf der Studie vernichtet. Alle Daten werden mit diesem Code versehen.Zu Beginn der Datenverarbeitung werden die Gesichtskonturen, welche man auf den MRT-Bldern sehen kann, entfernt. Dadurch ist es nicht mehr möglich, Sie auf den Bildern zu erkennen.

**Zufallsbefunde**

Obwohl die Messungen an einem klinisch üblichen Magnetresonanztomographen stattfinden, handelt es sich bei den Messungen **um keine medizinische Untersuchung**. Die Messungen sind daher auch nicht dazu geeignet, pathologische Veränderungen zu entdecken. Auch werden die Daten nicht von fachkundigen Neuroradiologen oder Neurologen begutachtet. Deshalb können keine Rückschlüsse auf den gesundheitlichen Status gezogen werden. Trotzdem besteht die Möglichkeit, dass sich in den aufgezeichneten MRT-Bildern strukturelle Anomalien, sog. Zufallsbefunde, finden lassen. Im Falle eines Zufallsbefundes oder eines Verdachts auf einen Zufallsbefund werden wir Ihnen diese Beobachtung mitteilen. Nach vorheriger Absprache mit ihnen werden repräsentative Bilder einem fachkundigen Arzt vorgelegt, um eine erste Einschätzung einzuholen. Falls der Verdacht auf einen Zufallsbefund weiterhin vorliegt, wird Ihnen die Vorstellung bei einem Facharzt empfohlen.

Ihr Einverständnis dazu ist Voraussetzung dafür, an der Untersuchung teilnehmen zu können.

## 8.2.2 Document 2B – Consent form

**ZKW**

✉ Universität Bremen ● **ZKW**·Cognium–Gebäude ●·Hochschulring 18 ● 28359 Bremen

**Zentrum für Kognitions-
wissenschaften**

**Institut für Hirnforschung V**

**Abteilung für Neuropsychologie und
Verhaltensneurobiologie**

Cognium-Gebäude
Hochschulring 18
28359 Bremen

Telefon (0421) 218 - 68749
Fax      (0421) 218 - 68759
eMail   doehring@uni-bremen.de
http:    www.neuropsychologie.uni-bremen.de

Einwilligungserklärung

Über Art und Durchführung der geplanten MRT- Untersuchung im Rahmen dieser
wissenschaftlichen Studie hat mich Herr Niels Doehring in einem
Aufklärungsgespräch ausführlich informiert. Das Informationsblatt für
Proband*innen ist mir ausgehändigt worden. Ich konnte alle mir wichtig
erscheinenden Fragen, z.B. über spezielle Risiken und mögliche Komplikationen
oder Maßnahmen stellen, die zur Vorbereitung oder während der Untersuchung
erforderlich sind. Die mir erteilten Informationen habe ich verstanden.

Ich erkläre mich hiermit bereit, an der im Informationsblatt beschriebenen
freiwilligen Untersuchung im Rahmen der oben genannten wissenschaftlichen
Studie teilzunehmen und gebe meine Einwilligung, dass bei mir im Rahmen der
wissenschaftlichen Studie eine MRT-Untersuchung des Gehirns durchgeführt
wird.

Ich erkläre mich damit einverstanden, dass die im Rahmen der Messungen
erhobenen Daten in verschlüsselter Form (pseudonymisiert) auf elektronischen
Datenträgern gespeichert und verarbeitet werden dürfen. Ich habe davon
Kenntnis genommen, dass sofort nach Auswertung und Abschluss der Studie –
spätestens jedoch Ende April 2020, die personenbezogenen Daten gelöscht
werden und so keine Zuordnung der erhobenen Untersuchungsdaten zu meiner
Person mehr möglich sein wird. Mir ist bekannt, dass die Daten während der
Verarbeitung durch digitale Entfernung der  Gesichtsoberfläche anonymisiert
werden.

Mir ist bekannt, dass es sich bei der magnetresonanztomographischen
Untersuchung nicht um eine medizinische Untersuchung handelt und ich daher
keine Rückschlüsse auf meinen gesundheitlichen Status ziehen kann. Im Falle
eines Zufallsbefundes oder eines Verdachts auf einen Zufallsbefund im Rahmen
der MRT-Messung möchte ich informiert werden.

Bremen,_____   _____   _____

Unterschrift                          Unterschrift
Untersuchungsteilnehmer*in            Untersucher

**Leitung**
Prof. Dr. Dr. Manfred Herrmann

**Verwaltung/Sekretariat**
Barbara Muntz

## 8.2.3 Document 2C – MRI-safety questionnaire

# Fragebogen zur Teilnahme an Magnetresonanzuntersuchungen

**Beantworten Sie bitte folgende Fragen zu möglichen Gegenanzeigen für Ihre Teilnahme an der Untersuchung (Zutreffendes bitte ankreuzen):**

Tragen Sie einen <u>Herzschrittmacher</u> oder ein anderes elektrisches/medizinisches Gerät (z.B. Insulinpumpe, elektronisches Implantat / Chip)?   o ja   o weiß nicht   o nein

Besitzen Sie <u>metallische Implantate</u> (z.B. Zahnschrauben, Zahnspangen, Metallplatten, Katheder, Stent o.ä. oder mechanische, metallische <u>Verhütungsmittel</u>)?   o ja   o weiß nicht   o nein

Befinden sich in Ihrem Körper andere <u>metallische Fremdkörper</u> wie Metallplatten, Geschosssplitter o.ä.?   o ja   o weiß nicht   o nein

Leiden Sie unter <u>Raum- oder Platzangst</u>?   o ja   o weiß nicht   o nein

Sind bei Ihnen oder in Ihrer Familie Anfallsleiden (<u>Epilepsie, Fallsucht</u>) aufgetreten?   o ja   o weiß nicht   o nein

Besteht die Möglichkeit, dass Sie <u>schwanger</u> sind?   o ja   o nein

Sind Sie Brillenträger/in?   O ja   o weiß nicht   o nein

Tragen Sie Kontaktlinsen?   o ja   o weiß nicht   o nein

Haben Sie Tätowierungen?   o ja   o nein

Wurden Sie schon einmal operiert?   o ja   o weiß nicht   o nein
Art der Operation / welches Jahr _____

Wurde bei Ihnen eine Gefäßoperation durchgeführt?   o ja   o weiß nicht   o nein

**Erklärung:**
**Ich habe alle Fragen auf dieser Seite wahrheitsgemäß und nach bestem Wissen beantwortet.**

_____   _____   _____
Ort                          Datum                  Unterschrift

## Persönliche Daten:

Name ...............................................................................................................
Geschlecht .......................
Größe ................................
Gewicht ...........................
Alter .................................

### 8.2.4 DOCUMENT 2D – WRITTEN INFORMATION ON DESIGN

Note: Handed to the participants to read before the measurement started; used to provide context for the decisions made in the scanner.

*Im Folgenden wird eine Rahmengeschichte für das kommende Experiment beschrieben. Bitte versetzen Sie sich so gut wie möglich in die beschriebene Situation.*

Sie befinden sich auf einem Stadtfest, bei dem viele Kinder und Erwachsene anwesend sind. Sie haben einen Stand, an welchem Sie mit einer Maschine Luftballons befüllen. Drücken Sie auf einen Knopf, befüllt die Maschine den aktuellen Luftballon. Drücken Sie auf einen anderen Knopf, wird der Ballon zugeknotet.

Jeder Ballon hat eine Ihnen unbekannte maximale Kapazität. Überschreiten Sie diese, platzt der Ballon.

Sowohl Erwachsene als auch Kinder kommen zu ihrem Stand. Den Erwachsenen verkaufen Sie Ihre Ballons. Für Ballons, welche Sie häufiger aufgepustet haben, bekommen Sie von den Erwachsenen mehr Geld. Kindern schenken Sie die Luftballons. Je häufiger sie den Ballon aufgepustet haben, desto mehr freut sich das Kind, welches ihn geschenk bekommt hat. Beide Belohnungen werden nach dem Experiment ins echte Leben übertragen: je häufiger Sie Luftballons für Erwachsene erfolgreich aufgepustet haben, desto mehr Geld bekommen Sie ausgezahlt. Je häufiger Sie Ballons für Kinder erfolgreich aufgepustet haben, desto mehr Wundertüten werden wir nach Abschluss der Studie Kindern einer Bremer KiTa schenken.

Die Maschine hat auch einen Automatik-Modus. In diesem müssen sie immer nur dieselbe Taste (mittlere Maustaste) drücken. Die Maschine entscheidet selber, ob der Ballon weiter aufgepustet oder zugeknotet wird. Manchmal platzen auch beim automatischen Befüllen Ballons.

Bevor Sie einen neuen Ballon aufpusten, wird Ihnen auf dem Bildschirm angezeigt, ob Sie diesen Ballon im Automatik-Modus aufpusten, oder ob sie selber entscheiden dürfen, wie lange sie aufpusten möchten. Der Automatik-Modus wird durch das Wort "Passiv" angekündigt. Dürfen Sie selber entscheiden, steht das Wort "Aktiv" vor Beginn in der Mitte des Bildschirms.

Sowohl Erwachsene als auch Kinder wollen nicht zu lange warten - brauchen sie länger als 4 Sekunden, um sich im Aktiven Modus zu entscheiden oder um im Passiven Modus die mittlere Maustaste zu drücken, gehen Sie für den jeweiligen Ballon leer aus.

Auch wenn einer der Ballons platzt, bekommen Sie keine Belohnung - die Erwachsenen geben Ihnen kein Geld und die Kinder freuen sich nicht.

## 8.2.5 Document 2 E – Guideline for verbal information for participants

Note: The text was read to participants to inform them on the experiment before the measurement started. Participants could ask questions at any moment and the text mostly served as a guideline. A presentation was used in parallel to accustom participants to the stimuli. "click" notes where the slide was changed.

Ich werde Ihnen nun ihre Aufgabe in der folgenden Studie erklären. Bitte hören Sie aufmerksam zu. Sie werden eine gekürzte Form der Instruktionen auch noch einmal vor der Messung an einem Computerbildschirm gezeigt bekommen. Außerdem werden Sie die Möglichkeit haben, 10 Probeballons aufzupusten, bevor die richtige Messung beginnt.

Wie Sie gerade gelesen haben, ist es Ihre Aufgabe in der folgenden Studie, virtuelle Luftballons per Tastendruck aufzupusten. Manche der Ballons pusten Sie für Erwachsene auf, andere für Kinder.

Vor jedem Ballon bekommen Sie angezeigt, ob der Ballon für einen Erwachsenen oder ein Kind ist. Ist der Ballon für jemand Erwachsenes, sehen Sie folgendes Bild **click**.

Ist der Ballon für ein Kind, sehen Sie folgendes Bild **click**.

Bei manchen der Ballons können Sie selbst entscheiden, ob sie weiter aufpusten können, bei anderen wird es Ihnen vorgegeben. Können sie selbst entscheiden, wird Ihnen dies vor dem Ballon wie folgt angekündigt: **click**

Können Sie nicht selbst entscheiden, wird es Ihnen wie folgt angekündig: **click**.

Nachdem Ihnen die Informationen angezeigt wurden, geht es mit dem eigentlichen Aufpusten los. Im Folgenden werden wir erst die *altive* Bedingung besprechen, bei der sie selbst entscheiden können ob sie weiter aufpusten wollen oder nicht.

Zu Beginn jedes Ballons wird ihnen ein kleiner Luftballon mit einem Fragezeichen darauf angezeigt. **click** Sie müssen sich nun entscheiden, ob Sie weiter aufpusten wollen oder nicht. Dies kommunizieren Sie über die linke bzw. rechte Maustate. Die genaue Zuweisung der Tasten wird Ihnen gleich beim Übungsdurchlauf am Computer angezeigt.

Sie müssen in dieser Studie *ausschließlich* dann klicken, wenn Sie einen Luftballon mit einem Fragezeichen sehen, oder explizit zum klicken aufgefordert werden. Zwischenzeitlich werden immer wieder sogenannte Fixationspunkte angezeigt. Diese sehen wie folgt aus: **click** Fixationspunkte verschwinden nach einer Variablen Zeit. Manchmal kann dies etwas länger dauern, sie brauchen jedoch in keinem Fall bei einem Fixationspunkt zu klicken. Bitte halten Sie einfach ihren Blick auf das Kreuz in der Mitte des Bildschirms gerichtet und warten Sie entspannt den nächsten Stimulus ab.

**click**

Entscheiden Sie sich nun bei einem Luftballon zum Aufpusten, gibt es zwei mögliche Folgen: entweder der Ballon platzt, oder er wird erfolgreich aufgepustet.

Wenn der Ballon platzt, wird Ihnen, nach einem Fixationspunkt **click** der geplatzte Ballon angezeigt **click**. Anschließend sehen Sie **click**, je nach dem, ob der Ballon für jemand Erwachsenes oder für ein Kind war, ein Feedback darüber, dass Sie kein Geld gewonnen haben, bzw. dass das Kind nicht glücklich ist. Danach geht es weiter mit dem nächsten Ballon.

**click**

Wenn sie den Ballon aufblasen und er nicht platzt, sehen Sie, wieder nach einem kurzen Fixationspunkt **click** , wie glücklich das Kind aktuell ist bzw. wie viel Geld sie aktuell bekämen. Anschließend sehen Sie noch als Animation wie der Ballon größer **click** wird , bevor dann wieder ein Fragezeichen auf dem Ballon erscheint, und Sie sich erneut entscheiden müssen **click**.

Wenn Sie sich dafür entscheiden, den Ballon nicht weiter aufzublasen, wird Ihnen angezeigt, wie viel Sie für diesen Ballon bekommen, bzw wie glücklich das Kind aktuell ist. Anschließend sehen Sie noch mal einen Fixationspunkt, bevor es mit dem nächsten Ballon weitergeht. **click**

Die passiven Trials laufen genau so ab, wie die aktiven. Der einzige Unterschied ist, dass Sie hier nicht bestimmen können, was mit dem Ballon passiert. Sie müssen stets die mittlere Maustaste drücken, wenn ein Ballon mit Fragezeichen darauf erscheint. Dann "entscheidet der Computer" ob der Ballon weiter aufgepustet wird oder nicht. Wenn der Computer entscheidet, dass der Ballon weiter aufgepustet wird, kann es auch sein, dass der Ballon platzt.

Treffen Sie ihre Entscheidungen wohl überlegt - es gibt eine feste Anzahl von Ballons, und jeder geplatzte Ballon kommt nicht wieder zurück. Lassen Sie sich aber auch nicht zu viel Zeit: Warten Sie länger als 4 Sekunden mit dem aufpusten eines Ballons, geht der Erwachsene oder das Kind und Sie bekommen keine Belohnung für diesen Ballon.

Die Luftballons kommen alle aus der selben Kiste. Auch wenn Aktive und Passive Ballons verschiedene Farben haben, sind die Explosionswahrscheinlichkeiten bei beiden gleich. Dabei gilt, dass kleinere Ballons mit geringerer Wahrscheinleichkeit explodieren als größere. Trotzdem kann es auch mal vorkommen, dass ein sehr kleiner Ballon schon explodiert oder ein sehr großer es nicht tut. Beide Ereignisse sind aber eher unwahrscheinlich.

Die Explosionswahrscheinlichkeit der Ballons hängt ausschließlich von ihrer Größe ab. Weder ihr Verhalten innerhalb der Aufgabe, noch die Explosionen früherer Ballons haben einen Einfluss auf den jeweils aktuellen Ballon.

Sie bekommen am Ende sowohl die Belohnungen von den aktiven, wie auch von den passiven Ballons. Das Geld, welches Sie erspielen, wird Ihnen bar ausgezahlt. Für die Smileys verschenken wir Wundertüten an Kinder einer Bremer KiTa. Die Smileys addieren sich dabei zusammen - viele leicht glückliche Kinder zählen so viel, wie wenige sehr glückliche. Die Wundertüten beinhalten kleine Spielzeuge sowie Sticker, Abziehtattoos, und Luftballons.

Während der Messung gleich im Scanner wird es drei kurze Pausen geben. Vor jeder Pause wird Ihnen angezeigt, wie viel Geld und Wundertüten Sie bisher insgesamt erspielt haben. Durch ein Klick gelangen Sie dann zum eigentlichen Pause - Bildschirm. Dieser verschwindet ebenfalls durch einen Klick Ihrerseits, sobald Sie weiter machen wollen. Bitte nutzen Sie die Pausen um sich kurz zu entspannen, passen Sie aber auf, dass Sie sich nicht bewegen, da sonst die MR-Messergebnisse leicht gestört werden können.

Gleich vor der Messung werden Sie dann noch die 10 Übungsballons hier am Computer aufpusten können. Sie bekommen für diese Ballons noch keine Belohnung, das heißt Sie können die Gelegenheit nutzen, um herauszufinden wie groß die Ballons Circa werden.

Haben Sie noch Fragen?

## 8.2.6 Document 2F – Guideline for demographic interview

Note: The questionnaire was not handed over to participants directly but used as a guideline for an interview to circumvent any misunderstanding and follow up on possibly relevant conditions.

Anamnese – RiSEco - MRI

Datum: _____

Versuchsleitung: _____

Probandencode: _____

Allgemeines:

Alter: _____ Jahre

Geschlecht: männlich O weiblich O divers O

Nationalität: _____

Bildungsstand (Ausbildungsjahre):_____

Beruf: _____

Konsum von Tabak: wie oft?: _____ wann zuletzt?: _____

Konsum von Alkohol: wie oft?: _____ wann zuletzt?: _____

Konsum von Kaffee: wie oft?: _____ wann zuletzt?: _____

Konsum andere Drogen: wie oft?: _____ wann zuletzt?: _____

Erkrankungen: _____

Einnahme von Medikamenten: was?:_____

wie oft?: _____ wann zuletzt?: _____

Händigkeit: Rechtshänder*in O Linkshänder*in O

Sehvermögen (normal/korrigiert): normal O korrigiert: Brille O Kontaktlinsen O

Andere visuelle Einschränkungen: _____

Schlafverhalten (letzte Nacht): wenig O normal O viel O

War das Schlafverhalten normal? : _____

Müdigkeit: (nicht müde) 1 2 3 4 5 6 7 8 9 10 (sehr müde)

## 8.2.7 DOCUMENT 2G – QUESTIONS ON MOTIVATION

Note: The questionnaire was handed out right after the measurement.

# RiSEco - Zusatzfragebogen 1

ID:_ _____

*Bitte beantworten Sie die folgenden Fragen wahrheitsgemäß mithilfe der Angegebenen Skalen.*

Wie motivierend fanden Sie die Wundertüten?

Gar nicht motivierend | 1 - 2 - 3 - 4 - 5 - 6 - 7- 8 - 9 - 10 | Sehr motivierend

Wie motivierend fanden Sie den finanziellen Gewinn?

Gar nicht motivierend | 1 - 2 - 3 - 4 - 5 - 6 - 7- 8 - 9 - 10 | Sehr motivierend

Wie motiviert waren Sie insgesamt?

Gar nicht motiviert | 1 - 2 - 3 - 4 - 5 - 6 - 7- 8 - 9 - 10 | Sehr motiviert

## 8.2.8 Document 2H – Certificate on acquired gift-bags

# URKUNDE

_____

hat im Rahmen der Studie „RiSEco" an der Universität Bremen

_____

Wundertüten für Kinder einer Bremer KiTa erspielt.

Die Abteilung für Neuropsychologie und Verhaltensneurobiologie spricht
ihren Glückwunsch aus und verpflichtet sich hiermit,
ihrer Pflicht nachzukommen und die Wundertüten Kindern zukommen zu lassen.

Wir wünschen Ihnen alles Gute und viel Erfolg.

Bremen, den _____2019

_____

M.Sc. Niels Doehring, i.A.

**Abteilung für Neuropsychologie und Verhaltensneurobiologie**

## 8.3 Document 3 – AFNI preprocessing script

Note: Function call to afni_proc.py, generated through ubers_subject.py and adapted. The function was called once for each participant, $path_anatomy, $path_epi, $subj_id, and $path_timing were different for each participant. They indicated paths to the T1-scan, the functional data, a subject identifier, and a path to the stimulus timing files, respectively.

```
afni_proc.py -subj_id $subj_id                                             \
      -script proc_py_script -scr_overwrite                                \
      -blocks tshift align tlrc volreg blur mask scale regress             \
      -copy_anat $path_anatomy                                             \
      -dsets $path_epi                                                     \
      -tcat_remove_first_trs 0                                             \
      -align_opts_aea -cost lpc+ZZ -check_flip -ginormous_move             \
      -tlrc_base MNI152_T1_2009c+tlrc                                      \
      -tlrc_NL_warp                                                        \
      -volreg_align_to MIN_OUTLIER                                         \
      -volreg_align_e2a                                                    \
      -volreg_tlrc_warp                                                    \
      -mask_epi_anat yes                                                   \
      -blur_size 8.0                                                       \
      -regress_stim_times                                                  \
          $path_timing/inflate_1D_no1inf_eco_act_rt_param.1D               \
          $path_timing/inflate_1D_no1inf_eco_pas_rt_param.1D               \
          $path_timing/inflate_1D_no1inf_soc_act_rt_param.1D               \
          $path_timing/inflate_1D_no1inf_soc_pas_rt_param.1D               \
          $path_timing/feedback_exp_01.1d                                  \
          $path_timing/feedback_exp_00.1d                                  \
          $path_timing/feedback_exp_11.1d                                  \
          $path_timing/feedback_exp_10.1d                                  \
          $path_timing/feedback_win_01.1d                                  \
          $path_timing/feedback_win_00.1d                                  \
          $path_timing/feedback_win_11.1d                                  \
          $path_timing/feedback_win_10.1d                                  \
      -regress_stim_labels                                                 \
          risk_ea risk_ep risk_sa risk_sp                                  \
          expl_ea expl_ep expl_sa expl_sp                                  \
          win_ea win_ep win_sa win_sp                                      \
      -regress_basis_multi 'dmBLOCK' 'dmBLOCK' 'dmBLOCK' 'dmBLOCK'         \
                  'BLOCK(1.5,1)' 'BLOCK(1.5,1)' 'BLOCK(1.5,1)' 'BLOCK(1.5,1)'\
                  'BLOCK(1.5,1)' 'BLOCK(1.5,1)' 'BLOCK(1.5,1)' 'BLOCK(1.5,1)'\
      -regress_stim_types AM2                                              \
      -regress_censor_motion 0.3                                           \
      -regress_apply_mot_types demean deriv                               \
      -regress_motion_per_run                                              \
      -regress_censor_outliers 0.05                                        \
      -regress_opts_3dD                                                    \
          -jobs 4                                                          \
          -num_glt 20                                                      \
          -gltsym 'SYM: risk_ea[1] -risk_ep[1]' -glt_label 1 risk_ea-
ep_modulation\
          -gltsym 'SYM: risk_sa[1] -risk_sp[1]' -glt_label 2 risk_sa-
sp_modulation\
```

```
            -gltsym 'SYM: risk_ea[0] -risk_ep[0]' -glt_label 3 risk_ea-
ep_mean\
            -gltsym 'SYM: risk_sa[0] -risk_sp[0]' -glt_label 4 risk_sa-
sp_mean\
            -gltsym 'SYM: risk_ea[1] -risk_sa[1]' -glt_label 5 risk_ea-
sa_modulation\
            -gltsym 'SYM: risk_ea[0] -risk_sa[0]' -glt_label 6 risk_ea-
sa_mean\
            -gltsym 'SYM: risk_ep[1] -risk_sp[1]' -glt_label 7 risk_ep-
sp_modulation\
            -gltsym 'SYM: risk_ep[0] -risk_sp[0]' -glt_label 8 risk_ep-
sp_mean\
            -gltsym 'SYM: risk_ea[1] -risk_ep[1] -risk_sa[1] +risk_sp[1]' -
glt_label 9 risk_ea-ep-sa+sp_modulation\
            -gltsym 'SYM: risk_ea[0] -risk_ep[0] -risk_sa[0] +risk_sp[0]' -
glt_label 10 risk_ea-ep-sa+sp_mean\
            -gltsym 'SYM: expl_ea[1] -expl_sa[1]' -glt_label 11 expl_ea-
sa_modulation\
            -gltsym 'SYM: expl_ea[0] -expl_sa[0]' -glt_label 12 expl_ea-
sa_mean\
            -gltsym 'SYM: win_ea[1] -win_sa[1]' -glt_label 13 win_ea-
sa_modulation\
            -gltsym 'SYM: win_ea[0] -win_sa[0]' -glt_label 14 win_ea-sa_mean\
            -gltsym 'SYM: win_sa[1] -expl_sa[1]' -glt_label 15 win_sa-
expl_sa_modulation\
            -gltsym 'SYM: win_sa[0] -expl_sa[0]' -glt_label 16 win_sa-
expl_sa_mean\
            -gltsym 'SYM: win_ea[1] -expl_ea[1]' -glt_label 17 win_ea-
expl_ea_modulation\
            -gltsym 'SYM: win_ea[0] -expl_ea[0]' -glt_label 18 win_ea-
expl_ea_mean\
            -gltsym 'SYM: win_ea[1] -expl_ea[1] -win_sa[1] +expl_sa[1]' -
glt_label 19 wea-eea-wsa+esa_modulation\
            -gltsym 'SYM: win_ea[1] -expl_ea[1] -win_sa[0] +expl_sa[0]' -
glt_label 20 wea-eea-wsa+esa_mean\
        -regress_reml_exec                                              \
        -regress_compute_fitts                                          \
        -regress_make_ideal_sum sum_ideal.1D                            \
        -regress_est_blur_epits                                         \
        -regress_est_blur_errts                                         \
        -regress_run_clustsim no                                        \
        -html_review_style pythonic
```

## 8.4 Figure 1 – EV based on participants self-report
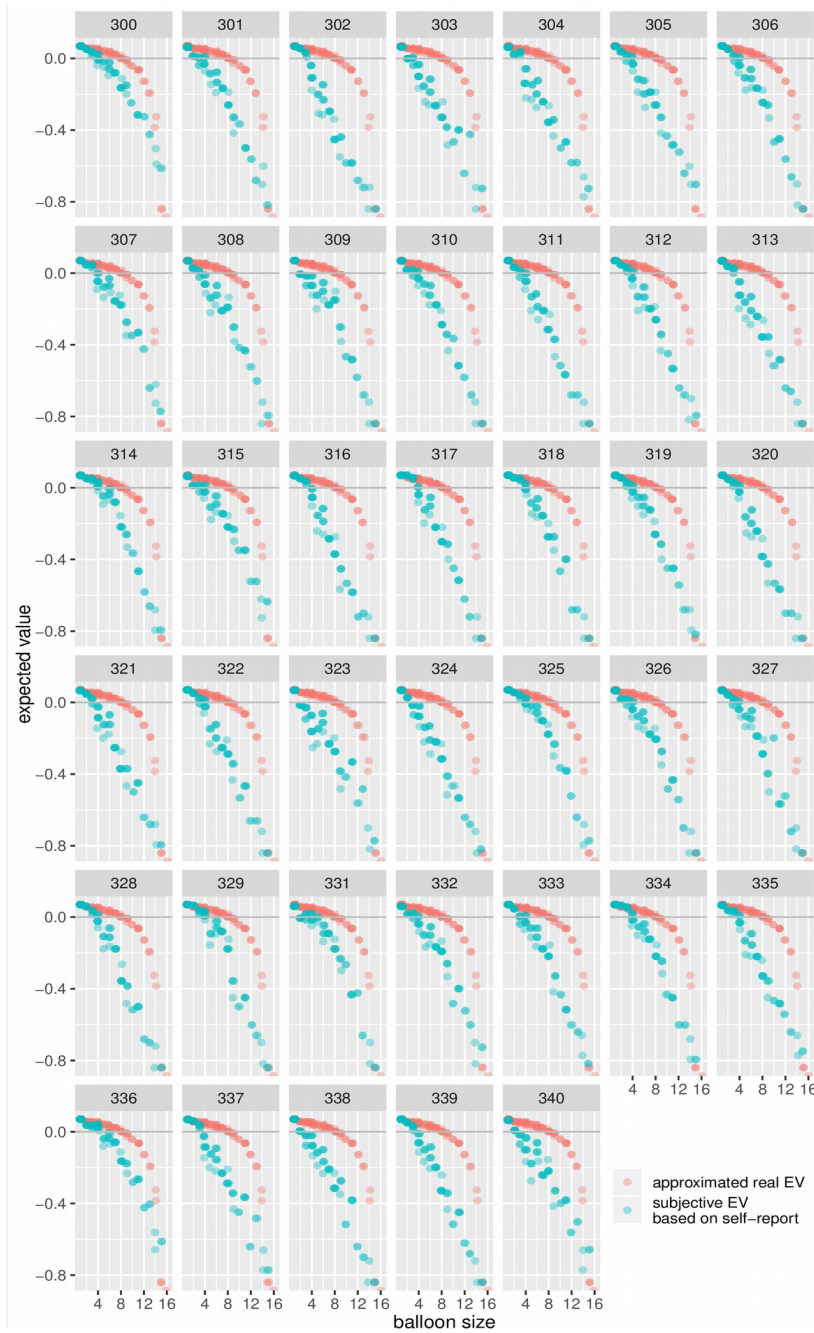


Note: EV is approximated, real EV varies, c.f. figure 12. Subjective EV is calculated based on participants self-reported explosion probabilities for balloons from active and passive condition. Participant 300 was a pilot participant not included in the main analysis.

## Versicherung an Eides Statt

Ich, Niels Doehring, _____

            (Anschrift)

versichere an Eides Statt durch meine Unterschrift, dass ich die vorstehende Arbeit selbständig und ohne fremde Hilfe angefertigt, meine Eigenleistung und Beiträge der Koautorinnen und Koautoren im Falle einer kumulativen Dissertation entsprechend richtig ausgewiesen habe.

Ich versichere an Eides Statt, dass ich alle Stellen, die ich wörtlich dem Sinne nach aus Veröffentlichungen entnommen habe, als solche kenntlich gemacht habe, mich auch keiner anderen als der angegebenen Literatur oder sonstiger Hilfsmittel bedient habe.

Ich versichere an Eides Statt, dass ich die vorgenannten Angaben nach bestem Wissen und Gewissen gemacht habe und dass die Angaben der Wahrheit entsprechen und ich nichts verschwiegen habe.

Die Strafbarkeit einer falschen eidesstattlichen Versicherung ist mir bekannt, namentlich die Strafandrohung gemäß § 156 StGB bis zu drei Jahren Freiheitsstrafe oder Geldstrafe bei vorsätzlicher Begehung der Tat bzw. gemäß § 161 Abs atz 1 StGB bis zu einem Jahr Freiheitsstrafe oder Geldstrafe bei fahrlässiger Begehung.

Ort, Datum                                        Unterschrift